Characterization of the functions of Upf1 in the nucleus of *Schizosaccharomyces pombe*

Jianming Wang

Supervised by Dr. Saverio Brogna

A thesis submitted to

The University of Birmingham

For the degree of

DOCTOR OF PHILOSOPHY

School of Biosciences

College of Life and Environmental Sciences

The University of Birmingham

November 2015

Abstract

Up-frameshift protein 1 (Upf1) is a conserved protein across eukaryotes which is required for nonsense mediated mRNA decay (NMD). While NMD is linked to translation, it has been reported that Upf1 has also nuclear functions, which are independent of its role in NMD in the cytoplasm. However, it is not clear whether the known nuclear role of Upf1 in mammalian cells is conserved in *Schizosaccharomyces pombe* (*S. pombe*). The research work in this study is to investigate whether Upf1 functions in the nucleus and its other possible molecular functions in *S. pombe*. Similar to what has been previously reported in mammalian cells, I found that *upf1* deletion mutant of *S. pombe* was hypersensitive to the DNA replication inhibitors hydroxyurea (HU) and methyl methanesulfonate (MMS), suggesting increased DNA damage in this mutant. Additionally, each of *upf1*, *upf2* and *upf3* has shown synthetic sick with *rad52*, which is known to play a central role in homologous recombination and DNA double-strand break repair in *S. pombe*. Moreover, I found that S-phase progression is slower in NMD mutants. I have assayed the chromosomal association of Upf1 by chromatin immunoprecipitation (ChIP) experiments, and found an RNA dependent selective association of Upf1 with highly transcribed gene loci including both protein coding and noncoding genes, implying its association with nascent RNA. Furthermore, deletion of Upf1 leads to increased RNA levels of *tf2* and rDNA, which are bound by Upf1, suggesting it has a direct role in regulating transcription. The direct role of Upf1 in transcription will be assessed using reagents described in this thesis for an investigation of whether the loading pattern of RNA polymerase II on chromatin changes in the absence of Upf1 using ChIP-Seq. The hypothesis is that Upf1 has a direct role at transcription sites. Additionally, a genome-wide genetic screen was performed in this study to uncover other possible nuclear functions of Upf1, which identified genetic interaction of Upf1 with genes involved in nuclear activities including nucleosome remodelling, transcription and cell cycle regulation.

Acknowledgements

Firstly, I would like to express my very great appreciation to my supervisor Dr. Saverio Brogna for the continuous support of my PhD study, for his huge patience, and immense knowledge. His persistence, enthusiasm for science have greatly encouraged me to make efforts for the research work.

I am particularly grateful for the lab training and valuable advice provided by Dr. Jikai Wen. I would also like to thank Dr. Yun Fan, Dr. Klaus Fütterer, Prof. Robin May, Dr. Sandip De, Dr. Wazeer Versally for their insightful comments, constructing discussion and encouragement on my research work. Thanks for Dr. Alicia Hidalgo and Dr Matthias Soller for sharing equipment. I would like to offer my special thanks to Tina Mcleod and Marija Petric, who have spent their precious time on my thesis correction.

My grateful thanks are also extended to Dr. Samira Khaliq, Kim Piechocki, Roy Subhendu Choudhury, Dr. Akilu Abdullahi, Dr. Anand Kumar Singh and other colleagues from 6th floor of Biosciences building for their support during my PhD. I will always remember all the fun we have had in the last four years. I am also very proud of my Chinese friends in UK and in China, with whom I shared many wonderful moments and no longer feel cold in UK.

My sincere thanks also goes to the Darwin Trust of Edinburgh PhD studentship, which allowed me not to struggle for living in Birmingham during my four-year PhD. I also appreciate the travel funds, excellent teaching and research services provided by School of Biosciences, the University of Birmingham.

Thanks to my previous colleagues in Lanzhou Institute of Biological Products, especially Prof. Xu Zhou and Prof. Guilin Xie for introducing me to the molecular biology fields, and for recommending me to study PhD degree at the University of Birmingham.

Finally, I would like to thank my family: my parents, my elder brother and younger sister for their unconditional support, for giving me infinite strength to overcome tough life. You are my sunshine, and I love you forever!

Jianming Wang

List of Abbreviations

BSA	Bovine serum albumin
CBC	Cap binding complex
CBP	Cap binding protein
DMSO	Dimethyl sulfoxide
DSE	Downstream sequence
EDTA	Ethylenediaminetetraacetic acid
eIF3/eIF4AIII/eIF4G	Eukaryotic translation initiation factors
EJC	Exon junction complex
eRF1/eRF3	Eukaryotic release factor 1 and 3
FISH	Fluorescent *in situ* hybridization
GFP	Green fluorescent protein
HA	Hemagglutinin
HR	Homologous recombination
NHEJ	Non-homologous end joining
NMD	Nonsense-mediated mRNA decay
NPC	Nuclear pore complex
PABPC	Poly (A) binding protein, cytoplasm
PEG	Polyethylene glycol
PTC	Premature termination condon
RNAPII	RNA polymerase II
Rpb3	RNA polymerase II subunit 3
RpL	Ribosomal protein large subunit
RpS	Ribosomal protein small subunit
SDS	Sodium dodecyl sulfate
SMG	Suppressor with morphological effect on genitalia
Tris	Tris (hydroxymethyl) aminomethane
UPF	Up-frameshift

UTR	Untranslated region

Abbreviations names are usually given in full when they are first mentioned. This list only shows the most frequently used and those for which full names were not given in the text.

Table of Contents

Chapter 1

1.0 Introduction

1.1 Eukaryotic gene expression

Protein-coding gene expression in eukaryotes begins with the transcription of DNA into mRNAs, which are eventually converted to functional proteins. Unlike prokaryotes, eukaryotic genomic DNA is located in a membrane-encircled compartment called the nucleus. Thus, regulation of eukaryotic gene expression happens at many different levels, including chromosome remodelling, nuclear organization, transcription, mRNA processing, export of mRNA and translation, as well as quality control processes coupled to each step. Eukaryotic protein-coding genes are firstly transcribed by RNA polymerase II, one of three distinct nuclear RNA polymerases that each transcribe different types of genes. All prokaryotic genes on the other hand are transcribed by a single RNA polymerase (Cooper, 2000). Most eukaryotic precursor mRNAs (pre-mRNAs) undergo several processing steps to become mature messenger RNAs (mRNAs). These steps include the attachment of a 7-methylguanosine cap at the 5' end, intron removal coupled with exon ligation, and formation of a 3' end by cleavage and addition of a non-templated poly(A) tail (Bentley, 2014). The co-transcriptionally processed mRNA in the nucleus is packaged into messenger ribonucleoprotein (mRNP) complexes, which are translocated through nuclear pore complexes (NPCs) and directionally released into the cytoplasm (Carmody and Wente, 2009). Proteins are synthesized by ribosomes, with a variety of tRNAs serving as a bridge between the mRNA template and the amino acids being incorporated into proteins. (Cooper, 2000). A modified outline of gene expression processes is illustrated in Figure 1.

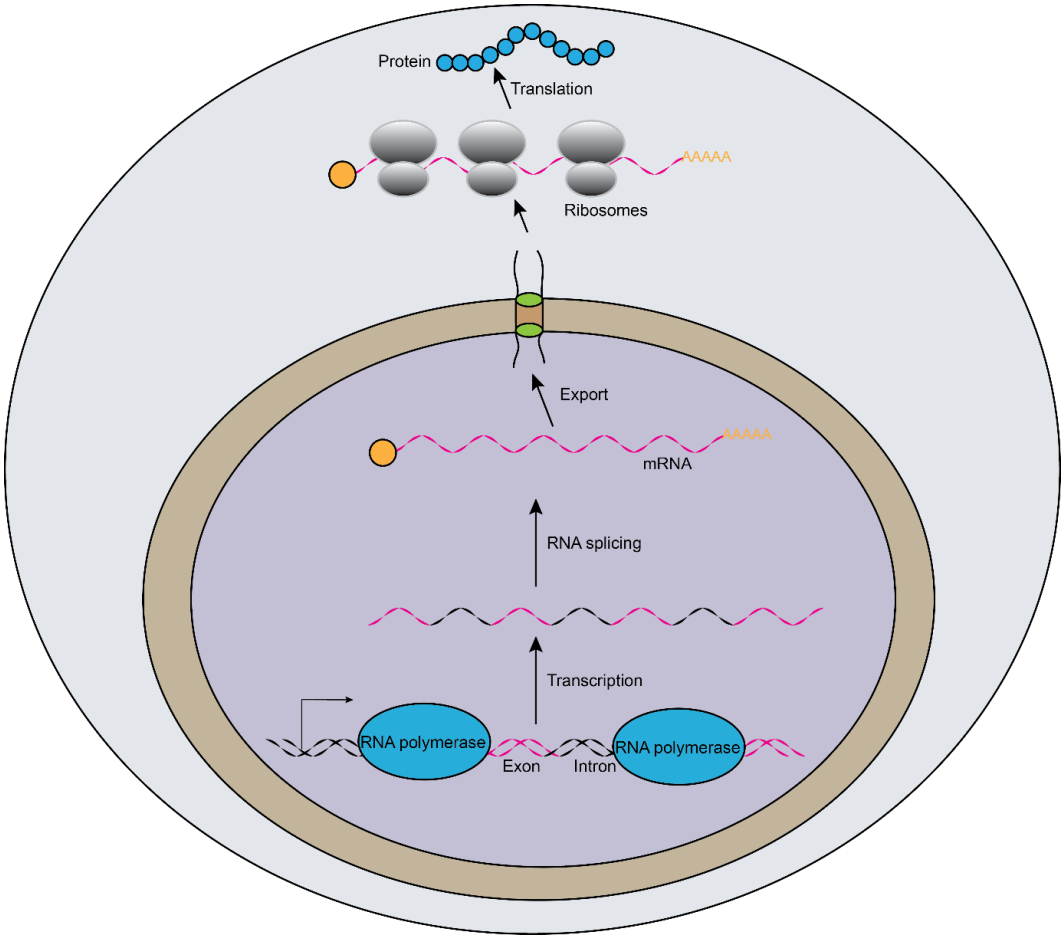

Figure 1. Outline of eukaryotic gene expression. Protein-coding genes are transcribed by RNA polymerase II in the nucleus. Following co-transcriptional pre-mRNA processing, the resulting mature mRNA, packaged into messenger ribonucleoprotein (mRNP) complexes, is exported through nuclear pore complexes (NPCs) to the cytoplasm. The mRNA is then used as a template by ribosomes to synthesize proteins.

1.2 Nonsense-mediated mRNA decay

Nonsense-mediated mRNA decay (NMD) is a conserved eukaryotic mRNA surveillance pathway where aberrant mRNAs carrying premature translation termination codons (PTCs) are recognised and degraded in a translation-dependent manner (Anders et al., 2003; Gonzalez et al., 2001; Holla et al., 2009; Kim et al., 2009; Metzstein and Krasnow, 2006). One role of NMD is probably to prevent translation of potentially toxic truncated proteins, but the NMD pathway has also been found to be involved in the general regulation of gene expression, affecting the stability of transcripts of genes without PTCs (Matia-Gonzalez et al., 2013; Rodriguez-Gabriel et al., 2006).

1.2.1 Sources of nonsense mRNAs

There are several sources of NMD substrates. Firstly, PTCs can result from three types of DNA mutations, including single base substitutions, insertions and deletions as well as chromosomal mutations. Substitution of a single nucleotide may change an amino acid codon into one of the stop codons (TAA, TAG, TGA). In addition, a piece of DNA deletion or addition, or chromosomal aberrations that alter the reading frame, may also account for the formation of premature stop codons. PTCs are also frequently produced during B lymphocyte maturation as a result of the somatic rearrangement of V, D, and J gene segments. In these processes, the addition of non-multiples of three nucleotides to the coding strand at the junctions of the segments leads to a non-productively rearranged allele that encodes PTC-containing transcripts (Muhlemann et al., 2008). As a result, those PTC-containing mRNAs become NMD targets, and efficiently degraded by NMD (Eberle et al., 2009). For example, there was significant reduction of the steady-state levels of PTC+ transcripts encoding immunoglobulin heavy and light

chains by NMD (Gudikote and Wilkinson, 2002). PTCs can also be introduced by transcription errors and alternative pre-mRNA splicing due to aberrant splicing (Lewis et al., 2003). Only 0.05% to 0.5% of all transcripts are estimated to acquire a PTC during transcription, based on the assumption that transcription error rate is 10^{-5} errors per nucleotide and a gene has 10^3 to 10^4 coding nucleotides (Cusack et al., 2011; Ninio, 1991).

1.2.2 NMD factors

NMD factors were initially identified in genetic screens in *Saccharomyces cerevisiae* and *Caenorhabditis elegans*. In *S. cerevisiae* they were identified as mutations that selectively stabilize mRNAs containing a premature translational termination signal. The screen was based on the use of a special strain which contains two mutations. One is *his4-38*, a +1 frameshift mutation near the 5' end of the *HIS4* transcript resulting in translational termination at an adjacent downstream stop codon (Leeds et al., 1991). Another is *SUFI-1* coding for a glycine tRNA frameshift suppressor that promotes a low level of read-through of the frameshift mutation via decoding a 4-base codon. The strains carrying both of these mutations confer a His^+ phenotype at 30 ℃, but are His^- at 37 ℃ (Leeds et al., 1991). Therefore, Up frameshift (*upf*) mutations were identified by selecting mutants which grew at 37 ℃, due to increased expression of the *his4* gene. The gene *upf1* was identified first using this method. Later, using the same genetic method a second gene, named *upf3* in *Saccharomyces cerevisiae*, was identified, due to a similar effect on nonsense mRNAs as *Upf1* (Leeds et al., 1992). Another yeast gene, *upf2/nmd2*, was found to be required for NMD at nearly the same time by two independent labs, either by investigating cellular factors that have specific interactions with the product of the *upf1* gene or by a genetic screen (Cui et al., 1995; He and Jacobson, 1995). In *C. elegans*, seven genes called *smg1* to *smg7* (suppressor with

morphogenetic effect on genitalia) are required for elimination of nonsense mRNA. The majority of *smg* mutations were originally identified in genetic screens as informational suppressors that affected specific mutations of different genes (Hodgkin et al., 1989). The essential role of *smg1* to *smg6* genes in NMD was thereafter demonstrated by analysing the stability of a number of mutant mRNAs of the *unc-54* gene encoding myosin heavy chain B (MHC B) in both *smg* mutants and wild-type cells (Pulak and Anderson, 1993). The quantity of nonsense mRNAs of *unc-54* increased in *smg* mutants compared to that in *smg* (+) genetic backgrounds suggesting the key role of SMG1 - SMG6 in rapid turnover of nonsense mRNAs (Pulak and Anderson, 1993). In addition, a new NMD factor named SMG7 in *C. elegans* was identified in a modified screen for *smg* mutants which avoided the isolation of additional alleles of *smg-1*, *smg-2*, or *smg-5* that accounted for nearly 90% of identified *smg* mutations (Cali et al., 1999).

The NMD factors are evolutionally conserved in different eukaryotic organisms. Orthologues of NMD factors SMG2-4 in *C. elegans* exist in both lower and higher eukaryotes. For example, SMG2, SMG3, and SMG4 from *C. elegans* are orthologues of *S. cerevisiae* Upf1, Upf2, and Upf3, respectively (Aronoff et al., 2001; Page et al., 1999; Serin et al., 2001). To date, all the orthologues for *C. elegans* NMD factors including SMGL-1 and SMGL-2 that were discovered by genome-wide RNA interference (RNAi) strategy are only present in mammals (Longman et al., 2007). Interestingly，unlike lower eukaryotic organisms (Table1), there are two mammalian Upf3 paralogs (Upf3a, Upf3b), one of which derives from the X chromosome (Upf3b) (Lykke-Andersen et al., 2000; Serin et al., 2001). These two Upf3 proteins are not expressed at the same levels in mammalian cells, since Upf3a expression is downregulated by Upf3b by destabilizing the Upf3a protein (Chan et al., 2009). Below is the table that summarizes the trans-acting factors involved in NMD from different

species (Table1). With the use of new bioinformatics tools and sequence comparisons, it is possible to reveal novel factors or orthologs of NMD factors already identified in other eukaryotic organisms.

Table 1. NMD factors from selected species

S. pombe	*S. cerevisiae*	*C. elegans*	*D. melanogaster*	Plants	Mammals
Upf1	Upf1	SMG2 (Upf1)	Upf1	Upf1	Upf1 (RENT1)
Upf2	Upf2	SMG3 (Upf2)	Upf2	Upf2	Upf2
Upf3	Upf3	SMG4 (Upf3)	Upf3	Upf3	Upf3a, Upf3b (Upf3X)
-	-	SMG1	SMG1	ND[a]	SMG1
-	-	SMG5	SMG5	ND[a]	SMG5
-	-	SMG6	SMG6	ND[a]	SMG6
-	-	SMG7	-	ND[a]	SMG7
-	-	SMG8	SMG8	-	SMG8
-	-	SMG9	SMG9	-	SMG9
-	-	SMGL-1	-	SMGL-1[b]	NAG (SMGL-1)
-	-	SMGL-2	SMGL-2b	-	DHX34 (SMGL-2)

[a] ND = not determined; [b] Role in NMD is not determined. (This table is modified from (Muhlemann et al., 2008), (Yamashita et al., 2009) and my unpublished work).

1.2.2.1 Upf proteins

Single, double or triple deletions of different combinations of yeast *upf1, upf2,* and *upf3* genes result in nearly the same abundance of unspliced *CYH2* transcripts, which contain an intron-encoded premature stop codon and are the target of NMD. This suggested that these three proteins may function as a complex (He et al., 1993). The interaction between Upf1， Upf2 and Upf3 was illustrated using a yeast two-hybrid system, and in human cells using a co-immunoprecipitation assay (He et al., 1997; He and Jacobson, 1995; Serin et al., 2001). During this interaction, Upf2 may serve as a bridge between Upf1 and Upf3, since interactions between Upf1 and Upf3 were not detected after the *upf2* gene in *S. cerevisiae* was deleted (He et al., 1997).

The amino acid sequences of Upf1, Upf2 and Upf3 were analysed in a variety of eukaryotic organisms and the sequence similarities are between 40.6-62.1% for Upf1, 16.8% to 34.2% for Upf2 and 11.4-25.5% for Upf3. Amino acid sequence comparison reveals that yeast Upf1, human Upf1 and other putative group I RNA helicases share seven helicase motifs (Applequist et al., 1997), but yeast and human Upf1 (HUpf1) have similar putative zinc finger motifs at their N-terminal ends, which are not present in other members of group I RNA helicases (Applequist et al., 1997). Sequence alignment of Upf1 in several eukaryotes revealed that this Zn finger-like region is enriched in cysteine and histidine amino acids, and interacts with Upf2 (He et al., 1997; Kadlec et al., 2006). The C-terminal region of Upf1 is rich in serine-glutamine clusters (SQ domain) which exist in higher eukaryotes but are absent in lower eukaryotic organisms such as yeast (Fiorini et al., 2013). In summary, the schematic representation of human Upf1 and yeast Upf1 domains are illustrated in Figure 2, based on sequence comparison (Applequist et al., 1997; Culbertson and Neeno-Eckwall, 2005; Imamachi et al., 2012; Kadlec et al., 2006). The putative RNA helicase activity and other

biochemical properties of the conserved Upf1 were demonstrated *in vitro* (Bhattacharya et al., 2000; Czaplinski et al., 1995). The ATPase activity of *S. cerevisiae* Upf1 was detected using a charcoal assay by incubating the purified protein in reaction mixtures with radiolabeled [γ-^{32}P]-ATP, in the presence or absence of nucleic acid (poly(rU)), and assaying the release of $^{32}PO_4$ (Czaplinski et al., 1995). This study showed that Upf1 ATPase activity is dependent on nucleic acid. Similar observations were made with HUpf1 (Bhattacharya et al., 2000). It also has 5' → 3' RNA and DNA helicase activities that were verified by a strand displacement assay (Bhattacharya et al., 2000; Czaplinski et al., 1995). Mutations in the helicase region of *S. cerevisiae* Upf1 abolished its ATPase activities and suppressed NMD (Weng et al., 1996). Furthermore, Upf1 has the ability to bind DNA or RNA，which was illustrated by a gel shift assay (Czaplinski et al., 1995); this binding activity appears to be regulated by ATP，since the presence of ATP resulted in the dissociation of the Upf1:RNA/DNA complex from one another (Bhattacharya et al., 2000; Czaplinski et al., 1995; Weng et al., 1996). However, binding of Upf1 is not affected by dysfunctions in its ATPase and helicase activities, caused by one missense mutation located in its ATP binding and hydrolysis motif (Weng et al., 1996). A single molecule of recombinant human Upf1 was recently demonstrated to be capable of travelling slowly over 10 kb of single-stranded nucleic acid, unwinding double-stranded nucleic acids and displacing the proteins associated with single-stranded nucleic acids (Fiorini et al., 2015). Immunological detection found yeast and mammalian Upf1 localized only in the cytoplasm, however, after treating HeLa cells with leptomycin B (LMB), a potent and specific protein nuclear export inhibitor in humans, it was also detected in the nucleus suggesting that this protein shuttles between the cytoplasm and the nucleus (Applequist et al., 1997; Atkin et al., 1995; Kudo et al., 1998; Mendell et al., 2002).

At least in *C. elegans* and human cells, Upf1 is phosphorylated, and its sequential phosphorylation and dephosphorylation are required for NMD (Ohnishi et al., 2003; Page et al., 1999). Genetic studies indicated that phosphorylation of SMG2 (Upf1) is regulated by SMG-1, SMG-3, and SMG-4, and its dephosphorylation are controlled by SMG-5, SMG-6, and SMG-7 in *C. elegans* (Page et al., 1999).

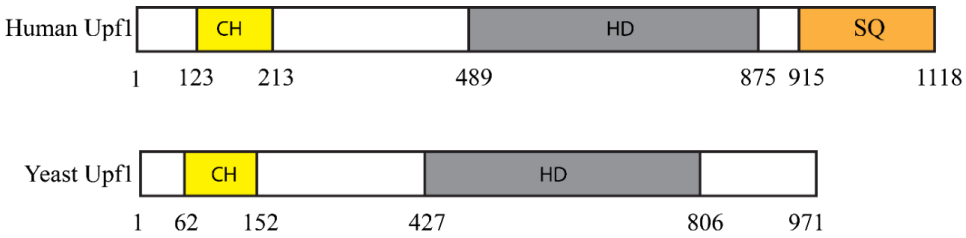

Figure 2. Schematic representation of human Upf1 and yeast Upf1 domain structure. The cysteine-histidine-rich (CH-rich) region is indicated by a yellow rectangle, the RNA helicase motifs by a grey rectangle and the serine-glutamine domain (SQ domain) by an orange rectangle (Applequist et al., 1997; Atkin et al., 1995; Kudo et al., 1998; Mendell et al., 2002).

The role of SMG-1 in the regulation of Upf1/SMG-2 phosphorylation was further investigated in human cells (Yamashita et al., 2001). In human cells, the kinase activity of hSMG-1, a human ortholog of *C. elegans* SMG-1, is required for HUpf1/SMG-2 phosphorylation and NMD (Yamashita et al., 2001). These conclusions were further supported by the observation that HUpf1 is phosphorylated by hSMG-1 both *in vivo* and *in vitro*. The degradation of PTC containing β-globin mRNA was significantly suppressed by the overexpression of a kinase-deficient point mutant of hSMG-1, but enhanced by that of wild-type hSMG-1 (Yamashita et al., 2001). The importance of the SMG-1 kinase activity and SMG-2 phosphorylation in NMD was also demonstrated in *C. elegans* (Grimson et al., 2004). Phosphorylated HUpf1 (P-HUpf1) associates with hSMG-5 and hSMG-7, which are human homologs of *C. elegans* SMG-5 and SMG-7, respectively, as well as protein phosphatase 2A (PP2A). It is suggested that this association process contributes to the dephosphorylation of HUpf1 and the NMD process, since failure of P-HUpf1 dephosphorylation suppresses NMD, due to overexpression of hSMG-5 mutants that preserve the ability to interact with P-HUpf1 but cannot induce its dephosphorylation (Ohnishi et al., 2003).

Table 2. Pairwise amino acid sequence identities for Upf1 proteins from selected eukaryotic organisms*.

	S. pombe			*S. cerevisiae*			*C. elegans*			*D. melanogaster*			*A. thaliana*		
	Upf1	Upf2	Upf3	Upf1	Upf2	Upf3	Upf1	Upf2	Upf3	Upf1	Upf2	Upf3	Upf1	Upf2	Upf3
S. cerevisiae	49.9	19.7	18.7												
C. elegans	46.4	17.8	18.7	40.6	16.8	11.4									
D. melanogaster	50.6	21.2	25.5	46.2	18.2	15.2	44.6	25.1	21.5						
A. thaliana	51.6	22.7	20.1	48.2	22.0	14.7	45.0	21.9	19.6	49.8	26.3	17.8			
H. sapiens	53.4	21.4	21.9	48.4	21.8	17.1	47.5	26.3	23.9	62.1	34.2	25.4	57.3	33.7	21.2

*The percent identities were derived from alignments of full-length sequences.

Although the Upf2 protein is less conserved than Upf1, it has some conserved structural features, inferred from sequence analysis, and can interact with both Upf1 and Upf3. In yeast, Upf2 contains highly acidic regions and a putative nuclear localization signal at the amino terminus of the protein; these were also identified in its homologues in fission yeast and humans (He and Jacobson, 1995; Mendell et al., 2000).The Upf1- and Upf3-interacting domains of Upf2 in yeast were defined using the yeast two-hybrid system. The 157-amino acid C-terminal region of Upf2 interacts with Upf1, whereas distinct domains of Upf2 are responsible for its interaction with Upf3 (He et al., 1996, 1997). The interaction of HUpf2 (human Upf2) with HUpf1, HUpf3 (human Upf3a) and HUpf3-X (human Upf3b) was also confirmed using immunoprecipitation of epitope-tagged Upf proteins transiently expressed in HeLa cells (Serin et al., 2001). In addition, Upf2 subcellular localization was investigated. Transiently expressed HUpf2 in HeLa cells was primarily identified as cytoplasmic by indirect immunofluorescence, even in the presence of leptomycin B which inhibits nuclear export (Mendell et al., 2000; Serin et al., 2001). The cytoplasmic distribution pattern of Upf2 was also revealed in living fission yeast cells by visualising yellow fluorescent protein (YFP) tagged Upf2 via fluorescence microscopy (Matsuyama et al., 2006). However, GFP tagged Upf2, which was expressed under the control of cauliflower mosaic virus 35S promoter, was localized in both the nucleolus and cytoplasm in *Arabidopsis* (Kim et al., 2009). Another biochemical property of Upf2 is that, like Upf1, it is a phosphoprotein, proven in yeast using an in-vivo labelling experiment, and in human HEK293T cells using two-dimensional gel analysis (Chiu et al., 2003; Wang et al., 2006).

As another NMD key factor，the subcellular localization and role in the NMD pathway of Upf3 were also studied in all tested eukaryotic organisms. Transiently expressed HUpf3-X in HeLa cells is primarily identified as nuclear and shuttles between nucleus

and cytoplasm as detected using indirect immunofluorescence (Serin et al., 2001). Overexpressed Upf3 in *S. cerevisiae* also shuttles between nucleus and cytoplasm, as opposed to the primarily cytoplasmic localization when expressed eightfold less from a centrometric plasmid, suggesting that the nucleolar distribution pattern may be due to abnormal intracellular accumulation (Shirley et al., 1998). One piece of evidence supporting this argument is that when GFP fused Upf3 is expressed in *S. cerevisiae*, using its endogenous promoter, it localizes to the cytoplasm (Mitchell et al., 2013). In addition to the investigation of Upf3 subcellular localization, other biochemical properties were studied. Firstly, using the yeast two-hybrid system, Upf3 was found to directly interact with Upf2, and its interaction with Upf1 is dependent on this interaction with Upf2 (He et al., 1997). The interaction among human Upf proteins was confirmed by coimmunoprecipitation of HUpf proteins (HUpf1, HUpf2, HUpf3a and HUpf3b) from HeLa cell extracts using anti-human Upf antibodies, and by GST pull-down assays (Kadlec et al., 2004; Lykke-Andersen et al., 2000). Secondly, the RNA binding activity of Upf3 was also studied in both human and yeast cells. The expressed human Upf3b construct, comprising a ribonucleoprotein-type RNA-binding domain (RNP domain), does not bind a non-specific single-stranded RNA probe using the gel-mobility assay, whereas Upf3 was identified to be associated with mRNA in a global identification of *Saccharomyces cerevisiae* mRNA-binding proteins (RBPs) by *in vivo* capture of RBPs (Kadlec et al., 2004; Mitchell et al., 2013). Finally, human Upf3 protein was identified to specifically bind spliced mRNA *in vivo* by using an hUpf3-RNA coimmunoprecipitation assay, and directly interacts with Y14, which is one of the key factors of exon-exon junction complex (described below), suggesting the functional link between NMD and splicing (Kim et al., 2001b; Le Hir et al., 2001; Le Hir et al., 2000; Lykke-Andersen et al., 2000).

1.2.3 Proposed NMD mechanisms

Although the NMD mechanism may vary from lower to higher eukaryotes, one of the shared features for NMD is its dependence on translation, based on several lines of evidence: (1) Yeast *CPA1* mRNA, which encodes the small subunit of arginine-specific carbamoyl phosphate synthetase, contains an upstream open reading frame (uORF). This uORF induced the downregulation of the transcripts of a *CPA1-LUC* chimeric reporter, due to NMD taking place in the presence of arginine, whereas the mutated D13N uORF, which abolishes the stalling of ribosomes, did not. After the initiation context was improved, the D13N uORF transcripts were more sensitive to NMD suggesting the importance of ribosome occupancy of the yeast *CPA1* uORF on the modulation of NMD (Gaba et al., 2005). (2) In yeast, the nonsense transcripts of *ade2-1*, an allele of the *ADE2* gene, were separated predominantly with the polysome fractions, and targeted for NMD, suggesting the active role of translation on NMD (Maderazo et al., 2003). (3) Yeast eIF4E is a eukaryotic translation initiation factor and eIF4E-bound nonsense RNAs were degraded by NMD but stabilized when cells were treated with the translational inhibitor cycloheximide (CHX) (Gao et al., 2005). (4) In HeLa cells, the β-globin mRNA decay triggered by transiently expressed human Upf1/2/3 proteins was also inhibited by cycloheximide (Lykke-Andersen et al., 2000). (5) In mammalian cells, CBP80 is a component of the nuclear cap binding complex that binds nascent RNA，and is involved in nuclear RNA processes (Lejeune et al., 2002). Ishigaki and co-workers found that nonsense-containing β-Globin (*GI*) was immunopurified using anti-CBP80 specific antibody, and was then targeted for NMD; this process could be blocked when translation was inhibited by cycloheximide, or disturbed by a suppressor tRNA, which inserts the amino acid serine at the nonsense codon of nonsense-containing *GI* mRNA (Ishigaki et al., 2001). Furthermore,

downregulation of CBP80 by siRNA inhibits NMD but not Staufen1 (Stau1)-mediated mRNA decay (SMD), which also requires Upf1 but is different from the NMD process (Hosoda et al., 2005). (6) The NMD factors Upf1, Upf2 and Upf3 were detected in mammalian cells in mRNP complexes immunopurified using an anti-CBP80 antibody, even though the association of Upf2 and Upf3 with CBP80 is dependent on RNA, while that of Upf1 may be not (Hosoda et al., 2005; Ishigaki et al., 2001). The interaction of Upf1 and Upf2 could be enhanced by CBP80 mediated translation, since when CBP80 was significantly downregulated by siRNA, transiently expressed Upf1 was not detected with immunopurified Upf2 (Hosoda et al., 2005). Combining these observations with the findings that Upf proteins were not detected in eIF4E associated mRNPs and that there was comparable NMD efficiency for nonsense codon containing mRNAs bound by CBP80 and eIF4E in mammalian cells, it was therefore proposed that NMD is dependent on a pioneer round of translation initiated on mRNAs associated with the cap-binding complex (Ishigaki et al., 2001). However, recent research showed that in human cells, eIF4E-associated nonsense codon containing mRNAs were not immune to NMD, but were in fact subjected to NMD (Durand and Lykke-Andersen, 2013; Rufener and Muhlemann, 2013). One clue is that, using an efficient method of isolating mRNPs, human Upf1 copurified with eIF4E in an RNA-dependent manner (Rufener and Muhlemann, 2013). More importantly, mRNA decay assays revealed that in human cells eIF4E-bound NMD substrates degraded as efficiently as those associated with CBP80, and that NMD can also act on nonsense codon containing RNA after translation inhibition was released by the removal of puromycin, a drug which releases ribosomes during the translation elongation step, resulting in repeated cycles of ribosome initiation (Durand and Lykke-Andersen, 2013; Rufener and Muhlemann, 2013). This evidence showed that NMD can also happen during eIF4F-dependent

translation in mammalian cells, make it possible that NMD is dependent on each round of aberrant translation in both lower and higher eukaryotes. In addition to the translation-dependent features of NMD, Upf1 in human cells was further shown to bind to both the coding-sequence regions (CDS) and 3′untranslated region (UTR) of mRNAs before translation, but was redistributed to 3′ UTRs during active translation, as observed by individual-nucleotide-resolution UV cross-linking and immunoprecipitation experiments. This suggested translation-independent binding of Upf1 to RNA, and its displacement from the CDS by translating ribosomes (Zund et al., 2013). The CH domain of Upf1 in yeast was demonstrated to interact with Rps26 of the 40S ribosomal subunit, indicating its possible function in dissociation of the premature termination complex in the NMD process (Min et al., 2013).

In mammalian cells, the exon-exon junction complex (EJC), which is a multiprotein complex deposited ~20 nucleotides upstream of the exon-exon junctions on spliced mRNAs, is also involved in NMD (Kim et al., 2001a; Kim et al., 2001b; Le Hir et al., 2000). Originally, endogenous Upf2 and Upf3 proteins in *Xenopus laevis* oocytes were identified, by coimmunoprecipitation, as associating with spliced mRNAs, upon which the EJC had also been deposited (Le Hir et al., 2001). Around the same time, Kim and co-workers found that the two forms of transiently expressed Upf3 were coimmunoprecipitated with Y14, one of the EJC key factors (Kim et al., 2001a). In addition, like the EJC complex, the binding site of Upf3 on spliced mRNAs was also mapped to be ~20 nucleotides upstream of the exon-exon junctions, using an RNase H footprinting assay (Kim et al., 2001a; Kim et al., 2001b; Le Hir et al., 2000). Thus, these results provided a link between splicing and NMD (Kim et al., 2001a; Kim et al., 2001b; Le Hir et al., 2001; Le Hir et al., 2000). Y14 was subsequently demonstrated to be required for NMD (Gehring et al., 2003): (1) Endogenous Y14 copurified with

transiently expressed FLAG-tagged hUpf3b. (2) Functional tethering of λN-Y14 fusion protein to the β-globin 5boxB reporter, which is an NMD substrate, resulted in a significant reduction of reporter mRNA abundance. (3) Knockdown of Y14 stabilized both the mRNA of β-globin 5boxB reporter in a hUpf3b tethering assay, and a PTC-containing NMD substrate.

Given the above findings, two PTC recognition models have been proposed. One is the faux 3' UTR model, based on observations of NMD in yeast, another is the exon junction complex (EJC) model (Brogna and Wen, 2009; Celik et al., 2015; Min et al., 2013; Zund et al., 2013). However, neither can fully explain the discrimination of nonsense codons from natural stop codons. The faux 3' UTR model suggests the importance of the 3' UTR in translation termination events. Translation termination of mRNA with normal stop codons is efficient because this event happens close to the poly (A) tail where associated poly (A)-binding protein interacts with peptide-release factor eRF3. However, the unconventional 3' UTR is distal to a premature terminator, thus a terminating ribosome cannot interact with poly (A)-binding protein, and instead associates with NMD factors. This defective termination fails to release a terminating ribosome effectively, thus stimulating mRNA decay (Amrani et al., 2004). The EJC model indicates that if a premature termination codon is ahead of at least one exon-exon junction, it is generally recognised as aberrant and then becomes the target of NMD (Le Hir et al., 2001). Interestingly, some studies showed that the EJC seemed to not be essential for NMD. In *Drosophila* cells, depletion of some EJC proteins did not result in the stabilization of the mRNA of the NMD reporter (Gatfield et al., 2003). Figure 3 summarizes the current NMD models in eukaryotes. Although NMD has evolved as a RNA surveillance mechanism in all tested eukaryotes, the detailed pathway of it may differ between different metazoans.

A

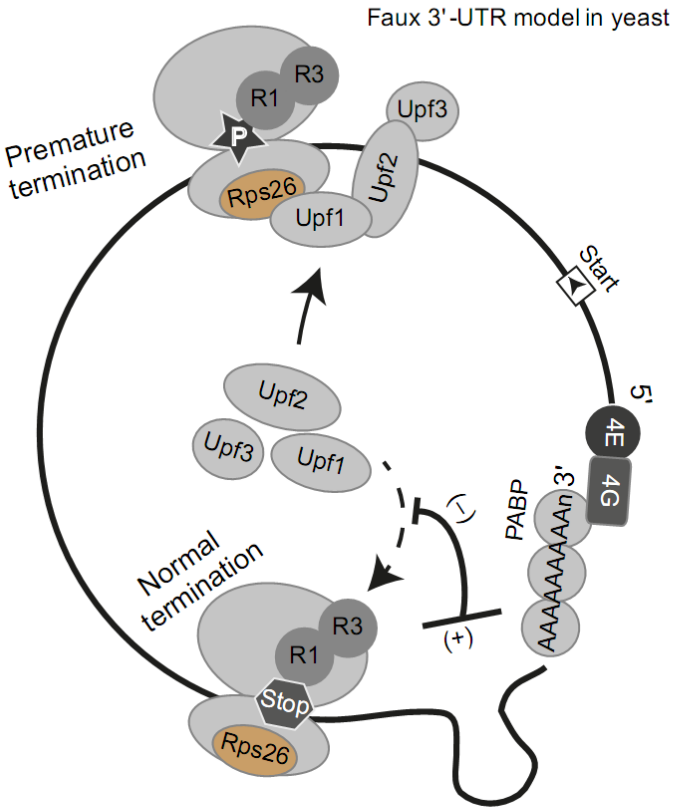
Faux 3'-UTR model in yeast
Premature termination
R3
R1
P
Upf3
Upf2
Rps26
Upf1
Start
5'
4E
4G
PABP
3'
AAAAAAAAAn
Upf2
Upf3
Upf1
(-)
(+)
Normal termination
R3
R1
Stop
Rps26

B

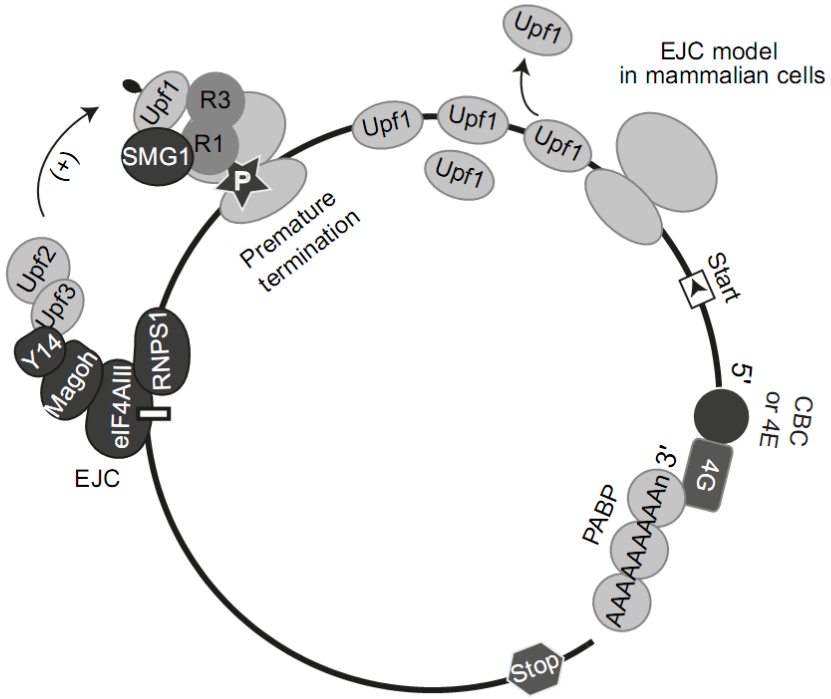
EJC model in mammalian cells
Upf1
Upf1
Upf1
Upf1
Upf1
Upf1
R3
R1
SMG1
P
(+)
Premature termination
Upf2
Upf3
Y14
Magoh
eIF4AIII
RNPS1
EJC
Start
5'
CBC or 4E
4G
PABP
3'
AAAAAAAAAn
Stop

Figure 3. NMD mechanisms. (A) The modified false 3′ UTR model. Efficient translation termination happens since poly (A) binding protein (PABP) can bind peptide-release factor eRF3 (R3) which interacts with the terminating ribosome. Premature translation termination takes place since the terminating ribosome fails to bind PABP resulting in the recruitment of NMD factors. The interaction of Upf1 with Rps26 may aid the dissociation of the termination complex. R1 denotes peptide-release factor eRF1; 4E and 4G stand for eIF4E and eIF4G, respectively. (B) The modified EJC model. During initial translation or translational elongation steps, translating ribosome removes Upf1 which binds to coding sequencing region (CDS). When a translating ribosome comes across a premature stop codon (PTC), NMD is triggered if this occurs upstream of an EJC, by activating or recruiting NMD factors on the terminating or post-termination ribosome. The black dot represents phosphorylation of Upf1. EJC constituents are also shown in the figure. The cap binding complex is indicated by CBC. This picture was modified based on (Brogna and Wen, 2009; Celik et al., 2015; Min et al., 2013; Zund et al., 2013).

1.3 Upf1 additional functions

1.3.1 Upf1 is required for replication-dependent histone mRNA degradation

In eukaryotic cells, the rates of histone and DNA synthesis are tightly coordinated. Suppression of histone gene expression causes DNA damage and inhibits DNA replication. Likewise, inhibition of DNA synthesis leads to a decrease of histone synthesis as a result of the rapid degradation of histone mRNA in mammalian cells (Kaygun and Marzluff, 2005). Upf1 was revealed to have a role in histone mRNA degradation, as siRNA-mediated knockdown of Upf1 stabilized histone H2a mRNA upon hydroxyurea (HU) treatment, which inhibits DNA replication by depleting dNTP pools (Kaygun and Marzluff, 2005). The role of Upf1 in the degradation of histone H2a mRNA may be independent of NMD, since downregulation of Upf2 by siRNA did not stabilize histone H2a mRNA (Kaygun and Marzluff, 2005). Metazoan replication-dependent histone mRNAs are mainly produced during S-phase in somatic cells and are the only eukaryotic mRNAs that are not polyadenylated (Marzluff et al., 2008). However, they have an RNA stem-loop structure which is close to the 3' end of the mature RNA, which is bound by the stem-loop binding protein, SLBP (Martin et al., 1997; Wang et al., 1996). SLBP is involved in histone pre-mRNA processing and mRNA translation (Marzluff et al., 2008). SLBP coimmunoprecipitated with Upf1, but not Upf2, in an RNase insensitive way and this interaction was enhanced by HU treatment, suggesting that Upf1 may have a direct role in the regulation of histone mRNA degradation instead of regulating expression of some other proteins participating in histone mRNA degradation (Kaygun and Marzluff, 2005). Recently, hyperphosphorylation of Upf1 by activated ATR (an important factor for regulating the DNA damage checkpoint pathway during replication stress) and DNA-dependent protein kinase upon the inhibition of DNA synthesis, was shown to play important roles

in histone mRNA degradation (Choe et al., 2014). Hyperphosphorylated Upf1 interacted more strongly with SLBP, which stimulated the release of cap-binding complex (CBC)-dependent translation initiation factor (CTIF) and eukaryotic initiation factor 3 complex (eIF3) from SLBP-containing histone mRNPs. The consequence was the translational suppression of histone mRNAs (Choe et al., 2014). In addition, coimmunoprecipitation studies showed that the association of SLBP with the proline-rich nuclear receptor coregulatory protein 2 (PNCR2), SMG5 and mRNA-decapping enzyme 1A (DCP1A), also depended on Upf1 phosphorylation, consequently directing histone mRNAs towards rapid degradation (Choe et al., 2014; Muller et al., 2007).

1.3.2 Upf1 is involved in Staufen-mediated mRNA decay (SMD)

Human Upf1 is required for SMD in a translation-dependent, but NMD independent, manner. The SMD process was firstly characterized to involve STAU1, a double-stranded RNA (dsRNA)-binding protein, HUpf1 and a termination codon (Kim et al., 2005). The NMD-independent role of Upf1 in SMD comes from experimental evidence showing that mRNA decay, induced by tethering MS2-fused STAU1 to an MS2 coat protein-binding site that was located downstream of a termination codon, was suppressed by siRNA-mediated downregulation of Upf1 but not by either of the other NMD factors, Upf2 and Upf3X (Kim et al., 2005). The inhibition of SMD by a cycloheximide-mediated block in translation suggests that the SMD pathway depends on translation.

The natural SMD substrates and the features of the STAU1-binding site (SBS) of the 3’UTR were also investigated. A region of around 230 nucleotides within the 3'UTR of ADP ribosylation factor 1 (ARF1) mRNA, an SMD target, has been identified as a STAU1-binding site (Brognard et al.; Kim et al., 2005). The STAU1-binding site of

ARF1 mRNA that is critical for STAU1 binding was subsequently delimited to a 19-base-pair stem with a 100-nucleotide apex via generating sets of deletions, and analysis of the folded secondary structure using RNAfold (Kim et al., 2007). The importance of the predicted stem structure for STAU1 binding, which is conserved among *Homo sapiens*, *Mus musculus* and *Rattus norvegicus*, was verified using a series of deletion and point-mutation constructs (Kim et al., 2007). Although some other SMD targets, including plasminogen activator inhibitor type 1 (SERPINE1) mRNA, were revealed and verified, their 3'UTRs do not contain comparable stem structures as predicted by RNAfold (Kim et al., 2007). However, several SMD targets such as SERPINE1 mRNA contain Alu elements, which are short interspersed and the most abundant repetitive elements in human genome, in their 3'UTR. The 3'UTR Alu element of an SMD substrate could partially base-pair with another Alu element-containing cytoplasmic and polyadenylated long noncoding RNA (lncRNA), thus forming an intermolecular STAU1-binding site required by SMD (Gong and Maquat, 2011). Furthermore, a subset of SMD targets can be downregulated by the same individual lncRNAs, and the same SMD target can be downregulated by different lncRNAs, suggesting the complex and regulatory mechanisms controlled by lncRNA-mRNA duplexes (Gong and Maquat, 2011).

STAU2, which is the paralog of STAU1, was also shown to directly interact with Upf1 and to be involved in SMD (Park et al., 2013). Furthermore, immunopurification revealed the formation of STAU1-STAU1, STAU1-STAU2 and STAU2-STAU2 complexes *in vitro* and *in vivo*; in other words, STAU1 and STAU2 paralogs associate with themselves and with one another. Moreover, Park and co-workers demonstrated that the reduction in mRNA abundance due to tethering siRNA-resistant STAU2 or STAU1 to an mRNA 3'UTR is blocked by downregulation of the cellular levels of

STAU1, STAU2, or Upf1 (Park et al., 2013). Taken together, it is more likely that STAU1 and/or STAU2 form homo-dimers or hetero-dimers, if not multimers, that bind to the STAU-binding site of the 3'UTR that can be formed by either intramolecular or intermolecular base-pairing. These then recruit and activate Upf1 and therefore induce SMD, if the STAU1-binding site resides sufficiently downstream of a termination codon so that bound STAU1 and/or STAU2 cannot be removed by the terminating ribosome during translation (Park et al., 2013; Park and Maquat, 2013).

1.3.3 Upf1 is involved in GR-mediated mRNA decay (GMD) in a translation-independent manner

Upf1 is shown to play an important role in GMD, which is not dependent on NMD or translation. The glucocorticoid receptor (GR) belongs to the nuclear receptor superfamily and functions as a transcription factor in the regulation of various physiological processes including inflammation and cell proliferation (Cho et al., 2015). Apart from these known functions, it is required for the rapid degradation of selected mRNAs. When HeLa cells were treated with a potent synthetic glucocorticoid, the GMD process occurs during which Upf1 promotes the interaction between the proline-rich nuclear receptor coregulatory protein 2 (PNRC2) and GR bound to the target mRNA such as chemokine (C-C motif) ligand 2 mRNA. In addition, the helicase activity of Upf1 was suggested to be involved in efficient GMD, because the inhibition of GMD of an mRNA substrate as a consequence of Upf1 downregulation by siRNA was significantly reversed by expression of siRNA-resistant Upf1-WT but not of its R843C variant which contains defects in the helicase activity (Cho et al., 2015).

Upf1-dependent GMD is mechanistically distinct from NMD and SMD. The first evidence came from the immunoprecipitation experiments which showed that GR

associated with Upf1 but not Upf2, Upf3 and Stau1 which is essential for SMD (Cho et al., 2015). Besides, knockdown of Upf1 but not Upf2 and Upf3X by siRNA significantly increased the mRNA levels of all tested endogenous GMD substrates (Cho et al., 2015). Unlike NMD and SMD which are coupled to translation, GMD is independent of translation because insertion of a stem-loop structure into the 5' UTR of GMD reporters drastically blocked their translation efficiency without disrupting their degradation efficiency by GMD, compared to the control GMD reporters not containing the SL structure (Cho et al., 2015). Thus, the data provided by the Kim laboratory presents a novel mRNA decay pathway (GMD) that requires participation of Upf1.

1.3.4 Upf1 functions in DNA replication or repair

In mammalian cells Upf1 has a direct role in DNA replication which is not dependent on NMD. Early studies revealed that delta helicase purified from fetal bovine thymus, which is the bovine homolog of human Upf1, co-purifies with DNA polymerase delta by immunoprecipitations, suggesting that Upf1 may take part in the DNA replication activities (Carastro et al., 2002). Knockdown of human Upf1 by short hairpin RNAs (shRNAs) resulted in DNA damage responses which were illustrated by the accumulation of the DNA damage marker ɣ-H2AX foci, in an ATR dependent manner (Azzalin and Lingner, 2006). Experimental evidence showed that Upf1 associated with chromatin and it was most enriched during S phase and upon γ irradiation in an ATR dependent manner, suggesting the direct role of Upf1 in DNA synthesis activities (Azzalin and Lingner, 2006). Furthermore, depletion of Upf1 in human cells caused significant increase in the total amount of both chromatid and chromosome breaks during metaphase. However, shRNA-mediated depletion of Upf2 did not significantly increase the levels of ɣ-H2AX as assayed by Western blotting; endogenous Upf2 did

not immunoprecipitate with DNA polymerase delta. These results suggested that human Upf1 plays an important role in DNA replication or repair which may be distinct from its role in NMD (Azzalin and Lingner, 2006).

Following the finding that human Upf1 is required for maintaining genome stability, Azzalin and co-workers showed that Upf1 binds telomeres *in vivo* (Chawla et al., 2011). Depletion of Upf1 leads to telomeric aberrations which include the absence of telomere and enrichment of telomeric repeat-containing RNA (TERRA) that is transcribed by RNA polymerase II (RNAPII) from several subtelomeric regions towards chromosome ends (Azzalin et al., 2007). Chawla and co-workers demonstrated that the enrichment of human Upf1 at telomeres was not only mediated by ATR but also by the length of telomere (Chawla et al., 2011). In addition, Upf1 associates with human telomerase reverse transcriptase (hTERT) and shelterin factor TPP1, and this association is not dependent on a nucleic acid, because it was not disrupted by the treatment of DNase I, RNase A or both (Chawla et al., 2011). Chromosome-orientation fluorescence *in situ* hybridization (CO-FISH) experiments further demonstrated that ATPase activity of Upf1 is required for maintaining the integrity of telomeres, predominantly by sustaining telomere leading-strand replication (Chawla et al., 2011). Although these discoveries suggest a direct role of Upf1 in maintaining the telomere replication, it is still not clear how Upf1 is recruited to the telomeric loci and whether Upf1 functions are restricted solely to telomere integrity preservation or whether Upf1 has a general role in securing the correct replication of several specific DNA loci.

1.4 Sources of DNA damage

DNA damage can be caused by both exogenous factors and cell metabolic processes that can either alter the DNA sequence directly or cause mutation when DNA is not faithfully repaired.

There are many exogenous mutagens accounting for DNA instability through different mechanisms. One of them is ultraviolet (UV) radiation which causes DNA damage (Sinha and Hader, 2002). The solar UV spectrum is, according to the wavelength (λ), classified into UVC (λ< 280 nm), UVB (λ<290–320 nm), and UVA (λ > 320–400 nm) (Pfeifer and Besaratinia, 2012). Dimerization of pyrimidines is the most abundant form of DNA lesions induced by UVB or UVC irradiation. As a result, the major DNA damage products - *cis-syn* cyclobutane pyrimidine dimers (CPDs) and pyrimidine (6-4) pyrimidone photoproducts [(6–4) photoproducts; (6-4)PPs] - are formed, in addition to other minor DNA damage base products (Pfeifer and Besaratinia, 2012). Although UVA can induce secondary photoreactions of existing DNA photoproducts or create DNA lesions through indirect photosensitizing, it is less efficient in causing DNA damage because it is not absorbed by native DNA (Sinha and Hader, 2002). In addition, ionizing radiation such as X-rays, γ-rays, and alpha particles, causes single strand breaks, double strand breaks (DSB), base damage and DNA-protein cross-links in the genomic DNA (Su et al., 2010). Heat shock, which represents the exposure of a whole organism (or particular cells) to an abnormally high environmental temperature, is another well-known exogenous stress factor that affects DNA integrity and DNA replication process (Mortensen et al., 2009; Velichko et al., 2012). Anthropogenic mutagenic chemicals can also lead to genomic instability via different mechanisms (Lord and Ashworth, 2012). For example, hydroxyurea inhibits the activity of the enzyme ribonucleotide reductase which causes reduced production of

deoxyribonucleotides. After prolonged drug treatment this chemical gradually inactivates DNA replication forks (Petermann et al., 2010; Poli et al., 2012).

Endogenous processes can also disrupt genome integrity. There are two types of elements contributing to DNA damage: the ones that act *in trans* to affect genome integrity, for instance, replication, repair and S phase checkpoint factors; the second type is represented by DNA sequences that are either highly transcribed. This leads to increased recombination frequency or fragile sites where, after partial inhibition of DNA synthesis, gaps and breaks occur on metaphase chromosomes (Aguilera and Gomez-Gonzalez, 2008). DNA damage can also arise from other factors, for example, cellular metabolism which generates reactive oxygen species that can oxidize DNA bases and cause single-strand breaks (SSBs). Likewise, DNA replication errors, because of deoxyribonucleoside 5´-triphosphate (dNTP) disincorporation, are potentially mutagenic and deleterious to DNA stability.

1.5 DNA damage repair

To counteract deleterious effects of DNA damage and maintain genomic integrity, different cellular DNA damage repair pathways have evolved based on the types of DNA lesions. These pathways include base excision repair, mismatch repair, nucleotide excision repair as well as double-strand break repair including homologous recombination (HR) and non-homologous end-joining (NHEJ).

DNA double-strand break repair mechanisms will be discussed in detail because double-strand DNA breaks (DSBs) are the most deleterious form of DNA damage (Papamichos-Chronakis and Peterson, 2013). DSB repair predominantly happens by means of homologous recombination in S and G2 phases of the cell cycle where a homologous DNA duplex, that originates from a sister chromatid, can be used as a

donor template for DNA-synthesis-dependent and error-free repair. However, the NHEJ pathway mostly occurs in G1 phase of the cell cycle and is the main mechanism of DNA repair in most mammalian cells, since they are predominantly in G1 phase (Papamichos-Chronakis and Peterson, 2013). By contrast, HR is the principal pathway in repairing DNA double-strand breaks in budding and fission yeast, as NHEJ mutants are insensitive to γ-radiation that causes DNA double-strand breaks, whereas HR mutants are hyper-sensitive to γ-radiation(Manolis et al., 2001; Siede et al., 1996). During NHEJ the ends of broken DNA are processed and re-ligated by relevant repair factors recruited to the damaged sites, resulting in either an error-free or error-prone repair. Major factors involved in these two DSBs repair pathways, as well as further details of how these processes are carried out, are shown in Figure 4.

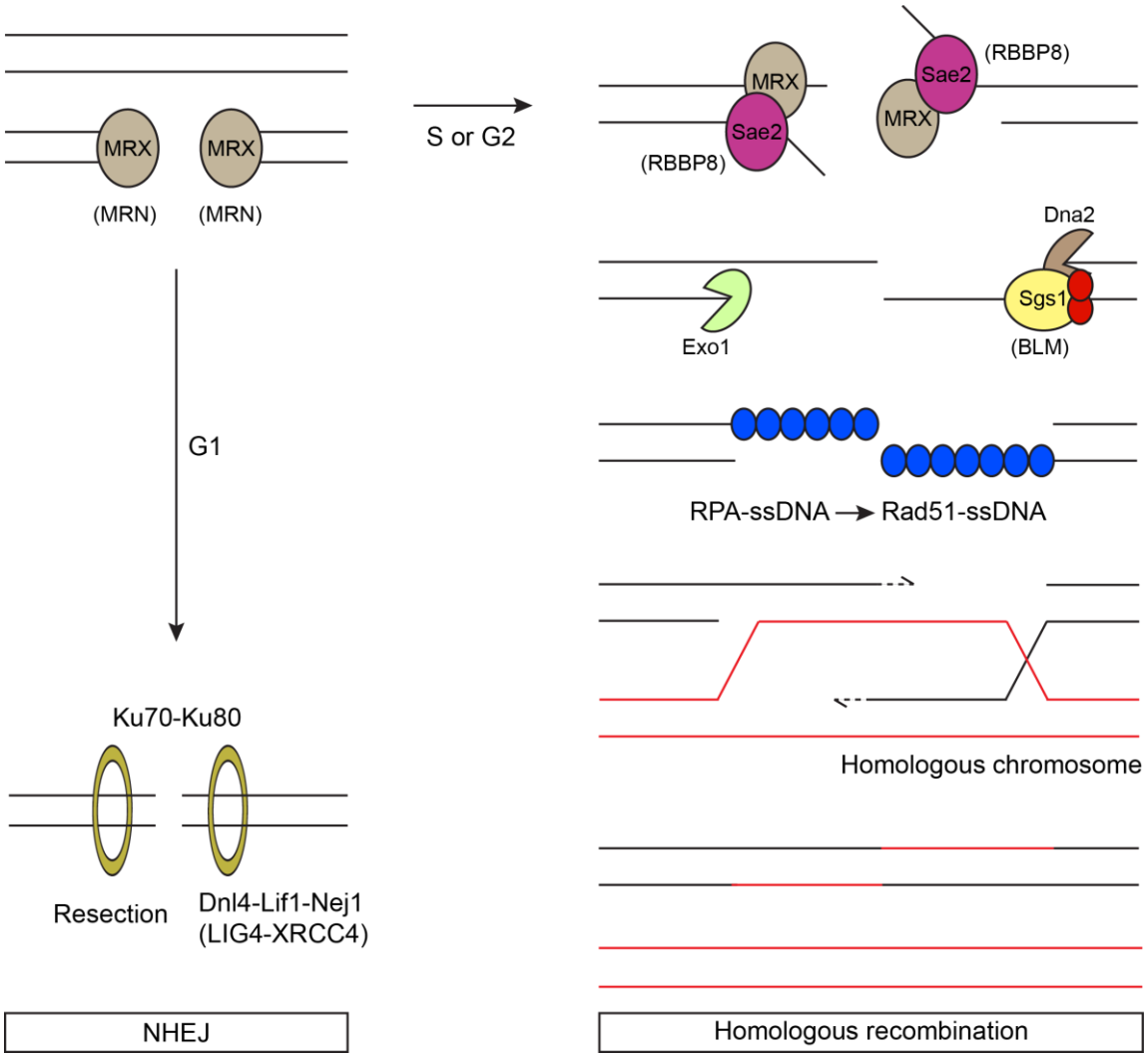

Figure 4. Two major pathways for double-strand DNA break repair.

Generated double-strand DNA breaks (DSB) are firstly bound by yeast Mre11–Rad50–Xrs2 (MRX) or human MRE11–RAD50–NBS1 (MRN) complex. Repair of the DSB formed in the G1 phase of the cell cycle is predominantly carried out by the non-homologous end-joining (NHEJ) pathway (left panel). During this process, recruitment of the Ku heterodimer (Ku70–Ku80) prevents extensive processing of the DSB by nucleases and further stimulates ligation of the DSB by the Dnl4–Lif1–Nej1 complex in budding yeast and the LIG4-XRCC4 factors in mammalian cells. By contrast, the homologous recombination repair pathway is initiated to repair the DSBs generated in

the S or G2 cell cycle phase (right panel). Fundamental steps of effective repair by homologous recombination include: initial processing of 5’ ends of the broken dsDNA into 3’ single-stranded tails by the yeast MRX complex and Sae2 enzyme (known as RBBP8 or CTIP in mammalian cells); further trimming by either exodeoxyribonuclease 1 (Exo1) or Dna2-Sgs1 DNA-end-processing enzymes (the human Bloom's syndrome protein (BLM) helicase is the homologue of yeast Sgs1); binding of the recombination protein A (RPA) to the ssDNA overhang that is subsequently replaced by Rad51 protein; effective tracking of homology and formation of heteroduplex DNA; DNA synthesis using the 3’ end of the broken DNA as the DNA replication template, resolution of the heteroduplex or a double-sided Holliday junction; final ligation of the ssDNA nicks. Protein or complex names shown in brackets in the figure are human homologues. The picture is adapted and modified from (Papamichos-Chronakis and Peterson, 2013).

1.6 *Schizosaccharomyces pombe* as a model organism

Schizosaccharomyces pombe (*S. pombe*), fission yeast, is a unicellular rod-shaped eukaryote. Wild-type cells are usually haploid in rich media; they only mate and sporulate due to nutrient limitation in a continuous pathway from conjugation through meiosis (Forsburg, 2003a). Haploid cells typically measure 3-4 μm in diameter and 12-15 μm in length at division. Generation time of *S. pombe* ranges from 2 to 5 h depending on the media, strain and temperature. The optimum growth temperature is 32 ℃, whereas the maximum and minimum permissive temperature is 36 ℃ and 17 ℃, respectively (Forsburg, 2003d). Haploid genome size, which consists of 3 chromosomes with the size ranging from 2.45 Mb to 5.58 Mb, is 13.8 Mb containing 5,049 protein-coding genes and at least 450 non-protein coding RNAs (Forsburg and Rhind, 2006; Wood et al., 2012).

Several features make *S. pombe* a popular model system for studying conserved eukaryotic processes. Firstly, wild-type haploid cells have regular cell shape and divide by medial fission to produce two daughter cells of equal sizes; this feature is widely used in cell cycle study. Paul Nurse, for instance, identified cyclin-dependent protein kinase Cdk1, which controls mitotic cell cycle, in *S. pombe.* He was subsequently awarded the 2001 Nobel Prize in Physiology or Medicine along with Leland Hartwell and Tim Hunt for their work on cell cycle regulation. Secondly, the genome of *S. pombe* has been sequenced and annotated, which allows more conserved genes, compared to their human counterparts, to be revealed and characterized. For example, fifty genes of *S. pombe* share significant similarity with human disease genes, which makes *S. pombe* a useful model organism for the functional study of human disease genes (Wood et al., 2002). In addition, *S. pombe* can be used to study the mechanism of RNA interference (RNAi), which is a gene-silencing pathway triggered by double-stranded RNA,

conserved among various eukaryotes except for another eukaryotic model organism, *Saccharomyces cerevisiae* (Nakayashiki et al., 2006). Similar to *Saccharomyces cerevisiae*, *S. pombe* is a powerful genetic model system because of its haploid life cycle. This trait enables identification of the physiological functions of individual genes by available and emerging genetic modification methods. For example, deletion of specific genes which leads to a complete loss of their function can be achieved by using a construct that contains a nutritional or antibiotic marker and homologous sequences to the target genes (Forsburg, 2001). Additionally, the CRISPR-Cas9 genome editing system was made available for rapid and efficient genome manipulation in *S. pombe*, since the constructs which produce the targeting guide RNA have been successfully developed for this model organism (Jacobs et al., 2014).

1.7 Aims and Objectives of this study

The Upf1 protein is an essential and evolutionally conserved molecular component in the NMD system in all eukaryotic organisms. The biochemical properties and the roles of Upf1 in NMD were extensively studied in past two decades. Intriguingly, the previous research in our lab indicated that this protein might involve in the maintenance of genome stability; this function seems to be independent of its role in NMD. Similar studies have also been reported in mammalian cells. However, functions of Upf1 within the nucleus remain unclear. My aim was to study whether Upf1 is required for maintaining genome stability and whether this process is NMD-independent as well as what is the molecular function of Upf1 in the nucleus of *S. pombe*.

I showed that Upf1 may have NMD-independent function in the suppression of DNA damaging phenotype. The hypersensitivity of *upf1* mutant to DNA replication reagent (HU) treatment in the spot growth assay suggests the requirement of Upf1 in the

inhibition of DNA damaging phenotype. The equal sensitivity of NMD mutants (*upf1Δ*, *upf2Δ* and *upf3Δ* strains) to HU treatment in the spot growth assay indicates the DNA damaging phenotype caused by deletion of Upf1 is because of its loss of function in NMD. However, the less sensitivity of *upf3Δ* strain to another DNA replication inhibitor (MMS) treatment than *upf1Δ* and *upf2Δ* strains supports the NMD-independent suppression of Upf1 and Upf2 in response to DNA-damaging drugs treatments. In addition, the less importance of Upf3 in the repression of the growth defects of *rad52Δ* strain (Rad52, a key regulator in repairing DNA double-strand breaks by homologous recombination pathway) than Upf1 and Upf2 as shown by spot growth assay strengthens the suggestions of the NMD independent role of Upf1 and Upf2 in either maintaining DNA replication or repairing DNA damages.

Verification of the binding of the functional Upf1 to the chromatin through nascent RNA in *S. pombe* by modified ChIP suggests that Upf1 regulates the transcription of the genes that it bind to, therefore maintains genome stability. This hypothesis would be tested by investigating whether lack of Upf1 changes the loading pattern of RNA polymerase II on genes using Chromatin Immunoprecipitation (ChIP) and Chromatin Immunoprecipitation Sequencing (ChIP-Seq). Additionally, to dissect the nuclear function of Upf1, I identified *upf1*-interacting genes including nucleosome remodelling protein Spt6, which have functions in the nucleus, using unbiased genome-wide genetic screens.

Chapter 2

2.0 Materials and Methods

2.1 Solutions and buffers

Buffers as well as other solutions were made from analytical grade reagents supplied by either Sigma-Aldrich, VWR, Fluka or Fisher, unless stated otherwise. Recipes for most solutions were obtained from Molecular Cloning 3rd edition (Sambrook and Russell, 2001). All solutions and buffers were made in purified water (Elix 5, Millipore) and sterilized by either autoclaving or filtration (0.22 μm, Millipore). All solutions used for RNA experiments were prepared in sterilized glassware and treated overnight with 0.1% (v/v) diethyl pyrocarbonate (DEPC), left overnight in a laminar flow hood and then autoclaved. Tris buffer solutions were not treated by DEPC but prepared with DEPC treated purified water.

2.2 DNA cloning in *Escherichia coli*

The majority of standard protocols were performed as described in Molecular Cloning 3rd edition (Sambrook and Russell, 2001). *E. coli* strain XL1-Blue (genotype: *recA1 endA1 gyrA96 thi-1 hsdR17 supE44 relA1 lac* [F´*proAB lacI*^{q}*ZΔM15* Tn*10* (Tet^{r})]) was used in this study.

2.2.1 Bacterial growth

LB broth or LB agar plates containing an appropriate selective antibiotic were used for growth and maintenance of *E.coli*. Bacteria cultures were grown in flasks in a shaking incubator overnight at 37 ℃, 220 rpm. *E. coli* transformants were grown on inverted 9-cm LB agar plates overnight at 37 ℃ and then kept at 4 ℃ for up to 6 months. Competent

XL1-Blue cells used for transformation were created using the Rubidium method by a previous lab member and stored at -80 ℃ (Wen, Jikai Ph.D. thesis, 2010).

2.2.2 Ligation and *E. coli* transformation

Ligation of DNA fragments was set up in a 10 µl reaction containing 100 ng of linearized plasmid, an insert (the molar ratio of insert to vector is used at around 3:1) and 400 units of T4 DNA ligase (NEB). The ligation reaction was incubated overnight at 18 ℃. 50 µl of *E. coli* competent cells was transformed by mixing 5 µl of ligation mixture with competent cells and keeping them on ice for 20 min. The cells were then heat shocked in a 42 ℃ water bath for 45 s and cooled on ice for 2 min. after which 450 µl of LB media was added, mixed and incubated at 37 ℃ for 45 min, with gentle shaking. They were then briefly centrifuged at room temperature and spread on an LB plate containing 100 µg/ml ampicillin which was incubated overnight at 37 ℃. The correct insertion of DNA fragment into vector was verified by restriction enzyme digestion of plasmids extracted from transformants.

2.2.3 Small-scale preparation of plasmids

The boiling prep method was primarily used to extract plasmids from cells transformed with a ligation mixture, which was followed by restriction enzyme digestion to confirm correct ligation of an insert into a plasmid vector (Wen, Jikai Ph.D. thesis, 2010). A single colony was inoculated into 5 ml of LB broth containing 100 µg/ml ampicillin and grown overnight. 1 ml aliquot of the culture was used for plasmid extraction (a detailed protocol in Appendix I).

2.2.4 Large-scale preparation of plasmid DNA

A single transformant was inoculated into 50 ml of LB broth in a 250 ml flask containing 100 μg/ml ampicillin and grown in a shaking incubator overnight at 37 ℃, 220 rpm. When cultures reached saturation plasmid DNA was extracted using PureLink® HiPure Plasmid Midiprep Kit (invitrogen). Extracted plasmid DNA was resuspended in 200 μl TE, pH 8.0, and the concentration was measured with a spectrophotometer (ND-1000, NanoDrop).

2.2.5 Restriction enzyme digestion

Restriction enzyme digestion to verify plasmid DNA was performed in a 10 μl reaction at an appropriate temperature for 1-2 h. In order to purify the resulting fragments, a 20 μl reaction was set up at a suggested temperature overnight. All restriction enzymes used in this study were purchased from New England Biolabs (NEB). The conditions of restriction enzyme digests were according to the NEB instructions.

2.2.6 Dephosphorylation of DNA

Antarctic phosphatase (NEB) was used to remove 5' phosphates from both ends of linear DNA, thus minimizing recircularization of plasmid DNA digested by a single restriction enzyme. After restriction enzyme digestion, 1 μl of Antarctic phosphatase (5 units/μl) was added into the reaction and incubated at 37 ℃ for 1 h. The reaction was then inactivated at 65 ℃ for 15 min, purified by gel purification as described below.

2.2.7 DNA purification

In this study DNA was either purified from agarose gels or the purification was carried out using the QIAquick PCR purification kit (QIAGEN). Gel purification was applied to PCR products and DNA digested by restriction enzymes. On the other hand, QIAquick PCR purification kit can only be used if the desired DNA fragments range

from 100 bp to 10 kb and the non-required DNA is below 100 bp. In order to perform gel purification, the desired DNA fragment was sliced out of a DNA agarose gel and placed into a 1.5 ml eppendorf tube. The DNA was then purified using the Silica Beads DNA Gel Extraction Kit (Fermentas).

2.2.8 Standard PCR

All primers used in this study are presented in Appendix II. Primers were designed using the NCBI Primer designing tool (http://www.ncbi.nlm.nih.gov/tools/primer-blast/) and obtained from Integrated DNA Technologies, Sigma or MWG. PCR programmes were set up according to the DNA polymerase type, melting temperature of the primers and the size of DNA required to be amplified. PCR was run in a thermal cycler (PTC-200, DNA Engine) and the PCR products were analysed by agarose gel electrophoresis.

2.2.8.1 Bacterial colony PCR

In order to perform bacterial colony PCR, fresh bacterial colonies were mixed with 20 µl PCR solutions which contained 1X PCR buffer, dNTP mixture (0.2 mM of each), 1.5 mM $MgCl_2$, 2 µM primers and 0.25 U GoTaq G2 Polymerase (Promega). DNA was amplified using standard cycling parameters: initial denaturation was conducted at 95 ℃ for 10 min, followed by 25 cycles of 95 ℃ for 30 s, 52 ℃ for 30 s and 72 ℃ for 1min. The final 72 ℃ cycle was extended by 5 min. After the reaction, PCR product was typically checked by electrophoresis in a 1% agarose gel.

2.2.8.2 PCR for molecular cloning

Q5 High-Fidelity DNA Polymerase (NEB) was used to PCR amplify specific DNA fragments intended for cloning. Either *S. pombe* genomic DNA (10 ng) or plasmid

DNA (1 ng) was used as a template to amplify a gene of interest in eight 25 µl PCR reactions which contained 1X Q5 Reaction Buffer, 200 µM dNTPs, 0.4 µM of each primer and 0.5 U Q5 High-Fidelity DNA Polymerase. The PCR programme was set up as described: initial denaturation at 98 ℃ for 3 min; 35 cycles of 98 ℃ for 10 s, (T_m-5) ℃ as the annealing temperature for 30 s, 72 ℃ extension for 1 min per kb of the expected DNA length; completed with 72 ℃ extension for 5 min.

2.2.9 Agarose gel electrophoresis of DNA

PCR products or DNA fragments digested by a restriction enzyme were resolved in 1% agarose gels to confirm and separate the correct bands by molecular weight. DNA samples were mixed with the gel loading dye (6X stock, NEB), loaded onto a 1% (w/v) horizontal agarose gel and run in 1X TAE buffer (40 mM Tris base, 40 mM acetic acid and 2 mM EDTA) containing 0.5 µg/ml ethidium bromide at a constant voltage of 100 V, along with either 1 kb or 100 bp DNA ladder (NEB) as a loading control and size reference. The expected size of the gene of interest was determined by referring to the size of a selected DNA ladder.

2.2.10 DNA sequencing

Purified DNA samples were sequenced and analysed by GATC biotech (Germany). The volume and the concentration of DNA samples and primers for sequencing were prepared as required by GATC biotech.

2.3 *S. pombe* growth, maintenance and manipulations

2.3.1 *S. pombe* strains

S. pombe strains used in this study are presented in Appendix III. All strain stocks were stored at -80 ℃ in either YES or EMM media containing 32% sterile glycerol. Specific gene deletion strains were validated by PCR using extracted genomic DNA or a grown colony as the DNA template. Primers used in this study are listed in Appendix II.

2.3.2 Bioneer *S. pombe* Gene Deletion Library

A set of 2747 single-gene deletion strains with the following genotype: gene X::kanMX4 h+ ade6-M216 ura4-D18 leu1–32 or gene X::kanMX4 h+ ade6-M210 ura4-D18 leu1-32) where gene X::kanMX4 means that a specific gene in the collection was replaced with the kanMX4 cassette, was used in this study. The deletion library construction and verification information is available at http://us.bioneer.com/products/spombe/spombetechnical.aspx.

2.3.3 *S. pombe* media and growth

Liquid cultures or solid agar plates consisting of rich media (YES) or synthetic minimal media (EMM) were used for growth and propagation of yeast strains. The recipes of these media is as described (Forsburg and Rhind, 2006) and they are listed in Appendix VI. G418 disulphate, hygromycin B and nourseothiricin (clonNAT) were purchased from Sigma Co., TOKU-E Co. and Werner BioAgents, respectively. These drugs were used in solid YES plates in concentrations of 100 μg/ml of each.

In order to recover strains stored at -80 ℃ they were streaked on YES or EMM plates and incubated at 30 ℃ or 25 ℃ (if strains were temperature sensitive) for 3-5 days until colonies could be easily visualized. To prepare a liquid culture, a single colony from a streaked plate was firstly inoculated into 3-5 ml of media. The resulting overnight culture was diluted to an OD_{600} of about 0.02 in the desired volume of media and grown

overnight again until reaching exponential phase (OD_{600}<1). Unless stated otherwise, the standard incubation temperature of the culture was 30 ℃.

2.3.4 *S. pombe* DNA transformation

Two slightly modified versions of DNA transformation by lithium acetate method were applied in this study. The first is the rapid version which is used for plasmid introduction into *S. pombe* cells (Forsburg, 2003b) (See a detailed protocol in Appendix I); The second is the long protocol used for DNA integration into *S. pombe* genome (Bahler et al., 1998; Xiao, 2006) (See detailed protocol in Appendix I).

2.3.5 Genomic DNA extraction

Two methods were used for *S. pombe* genomic DNA extraction depending on the way cells lysis was carried out. Cells lysis was achieved either by enzymatic digestion using zymolase or by physical agitation with glass beads. (detailed protocols are provided in the Appendix I). Before genomic DNA extraction, 10 ml cells of OD_{600} of 0.5-1 were prepared.

2.3.6 RNA extraction

S. pombe total RNA was extracted using the hot acidic phenol method (Collart and Oliviero, 2001).

2.3.7 Protein extraction

Two protein extraction methods were used depending on the characteristics of the protein detected by western blot. One is a quick protein extraction method which involves usage of sodium hydroxide (NaOH) (Matsuo et al., 2006) while the other is based on protein precipitation using 2,2,2-trichloroacetic acid (TCA). TCA protocol is

modified in this study according to the method provided by Professor Antony Carr from the University of Sussex (See detailed protocols in Appendix I).

2.3.8 Western blotting and Antibodies

Sodium dodecyl sulfate polyacrylamide gel electrophoresis (SDS-PAGE) gels were prepared as described in Molecular Cloning 3rd edition (Sambrook and Russell, 2001). In order to perform γH2A and H2A Western blotting, total cellular proteins were extracted using either NaOH or TCA protein extraction methods as described in the Appendix I, run in 13% SDS-PAGE gels and transferred onto a nitrocellulose membrane in CAPS buffer (10 mM CAPS, pH 11, 10% methanol). Polyclonal anti-γH2A antibody (courtesy of C. Redon, National Cancer Institute, National Institutes of Health, USA) was used for γH2A detection. Polyclonal anti-H2A antibody (07-146, Millipore) was used for the detection of H2A detection. Monoclonal anti-α-Tubulin antibody (clone B-5-1-2, Sigma) was used for α-Tubulin detection. Monoclonal anti-FLAG M2 antibody (Sigma) was used for the detection of FLAG-tagged Upf1, Upf2, Upf3 and RNA polymerase II subunit rpb3. Monoclonal anti-HA antibody (12CA5) was used to detect HA tagged proteins. Images were acquired on Syngene G:Box (GE).

2.3.9 Northern blot analysis of RNA samples

Total cell RNA was extracted from a 10 ml exponentially growing cell culture using hot acidic phenol method, as described in (Collart and Oliviero, 2001). RNA was separated on 1.2% agarose gels in the presence of formaldehyde. RNA was transferred onto a nylon membrane by means of overnight capillary transfer (Hybond-N, GE Healthcare) and hybridized with random-primer ^{32}P-labelled probes as described in (Yang et al., 1993). Probes were PCR amplified from plasmid clones (GFP) or from genomic DNA (RpL32 or rRNA). Images were acquired by phosphorimager

(Molecular Image-FX, Bio-Rad), and the band intensity was calculated using the Quantity One (Bio-Rad) software. Further details of the northern blot protocol are described in Appendix I.

2.3.10 Spot growth assay

Exponentially growing cell cultures (0.5×10^7~1.5×10^7 cells/ml) were diluted into ten-fold serial dilutions. Diluted samples containing 10^4, 10^3, 10^2, 10^1, respectively, were spotted on solid YES media containing no drugs or different concentrations of either hydroxyurea (HU, Sigma) or methyl methanesulfonate (MMS, Sigma). Cells were then grown for 2-4 days at either 25℃, 30℃ or 37℃. Drug concentrations used are indicated in the results part. Drug sensitivity was estimated by the number and/or size of colonies of different *S. pombe* strains relative to the wild type.

2.3.11 Survival assays

In order to carry out a survival assay for the acute exposure of cells to HU, an overnight cell culture was firstly diluted to an OD_{600} of 0.15. Cells were then cultured at 30℃ for another 3 h. At 0 h 1000 cells were plated onto YES agar plates in a triplicate and, at specific time points, the same volume of the culture was taken and cells were again plated in triplicates. Survival was estimated in relation to the untreated cells. Recovery was 2–3 days at 30℃ for all survival assays.

2.3.12 Flow cytometry analysis

Wild type (JM1), *upf1Δ* (JM2), *upf2Δ* (JM3) and *upf3Δ* (JM26) cell cultures were grown in 40 ml YES at 30℃ until they reached exponential phase. Cultures were incubated with 12 mM HU at 30℃ up to 4 h. HU was then washed out with prewarmed fresh YES media, and released into new prewarmed YES media and cultured at 30℃. At the specified time points, samples were taken for flow cytometry (FACS) analysis as

described in (Sabatinos and Forsburg, 2009). Cells were fixed in 70% ethanol, pelleted, washed in 50 mM sodium citrate and incubated for 2 h in 50 mM sodium citrate containing 0.1 mg/ml RNase A. Cells were stained with 4 μg/ml propidium iodide (Sigma) in 50 mM sodium citrate. Cells were vortexed just before processing. $3x10^6$ cells were used to perform flow cytometry on a BD FACSCalibur.

2.3.13 *S. pombe* colony PCR

GoTaq G2 Polymerase (Promega) was used for colony PCR. 25 μl of PCR reaction mix was made on ice, following protocol provided by Promega. A little amount of *S. pombe* colony was picked using 10 μl pipette tip and dispersed into the PCR tube by pipetting up and down several times. Hot-start PCR was used and the following PCR program: initial denaturation was conducted at 95 ℃ for 10 min, followed by 35 cycles of 95 ℃ for 30 s, 52 ℃ for 30 s and 72 ℃ for 1 min. The final 72 ℃ cycle was extended by 5 min. After the reaction, PCR product was checked by electrophoresis in a 1% agarose gel.

2.3.14 Construction of strains expressing C-terminus-tagged proteins

Either short (Bahler et al., 1998) or long tracts (Krawchuk and Wahls, 1999) of flanking homology strategy was used to generate C-terminal GFP or FLAG tagging cassette for a gene of interest. Primers used to amplify tagging cassettes are shown in Appendix II. Q5 high-fidelity DNA Polymerase (NEB) was used in PCR reactions. PCR products were purified using Silica Bead Gel Extraction Kit (Fermentas). Plasmids pFA6a-5FLAG-hphMX6 (Noguchi et al., 2008) and pFA6a-GFP(S65T)-hph (Sato et al., 2005) were used as DNA templates for amplifying C-terminal FLAG- and GFP- tagging cassette, respectively. Transformation of *S. pombe* cells by gene cassette containing drug-resistant genes was performed according to the previously described long DNA transformation procedure. Integration of the gene cassette into a specific gene locus was

confirmed by colony PCR using primers for the integrating construct and flanking genomic sequences.

2.3.15 Quantitative real-time PCR (qPCR)

Wild type (JM1), *upf1Δ* (JM2), *upf2Δ* (JM3) and *upf3Δ* (JM26) cultures were grown in 40 ml YES at 30 ℃ until exponential phase. At time 0, a 10 ml aliquot of cell culture was collected for RNA extraction. The remaining growing cultures were blocked with 12 mM HU for 4 h at 30 ℃ and an aliquot was collected for RNA preparation. 1 μg of total RNA, isolated, as previously described, using hot acidic phenol method, was reverse transcribed (RT) by means of qScript™ cDNA Synthesis Kit (Quanta BioSciences). Complementary DNA (cDNA) was used as a template for SYBR green qPCR analysis (Bioline). The same RNA sample was directly assayed without reverse transcription by qPCR as a no reverse transcription control.

2.3.16 Genome-wide screening of *upf1* putative interacting genes against Bioneer Library

The unbiased genetic screening protocol used in this study was modified from (Dixon et al., 2008) (See a detailed protocol in Appendix I). Before carrying out the screening, the G418-resistant marker (KanMX6) of the *upf1* deletion strain (JM10, genotype: *h- ade6- upf1::KanMX6,his3D leu1-32 ura4D18? arg?*) was switched to hygromycin to produce a new deletion strain (JM85, genotype: *h- upf1::hphMX6,his3D leu1-32 ura4D18 arg?*) using a standard technique as described in (Sato et al., 2005).

2.3.17 Chromatin immunoprecipitation (ChIP) for ChIP-sequencing (ChIP-seq)

Three ChIP protocols were used in my study.

The first protocol was originally used to investigate whether Upf1 binds to the chromatin: the JM94 strain was grown in 100 ml YES at 30 ℃ to exponential phase

(OD_{600} of 0.7). Cells in the media were fixed by 1% formaldehyde solution (from a 37% stock, Sigma) for 20 min before being broken up by acid washed glass beads (425-600 µm, Sigma). Chromatin extracted from cell lysates was fragmented by 6 sonicating cycles of 20 s using sonicator XL2020 (Misonix) with the following settings: level 3 and frequency 10%. Immunoprecipitations were performed using monoclonal anti-FLAG M2 antibody (Sigma). Protein G Dynabeads (Life Technologies) were pre-incubated with the antibody for 90 min at room temperature prior to an overnight IP at 4 ℃ (See a detailed protocol in Appendix I).

The second protocol was used to assess RNA-dependent protein association to chromatin by introducing the RNase A/T1 treatment (Schroder and Moore, 2005). This modified protocol was mainly based on Abruzzi et al. 2004, with the exception of dilluting chromatin samples with purified water (Elix 5, Millipore) in a 1:1 ratio prior to RNase treatment to dilute the SDS concentration to 0.05%. Samples were then incubated for 1 h at room temperature. Also, cross-linking time was 5 min instead of 20 min.

The third ChIP protocol was adapted from Bähler lab's ChIP-chip protocol (See a detailed protocol in Appendix I) mainly because the first ChIP protocol could not yield enough purified chromatin for sequencing. In this protocol 400 ml of cells growing at 30 ℃ until they reached the OD_{600} of 0.8 were fixed by 1% formaldehyde treatment for 5 min before being broken up by acid washed glass beads. Chromatin extracted from cell lysates was fragmented by 8 sonicating cycles of 5 min with 30 s ON/ 30 s OFF at HIGH setting (Bioruptor plus). Immunoprecipitations were performed using monoclonal anti-FLAG M2 antibody (Sigma). Protein G Dynabeads (Life Technologies) were preincubated with the antibody for 90 min at room temperature

prior to an overnight IP at 4 ℃. Both ChIP and Input DNA were purified using MinElute PCR Purification Kit (QIAGEN).

Chapter 3

3.0 Upf1 is required for maintaining genome stability in *Schizosaccharomyces pombe*

3.1 Summary

As reviewed in the Introduction, nonsense-mediated mRNA decay (NMD) is a eukaryotic cellular quality control mechanism that selectively recognises and degrades aberrant mRNAs containing a premature translation stop codon (PTC). The evolutionarily conserved protein Upf1 is essential for NMD in all eukaryotic organisms. Although Upf1 predominantly localizes in the cytoplasm, recent observations show this protein is also found in the nucleus. Upf1 was reported to associate with DNA polymerase delta in mammalian cells and its depletion correlates with DNA damage and reduced genome stability. Additionally, a previous PhD student in this lab observed that deletion of *upf1* resulted in DNA-damaging phenotypes and endogenously HA tagged Upf1 associates with specific chromosomal regions in fission yeast (Sandip De Ph.D. thesis, 2011). However, the observed DNA-damaging phenotypes of *upf1Δ* strain might be due to the difference in the genetic background between wild type and NMD mutants, not because of the deletion of *upf1*. In addition, the normal function of HA tagged Upf1 was not validated and the growth defect of HA-tagged *upf1* strain might also affect its chromatin binding specificity. Therefore, I improved the work in my thesis. In this chapter, I describe experiments that assess whether deletion of Upf1 leads to the accumulation of DNA damage and more generally, to understand if and how Upf1 functions in the nucleus in fission yeast. To a lesser extent, I carried out parallel studies with two other known NMD factors, Upf2 and Upf3.

Firstly, I discovered that although growth of *upf1Δ* and *upf2Δ* mutants does not differ under normal conditions, both are more sensitive to the DNA-damaging drugs

hydroxyurea (HU) and methyl methanesulfonate (MMS) than the wild type strain (*wt*). The hyper-sensitivity of *upf1Δ* and *upf2Δ* to HU and MMS might be the result of NMD being required for the correct expression of genes directly or indirectly required in DNA replication or repair. Consistent with this hypothesis, a similar phenotype was observed in an *upf3Δ* mutant strain. This gene had not yet been studied in fission yeast thus I characterized it during my PhD. The simplest explanation as to why the potential DNA damage is increased in these mutants is that NMD is required for the expression of genes involved in DNA replication or repair. However, two alternative models are, as suggested by the chromosomal association of Upf1, that this and other NMD proteins may function at the chromosomes, either directly in DNA replication or transcription-linked DNA damage. In Chapter 4 I described how I have validated association of Upf1 with selective gene loci using chromatin immunoprecipitation (ChIP) experiments. These results confirm that Upf1 does indeed associate with specific highly transcribed gene loci, raising the possibility that the increased potential DNA damage in *upf1Δ* mutant might be caused by a lack of an important function of Upf1 at transcription sites.

3.2 Results

3.2.1 Deletion of either *upf1* or *upf2* in *Shizosaccharomyces pombe* stabilizes PTC+ mRNAs

Before embarking on my investigation into the role of Upf1 and other NMD factors in the nucleus, I verified that, as expected, NMD was suppressed in the *upf1* and *upf2* deletion strains used for this study. To verify this, I used Northern blotting to assess mRNA levels of plasmid GFP reporters with or without a PTC mutation (TAA) at codon 6 in wild-type, *upf1Δ* (SPJK030) and *upf2Δ* (SPJK031) strains (Appendix III), as previously reported (Wen and Brogna, 2010). The results confirmed that NMD is suppressed in both *upf1Δ* and *upf2Δ* strains (Figure 5A: the level of GFP mRNA containing the PTC in the wild-type strain was significantly lower than that in the *upf2Δ* strain (13.4% vs. 59%) and in the *upf1Δ* strain (93%). Band intensity measured by the Quantity One software (Bio-Rad) is within linear range. This was verified by Northern blotting of ribosomal protein Rpl32 (also named *rpl3202* in PomBase, (Wood et al., 2012)) mRNA as the loading control using different amounts of total RNA. As shown in Figure 5B, the intensity of Rpl32 from 4.8 μg total RNA was 1.89 folds higher than that from 2.4 μg total RNA, which is just about 5.8% less than expected (188.5% vs. 200%); while the intensity of Rpl32 from 9.6 μg total RNA was 1.78 folds higher than that from 4.8 μg total RNA, which is approximately 11.1% less than expectation (177.8% vs. 200%). Compared to 2.4 μg of RNA sample, the quantitation of Rpl32 from 9.6 μg RNA sample is around 16% less than expectation (335.2% vs. 400%) (Figure 5B). Therefore, I concluded that it is acceptable to use the Quantity One software to quantify the intensity of the bands. To minimize the system error which arised from the software, equal amount of total RNAs were used for each sample when doing Northern blotting.

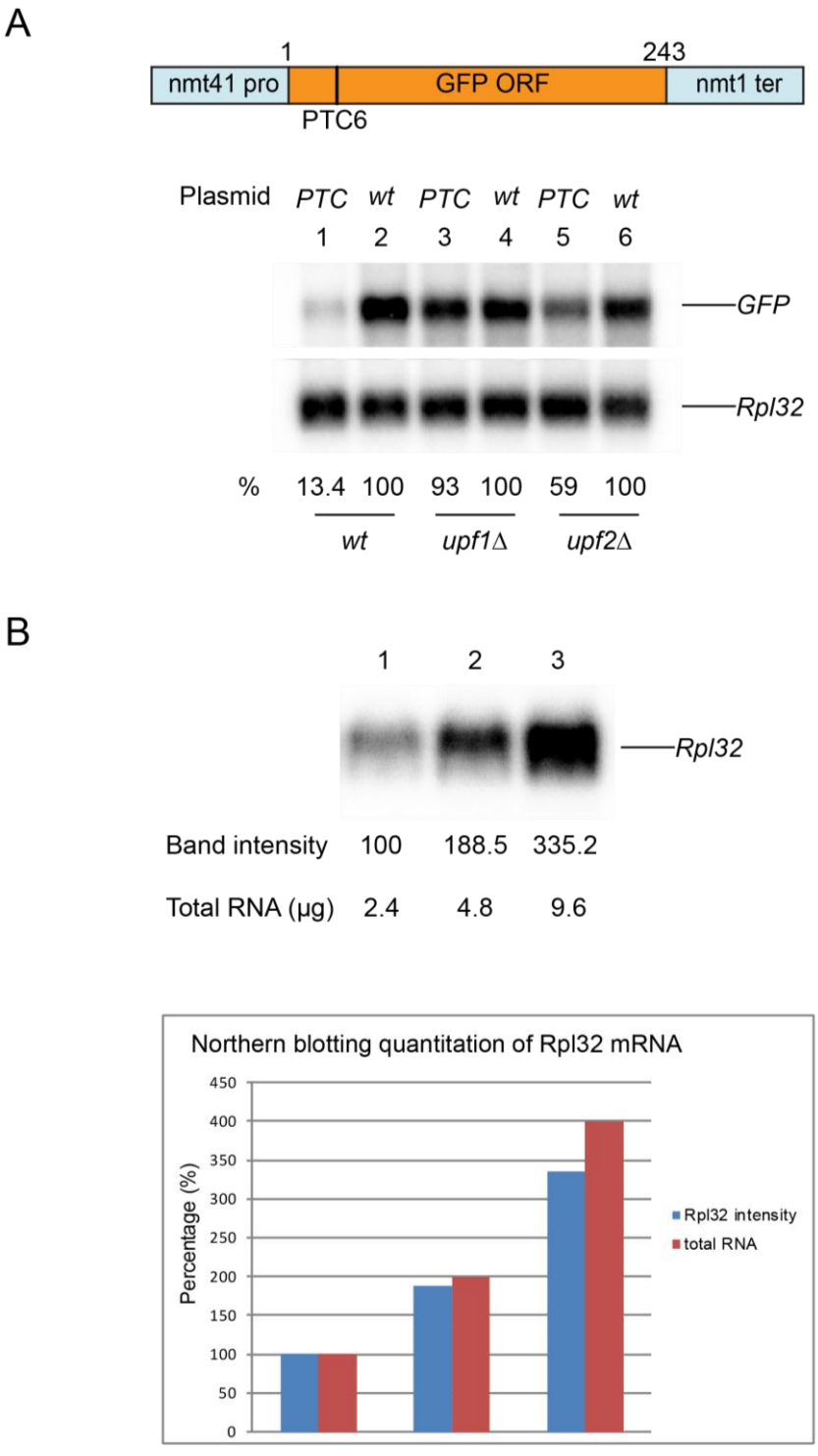

Figure 5. NMD is impaired in *upf1* and *upf2* deletion strain. (A) Nonsense mRNA produced from the NMD reporters in *upf1Δ* and *upf2Δ* strains was stabilized compared

to the wild type strain. Diagram of the NMD reporter carrying a nonsense mutation (TAA) at codon 6 of the *GFP* ORF is in the upper panel. The lower panel shows Northern blotting results for the listed strains. All the strains were transformed with GFP reporters which either contain a PTC or not. Total RNA was analysed. GFP mRNA was detected by hybridization with a radiolabelled DNA probe. The same membrane was stripped and hybridized with probes specific to *Rpl32* mRNA. Numbers indicate the levels of GFP mRNA in different samples after normalization with *Rpl32* signal. (B) Northern blotting quantitation of the mRNA levels of *Rpl32* from different amounts of the same total-RNA sample (indicated at the bottom). Band intensity was calculated using Quantity One software (Bio-Rad). The membrane was probed for *Rpl32* mRNA with specific radiolabelled probe (See Material and Methods). The intensity of the bands was normalized to that in lane 1 which contains 2.4 μg RNA (top panel). Bottom panel shows a graph of normalized Rpl32 band intensities in the three lanes (blue) and amounts of total RNA (red).

3.2.2 *upf1Δ and upf2Δ* mutants are hypersensitive to DNA replication inhibitors

It was suggested that UPF1 is directly involved in DNA replication in mammalian cells and that this function is independent of NMD (Azzalin and Lingner, 2006). To understand whether *S. pombe* Upf1, the homologue of mammalian UPF1, is also involved in DNA replication, I tested whether the *upf1* deletion mutant is hypersensitive to genotoxic agents compared to wild type. Spot growth assays were performed to investigate the sensitivity of *upf1Δ* to hydroxyurea (HU） or methyl methanesulfonate (MMS), which stall DNA replication by different mechanisms (Groth et al., 2010; Petermann et al., 2010). Sensitivity of the *upf2Δ* mutant to these drugs was studied in parallel. *cdc17-K42*, which is a mutant allele of ATP-dependent DNA replication ligase (SPAC20G8.01), a temperature and DNA damage hypersensitive protein, was used as a positive control (Nasmyth, 1977). Growth was assayed at either 30 ℃ or 37 ℃ using different concentrations of HU or MMS. Consistent with previous studies, the temperature sensitive *cdc*17-*K42* strain did not grow at 37 ℃ even in the absence of either drug. The growth of both the *upf1Δ* and *upf2Δ* strains at 37 ℃ was delayed in presence of 10 and 12.5 mM HU compared to the wild-type (Figure 6, top two panels). Due to unknown reasons, all the strains grew better at 37 ℃ than at 30 ℃ in the presence of HU. At a lower concentration of MMS (0.002%) or HU (1 mM HU), there was no growth difference between *wt*, *upf1Δ* and *upf2Δ* mutants at 30 ℃ and 37 ℃ (Figure S2). No effect on growth was observed in the presence of 0.003%, 0.004%, or 0.005% MMS at 30 ℃. However, both *upf1Δ* and *upf2Δ* were more sensitive than wild type at 37 ℃ in presence of MMS at concentrations ranging from 0.003~0.005% (Figure 6, bottom panels). In conclusion, both *upf1Δ* and *upf2Δ* mutants were more sensitive than wild-type to both DNA replication inhibitors.

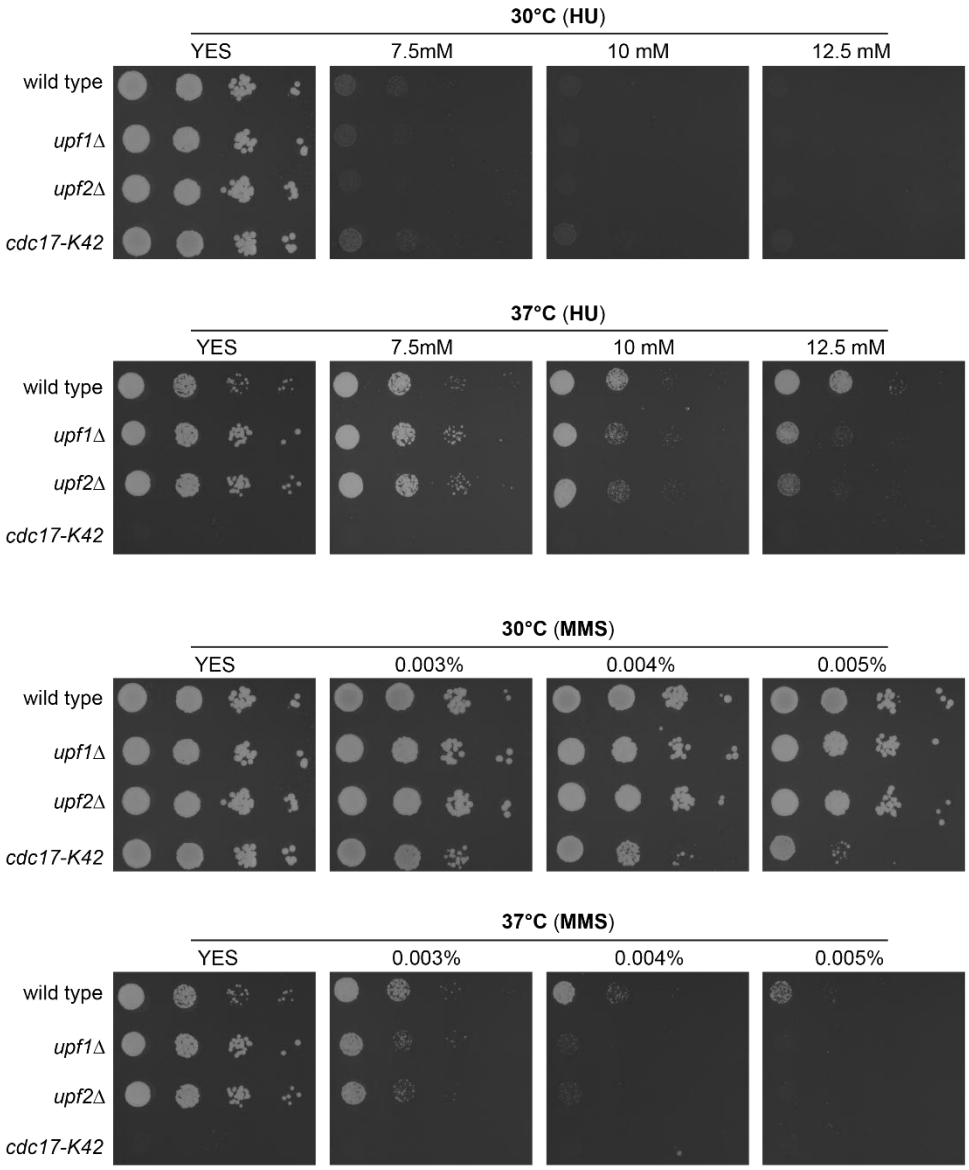

Figure 6. The *upf1Δ* and *upf2Δ* strains are hypersensitive to DNA-damaging drugs. The growth of *upf1Δ* and *upf2Δ* strains were sicker than the wild type on YES agar plates in the presence of HU and MMS at 37 ℃. The wild type (JM1, *upf1Δ* (SPJK030), *upf2Δ* (SPJK031) and *cdc17-K42* mutants were grown on rich media（YES）at 30 ℃. Approximately 10^4, 10^3, 10^2, and 10 cells were spotted and grown for 4 days at either

30℃ or 37℃ either in presence or absence of methyl methanesulfonate (MMS) or hydroxyurea (HU).

3.2.3 Upf3 is essential for NMD in *S. pombe*

Since both Upf1 and Upf2 are essential for NMD (Figure 5A), the hypersensitivity I have detected indicates either a role of NMD in DNA replication or repair or, as reported for UPF1 in mammalian cells, direct roles of these proteins in DNA replication or repair such as in replication. To distinguish between these two possibilities, I analysed *Upf3* which is yet another gene predicted to be required for NMD. Although Upf3 was predicted to be required for NMD in *S. pombe* as its protein sequence is similar to that of other organisms, this had not yet been confirmed in *S. pombe*. To verify that the *S. pombe* ortholog of Upf3 is indeed an NMD factor, I crossed an *upf3Δ* strain (Bioneer M3030H (Version2) to a wild-type strain (SPJK002) to remove possible genetic modifiers. This *upf3* deletion strain (JM26) was confirmed by PCR (Figure S3). In parallel, new *upf1Δ* (JM2) and *upf2Δ* (JM3) mutants were generated to make sure all strains have similar genetic backgrounds. I then tested whether Upf3 is involved in NMD by assaying GFP reporters which either contain a PTC or not (as described above, Figure 5A) in the *upf3Δ* strain, as well as in the newly generated *upf1Δ* (JM2) and *upf2Δ* (JM3) strains with homogenous genetic backgrounds. If Upf3 is required for NMD in *S. pombe*, the level of PTC+ mRNA should be stabilized. As expected, the Northern blotting showed a complete stabilisation of the NMD reporter mRNA in the *upf3Δ* strain (Figure 7A-7B). Stabilisation of the PTC+ mRNA in *upf3Δ* was even more apparent than in the *upf1Δ* and *upf2Δ* strains or when both genes were deleted (Figure 7). In this set of experiments NMD was less apparent compared to that detected previously (Figure 7 vs. Figure 5). These results demonstrated that Upf3 is an essential NMD factor in *S. pombe*.

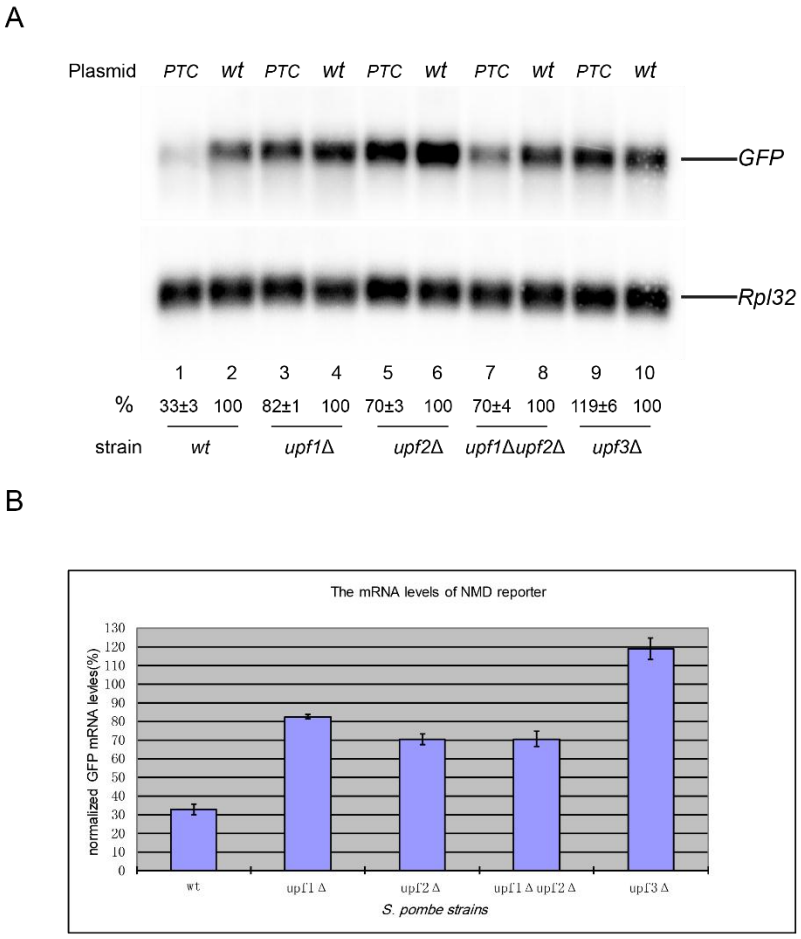

Figure 7. Deletion of *upf3* suppresses NMD in *S. pombe*. (A) Nonsense mRNA produced from the NMD reporters in *upf3Δ* strain was stabilized compared to the wild type strain. Northern blotting results for the listed strains. All the strains were transformed with GFP reporters which either contain a PTC or not. The total RNA was analysed. GFP mRNA was detected by hybridization with a radiolabeled DNA probe. The same membrane was stripped and hybridized with *Rpl32* mRNA specific probe. Values shown beneath lane numbers indicate the levels of GFP mRNA in the different samples after normalization with the *Rpl32* signal. The error bar is standard deviation (SD). (B) Graph of normalized PTC+ mRNA band intensities from (A). The quantification is based on three independent biological repeats.

3.2.4 *upf3Δ* is hypersensitive to hydroxyurea but not to methyl methanesulfonate

As shown above, *upf1Δ* and *upf2Δ* mutants are hypersensitive to HU and MMS, but at that stage it was not clear whether this phenotype results from the lack of NMD or from a direct function of these proteins in DNA replication or repair. Having demonstrated that Upf3 is also required for NMD in *S. pombe*, I investigated the sensitivity of the *upf3Δ* mutant to HU and MMS using the spot growth assay as above. In this instance and subsequently in this project, I used *cds1Δ* as a positive control, instead of the *cdc17-K42*, which is defective in the intra-S phase DNA damage checkpoint (Marchetti et al., 2002). There are two reasons why the *cds1Δ* strain is preferable: (1) the *cdc17-K42* mutant is inviable at 37 ℃ so it could not have been used at this temperature; and (2) the *cds1Δ* mutant is hypersensitive to HU (Shikata et al., 2007). The assay showed that the *upf3Δ* mutant is as hypersensitive to HU as the *upf1Δ* or *upf2Δ* strains (Figure 8A). Consistent to the previous growth assay results, all the tested strains including the wild type and the *cds1Δ* mutant were more sensitive to HU at 30 ℃ than at 37 ℃ (Figure 8A). Notably, the three NMD mutants differed regarding to methyl methanesulfonate (MMS) sensitivity. MMS hypersensitivity is apparent when the strains are grown at 37 ℃. At this temperature the *upf1Δ* and, to a slightly higher extent, the *upf2Δ* mutants were hypersensitive to the drug, but *upf3Δ* was not and grew comparably to the *cds1Δ* mutant, which was only slightly less sensitive to the drug than the wild-type. All the tested strains grew better in this latter set of experiments (Figure 8) than in the previous ones (Figure 6) in the presence of 0.004% MMS at 37 ℃. This was possibly because the strains used in the latter experiments were taken from exponential growing cultures while previous were taken from stationary cultures. An alternative explanation might be differences in genetic background.

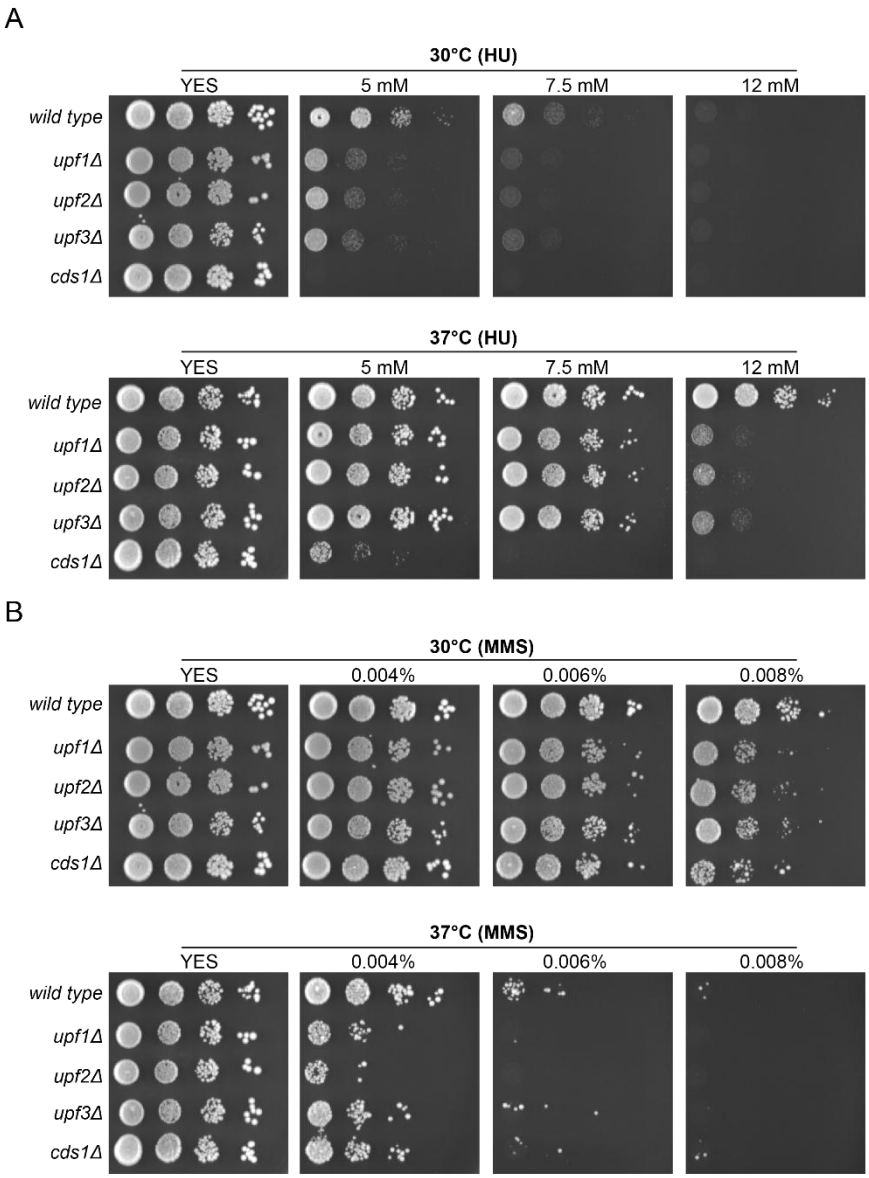

Figure 8. *upf3Δ* mutant is also hypersensitive to DNA-damaging agents. (A)The growth of the *upf3Δ* strain was sicker than the wild type strain on YES agar plates in the presence of HU. (B) The growth of the *upf1Δ* and *upf2Δ* strains were sicker than the *upf3Δ* strain on YES agar plates in the presence of MMS at 37 ℃. The wild type (JM1), *upf1Δ* (JM2), *upf2Δ* (JM3) and *cds1Δ* (JM26) mutants were grown on rich media (YES)

at 30℃. Approximately 10^4, 10^3, 10^2, and 10 cells were spotted on a YES agar plate and grown for 4 days at either 30℃ or 37℃, either in presence or absence of hydroxyurea (HU) (A) or methyl methanesulfonate (MMS) (B). The experiment was repeated twice independently and yielded similar results.

3.2.5 Modification of PCNA differs in NMD mutants

Ubiquitination of Proliferating Cell Nuclear Antigen protein (PCNA) is observed when *S. pombe* cells are exposed to DNA-damaging reagents, therefore, ubiquitinated PCNA can be used as a DNA damage marker (Frampton et al., 2006). Here, following my earlier observation that NMD mutants were more sensitive to DNA damaging drugs, I assayed whether PCNA modification levels were also affected. To do this, whole cell protein extracts were assayed by Western blotting using PCNA antibody. Unmodified and modified forms of PCNA, representing mono- and poly- ubiquitinated PCNA species were readily detected (indicated by arrows in Figure 9, panel A). No major differences in the modification of PCNA band patterns were observed at 30 ℃. However, there was more unmodified PCNA and slightly more poly-ubiquitinated PCNA species in both *upf2Δ and upf3Δ* mutants (Figure 9, panel A). When cells were pre-incubated at 37 ℃ for 4 h prior to cell lysis, which can change the level of the DNA damage in haemocytes of *Dreissena polymorpha* (Buschini et al., 2003), ubiquitinated PCNA was readily detected in all mutants, particularly in *upf3Δ* compared to wild type (Figure 9). A parallel reduction in unmodified PCNA was also detected (Figure 9).

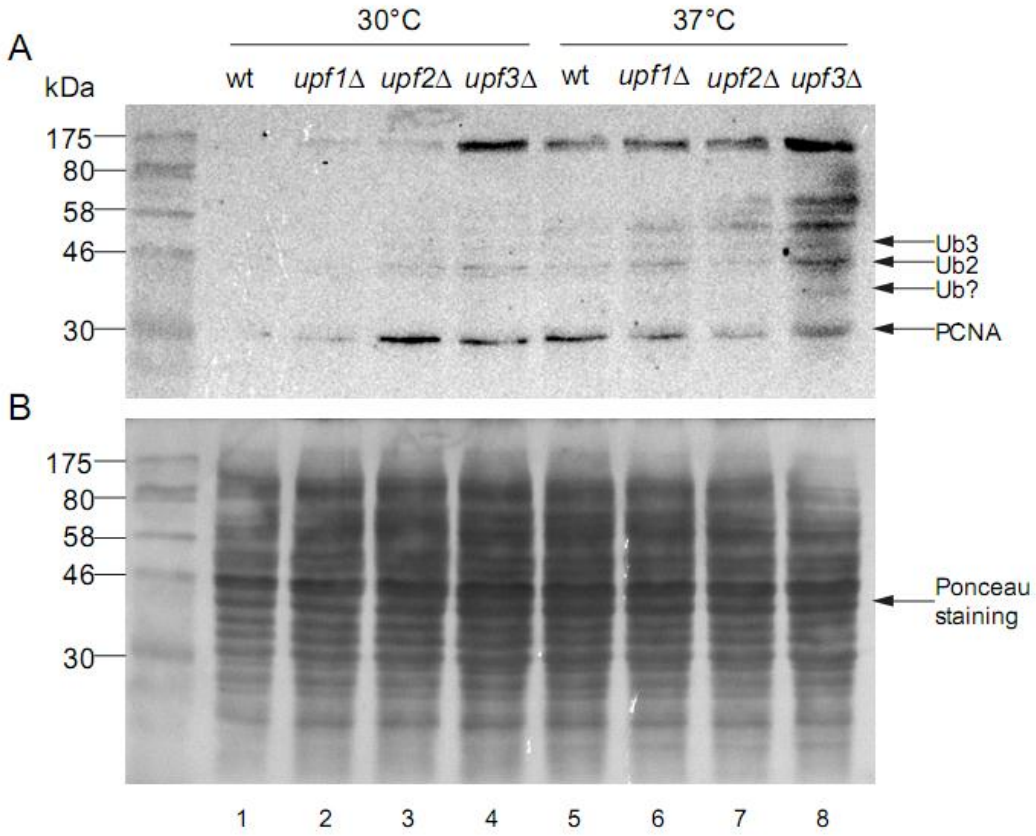

Figure 9. NMD mutants (the *upf1Δ*, *upf2Δ* and *upf3Δ* strains) accumulate ubiquitinated PCNA detected by Western blot. Exponentially growing cultures at 30 ℃ (OD_{600} of 0.1) were split into two: one aliquot was further incubated at 30 ℃ while the other was transferred to 37 ℃ and both cultures were further incubated for 4 h. Then, whole cell proteins were extracted and assessed by Western blot using anti-PCNA antibody (PC10, Thermo). Proteins transferred to the nitrocellulose membrane were detected by staining with Ponceau S solution. Western blotting results are shown in the panel A and the Ponceau S staining result is displayed in the panel B. Unmodified and polyubiquitinated PCNA species are indicated by respective arrows.

3.2.6 NMD mutants have a delayed S-phase but are not defective in S-phase checkpoints

Since all tested NMD mutants were hypersensitive to DNA replication inhibitors, this suggested they may have defects in cell cycle progression. To examine this I analysed changes in cell DNA content by flow cytometry (FACS). The *cds1Δ* mutant was used as a positive control since replication checkpoint kinase Cds1 is involved in DNA replication-monitoring by blocking mitosis when DNA replication is still in process (Sabatinos et al., 2012). Asynchronous wild type, *upf1Δ*, *upf2Δ*, *upf3Δ* and *cds1Δ* cells were blocked in S- phase by incubating in 12mM HU for 4h at 30℃ and released by washout with fresh media (Sabatinos et al., 2012). Cells were taken from the culture at different time points and fixed for FACS analysis. Wild type haploid cells in G1 phase contain two nuclei, each with a single, complete genome (termed 1C DNA) and thus contain the same total amount of DNA (2C) as cells in G2 phase, which have a single nucleus (Knutsen et al., 2011). Cells which have completed or are about to complete S-phase display a 4C peak, because cytokinesis occurs after S-phase (Yoshida et al., 2003). Since in asynchronous culture, 70% of wild type cells are in G2 phase, flow cytometry of exponentially growing *S. pombe* displays one major peak of 2C DNA and a shoulder stretching towards 4C DNA (Carlson et al., 1999; Forsburg, 2003c). Consistent with previous results, asynchronous wild type cells displayed two peaks with the larger peak corresponding to 2C DNA content (G2 phase) and the smaller peak corresponding to 4C DNA content (the end of S-phase) (Figure 10A) (Koulintchenko et al., 2012). Notably, there was no obvious 4C peak in asynchronous culture of all NMD mutants, and there were more cells with the DNA content between 2C and 4C (Figure 10B). This effect suggested a delay in S-phase and was most apparent in the *upf3Δ* and *cds1Δ* mutants (Figure 10B). At the 2h time point, wild type, *upf1Δ*, *upf2Δ*, and *cds1Δ* cells

displayed only one peak of around 2C DNA content, suggesting that DNA replication of all the cells was inhibited by HU. After 4h HU treatment, all the cells showed one sharp peak with the DNA content slightly less than 2C except for the *cds1Δ* mutant which still had a significant portion of cells in S- phase. The means that the NMD mutants can arrest at G1/S-phase border but not the *cds1Δ* mutant and indicates the *upf1Δ, upf2Δ* and *upf3Δ* mutants are not defective in intra-S phase checkpoints. After being released to a fresh culture for 2.5h, wild type cells progressed to the end of S-phase more than the NMD and *cds1Δ* mutants, as indicated by a lack of the obvious 4C peak seen in the wild-type (Figure 10B). In summary, these results demonstrate that NMD mutants have no defects in intra-S phase checkpoints, but have problems coming from the HU treatment.

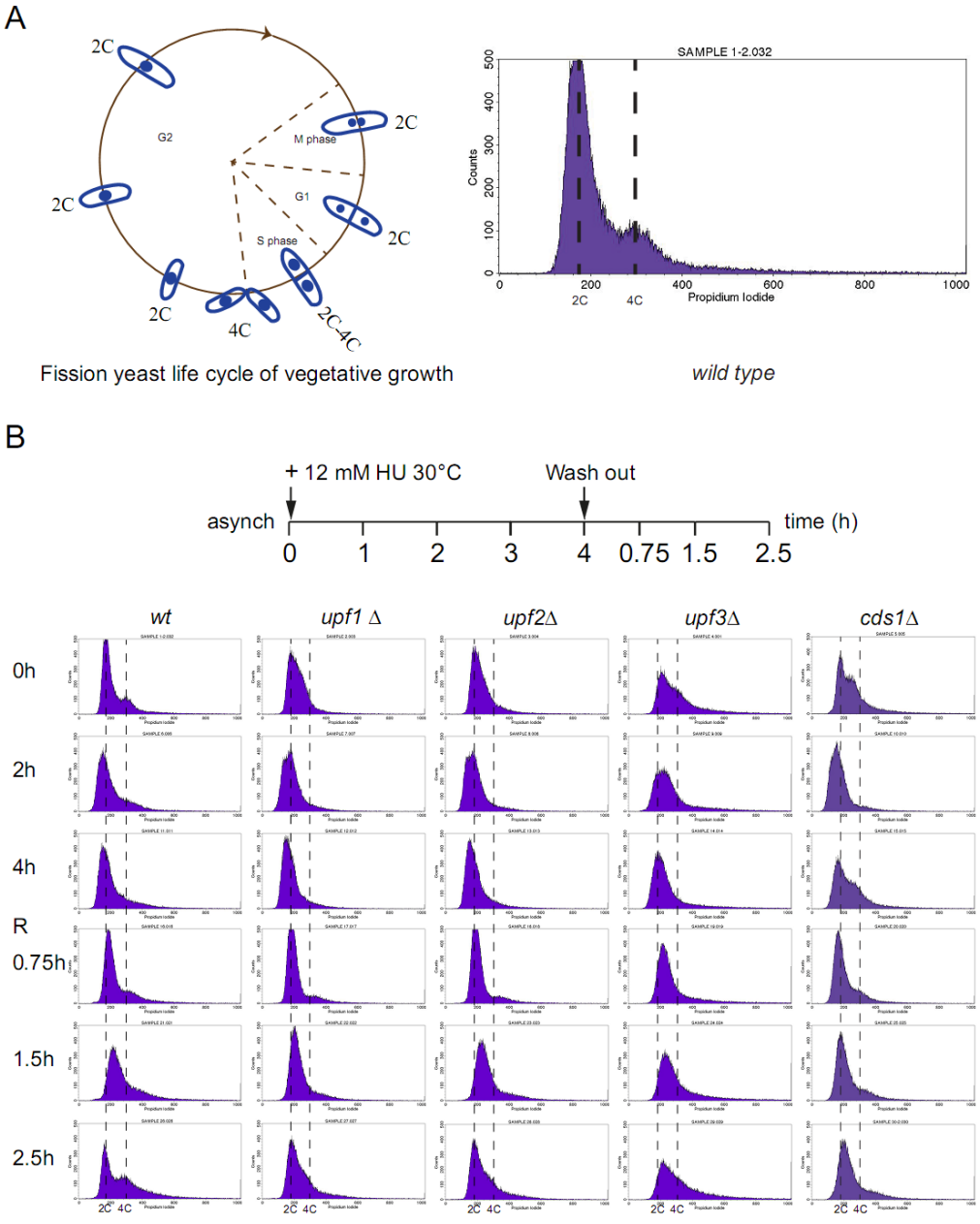

Figure 10. NMD mutants show delayed S-phase. (A) Diagram to the left shows the cell cycle of *S. pombe* in vegetative growth while the one to the right is an example of a FACS result of wild type cells in exponential growth stage which displays one major peak at 2C DNA content and one small peak at 4C DNA content. (B) NMD mutants accumulate more cells in S-phase with DNA content between 2C and 4C after 2.5 h release into fresh culture. Asynchronous wild type, *upf1Δ*, *upf2Δ*, *upf3Δ* and *cds1Δ* cells

were blocked in 12mM HU for 4h at 30 ℃ and then released into the fresh media. Cells were taken from the culture at indicated time points and assessed by FACS (upper panel). Lower panel is the FACS of the wild type, *upf1Δ*, *upf2Δ*, *upf3Δ*, and *cds1Δ* mutants.

3.2.7 The *upf1Δ* mutant contains more Rad52 mRNAs than the wild type

To investigate further whether there is more potential DNA damage in the *upf1Δ* mutant than in the wild type, with or without HU treatment, I assessed by real-time RT-PCR whether the Rad52 mRNA levels are increased. Rad52 is a DNA recombination protein that binds to the single-stranded DNA (ssDNA) during homologous recombination which results in the formation of Rad52 DNA repair foci (Noguchi et al., 2009). An increase in the total level of Rad52 is a sign of DNA damage accumulation (Sacher et al., 2006). Rad52 mRNA was quantified from total RNAs extracted from aliquots of the same cell cultures used for FACS analysis (Figure 10). The results showed more than a two fold increase of Rad52 mRNA in *upf1Δ* compared to wild type. There was no further increase after 4h HU treatment (Figure 11, right bars). In summary, a higher level of Rad52 mRNA was observed in *upf1Δ* than in wild type cells, with or without HU treatment.

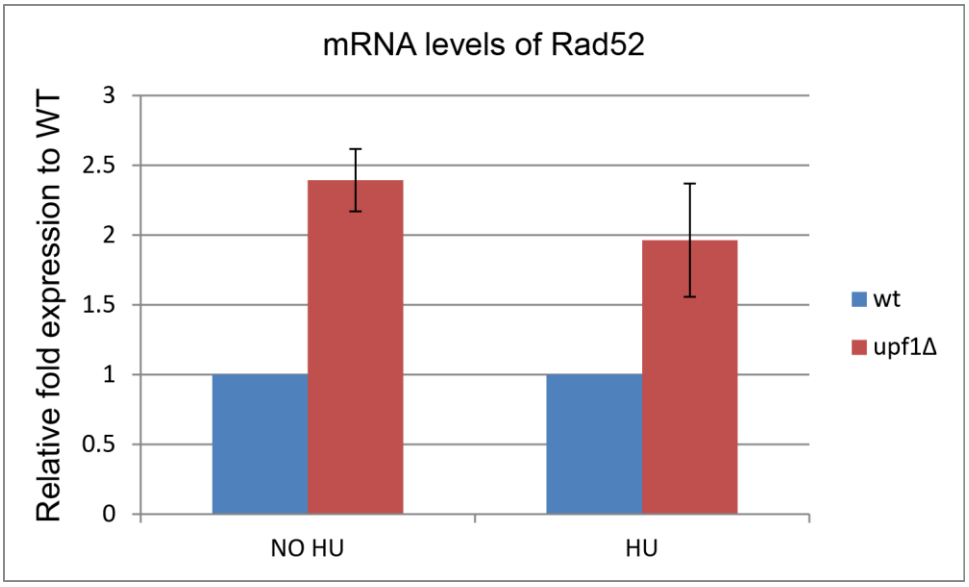

Figure 11. Increased levels of Rad52 mRNAs in *upf1Δ*. Exponentially growing cultures were incubated at 30℃ with or without 12 mM HU for 4 h. Total RNA was then extracted and Rad52 transcripts were quantified by RT-qPCR. The levels of Rad52 mRNA in each strain were firstly normalized to the mRNAs of an internal reference *act1* gene. The expression of Rad52 mRNA in the *upf1Δ* strain was then compared to that in the wild type strain. The quantification is based on three independent biological repeats. The error bar represents standard deviation (SD).

3.2.8 NMD mutants show synthetic sick with *rad52Δ*

HU treatment induces double strand DNA breaks (DSBs) in mammalian cells (Lundin et al., 2005). Therefore, the hypersensitivity observed for *upf1Δ* and other NMD mutants suggests an increase in DSBs. The expectation is that further deletion of key genes involved in either homologous recombination pathway such as *Rad52* or non-homologous end joining (NHEJ) pathway such as *pku70* from the *upf1Δ*, *upf2Δ* and *upf3Δ* strains might result in severer growth defects of the double mutants than NMD single mutants. To test this hypothesis I firstly constructed double mutants of Rad52 with each of the NMD mutants (Upf1, Upf2 and Upf3). As a control, I also constructed the double mutants of these NMD factors with *pku70* which is essential for non-homologous end joining. I then studied the sensitivity of these double mutants to different concentrations of HU at either 30 ℃ or 37 ℃. The growth assay results showed that *rad52Δ* is sicker compared to all the other tested strains in terms of colony size and is hypersensitive to as low as 1 mM HU at both 30 ℃ and 37 ℃. There was no growth difference between the wild type and NMD mutants at these HU concentrations (Figure 12A). However, *upf1Δrad52Δ* double mutant and *upf2Δ* were both synthetic sick at 30 ℃ even in the absence of HU (Figure 12). The synthetic sick phenotype was enhanced by 1 mM HU treatment at 30 ℃; *upf1Δrad52Δ* and *upf2Δrad52Δ* were synthetic lethal in presence of 3 mM HU at 30 ℃. Notably, *upf3Δrad52Δ* was significantly less sick than *upf1Δrad52Δ* and *upf2Δrad52Δ.* The synthetic sick phenotype of *upf1Δrad52Δ, upf2Δrad52Δ* and *upf3Δrad52Δ* was stronger at 37 ℃ (Figure 12A). In contrast to the *rad52Δ*, HU treatment did not impair growth of *pku70Δ* (Figure 12B). There was no obvious synthetic sick interaction between *pku70Δ* and the NMD mutants (Figure 12B).

In conclusion, *rad52Δ* showed synthetic sick with NMD mutants; however, *pku70* did not show such interactions.

A

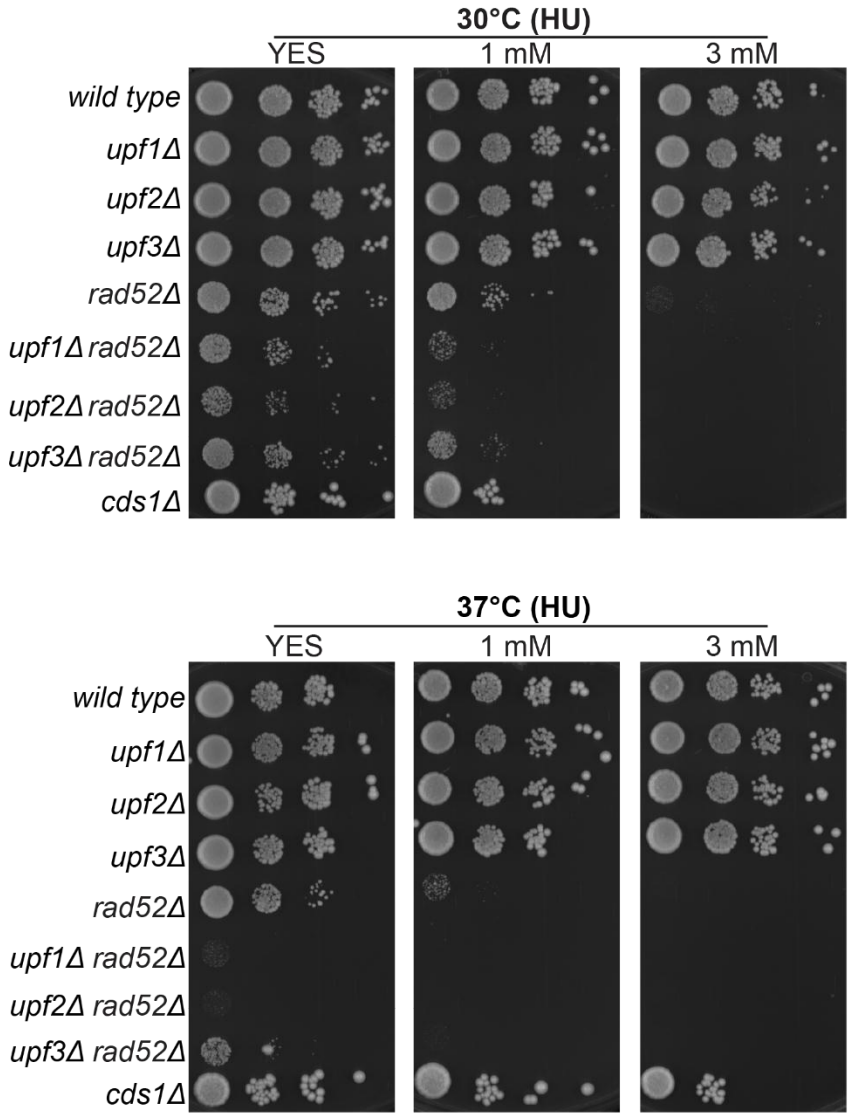
30°C (HU)
YES
1 mM
3 mM
wild type
upf1Δ
upf2Δ
upf3Δ
rad52Δ
upf1Δ rad52Δ
upf2Δ rad52Δ
upf3Δ rad52Δ
cds1Δ
37°C (HU)
YES
1 mM
3 mM
wild type
upf1Δ
upf2Δ
upf3Δ
rad52Δ
upf1Δ rad52Δ
upf2Δ rad52Δ
upf3Δ rad52Δ
cds1Δ

B

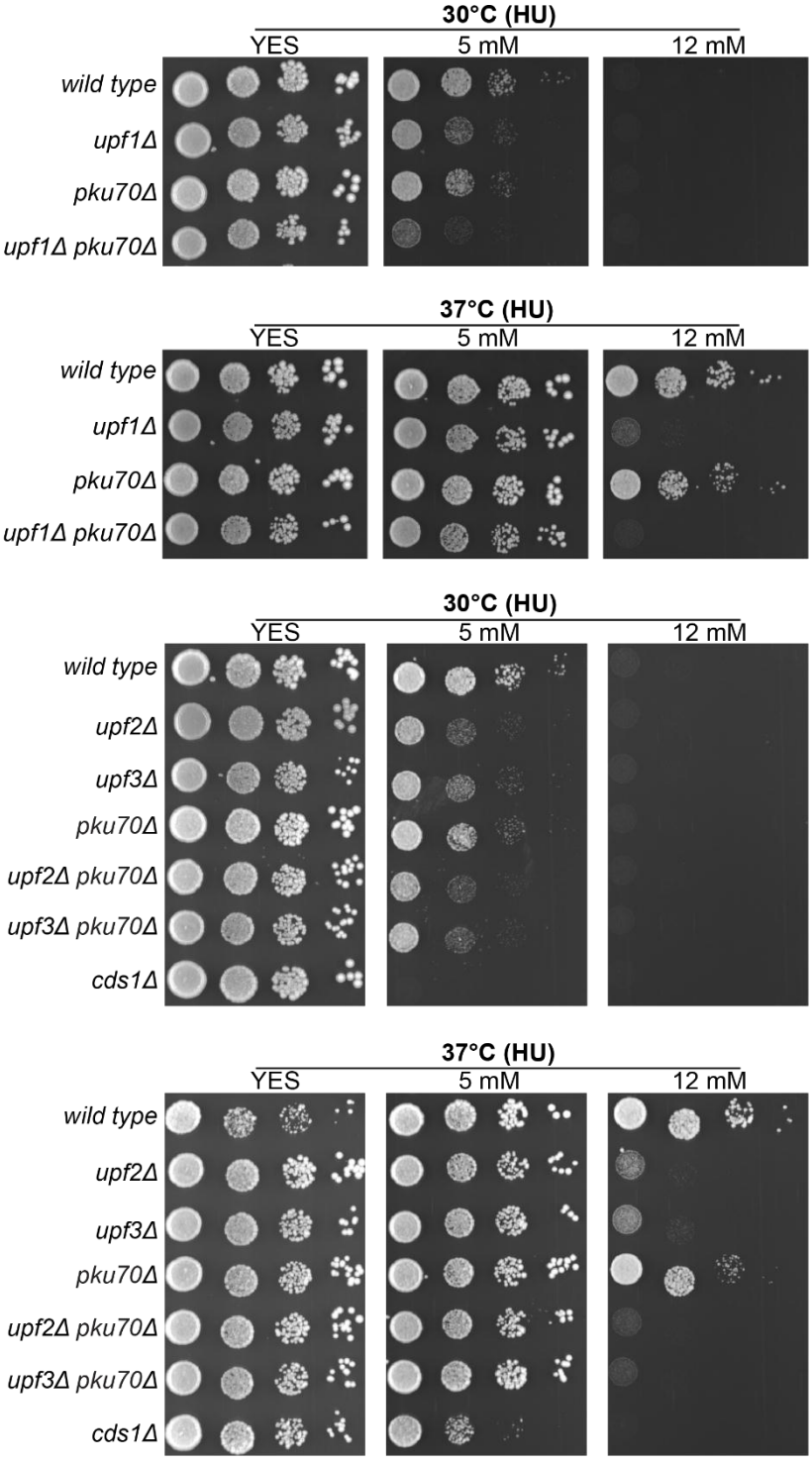

Figure 12．NMD mutants display a synthetic sick phenotype with *rad52Δ*, but not with *pku70Δ*. (A) Any of *upf1*, *upf2* and *upf3* are synthetic sick with *rad52*. Spot growth

assay of the *wild-type*, *upf1Δ*, *upf2Δ*, *upf3Δ*, *rad52Δ*, *upf1Δrad52Δ*, *upf2Δrad52Δ*, *upf3Δrad52Δ*, *cds1Δ* strains with or without HU. (B) Any of *upf1*, *upf2* and *upf3* are not synthetic sick with *pku70*. Spot growth assay of the *wild-type*, *upf1Δ*, *upf2Δ*, *upf3Δ*, *pku70Δ*, *upf1Δpku70Δ*, *upf2Δpku70Δ*, *upf3Δpku70Δ*, *cds1Δ* strains with or without HU. This experiment was done as described in Figure 6 and repeated twice.

3.3 Discussion

The data I presented in this chapter indicate that there is an accumulation of the potential DNA damage in all NMD mutants tested. This is in contrast to the report that only UPF1 is required for preserving genome stability in mammalian cells (Azzalin and Lingner, 2006). In *S. pombe* both *upf1Δ* and *upf2Δ* mutants showed hypersensitivity to DNA damaging agents HU and MMS (Figure 6). These observations suggest either an NMD-independent role of Upf1 and Upf2 in DNA replication or repair or the involvement of the NMD pathway in regulation of genes required for DNA replication or repair. The sensitivity of *upf3Δ* to both HU and MMS (Figure 8A and 8B) suggests a role of NMD in DNA replication or repair. However, the reduced sensitivity of *upf3Δ* to 0.004% MMS at 37℃ compared to either *upf1Δ* or *upf2Δ* mutants (bottom panel in Figure 8) and the slighter sensitivity to 7.5 mM HU at 30℃ and 12 mM HU at 37℃ than either of *upf1Δ* or *upf2Δ* mutants (top two panels in Figure 8) suggests that NMD factors may have NMD-independent roles in HU and MMS caused potential DNA damages. If the sensitivity of NMD mutants to DNA damaging agents was exclusively caused by a lack of NMD, all the single mutants should have shown quite similar sensitivity to these genotoxins.

In addition, the increased Rad52 mRNA in *upf1Δ* mutant even without HU treatment also indicated the existing damaged DNA (Figure 11). If *S. pombe* cells have DNA damage, the cell cycle checkpoint pathways would be activated and thus cell cycle would be delayed. Indeed, more cells of exponentially growing NMD mutants showed delayed S-phase (0h in Figure 10B). When NMD mutants were arrested by HU treatment at the same stage (4h HU, Figure 10B), and released into fresh media, the progress of the cell cycle in these mutants was slower than the wild type (2.5h release, Figure 10B).

Consistent with the NMD mutants being more sensitive to genotoxic agents, I observed an increase in the levels of ubiquitinated PCNA at 37 ℃, suggesting more heat-induced DNA damage in these mutants (lane 6-8 in Figure 9) (Buschini et al., 2003). Yet, it appears that the effect on PCNA is more apparent in *upf3Δ* than in either *upf1Δ* or *upf2Δ*; this observation supports the potential NMD-independent roles of NMD factors in reacting to DNA damaging agents (Figure 8A and 8B) which may not be simply explained by a lack of NMD.

HU can cause double strand DNA breaks (DSB) in mammalian cells (Lundin et al., 2005). Hypersensitivity of NMD mutants to HU (Figure 8A) suggests they are defective in either preventing DSB or repairing them. Although NHEJ is vital to repair DSB in G1, HR is the critical repair pathway in exponentially growing *S. pombe* cells as cells spend most of their cell cycle (70%) in G2 phrase (Ferreira and Cooper, 2004; Raji and Hartsuiker, 2006). If NMD factors have a role in repairing DSB, the double mutant of an NMD factor with *rad52Δ* would show similar sensitivity as the parental strain to HU. However, the synthetic sick phenotype of NMD mutants with the *rad52Δ* mutant (Figure 12A) suggests that NMD mutants are not involved in DSB repair. Based on the interpretation of the genetic interaction, it is implied that NMD factors may either have compensatory pathways or form protein complexes with Rad52 (Mani et al., 2008). However, there are no published results showing that Rad52 physically interacts with NMD proteins (Wood et al., 2012). It is likely that NMD factors are required to maintain genome integrity in a direct or indirect way. Failure in preventing genome stability in NMD mutants results in double strand DNA breaks, and as HR is responsible to repair the damaged DNA it keeps NMD mutants alive under replication stress (HU) or heat stress (37 ℃). Notably, the reduced sensitivity of the *upf3Δrad52Δ* strain compared to either *upf1Δrad52Δ* or *upf2Δrad52Δ* strains growing on YES at 37 ℃ (lower panel in

Figure 12A) or in the presence of 1 mM HU at both 30 ℃ and 37 ℃, may also indicate an NMD-independent function of NMD proteins in maintaining genome stability in *S. pombe*.

Chapter 4

4.0 The core NMD protein Upf1 associates with transcription sites in fission yeast

4.1 Summary

In Chapter 3, I have shown that NMD mutants accumulate potential DNA damage. This might be explained by the lack of NMD being required for the expression of genes involved in DNA replication or repair, however, it is also possible that the chromosomal association of Upf1, which was shown by a previous PhD student in this lab, could have a direct role in preventing potential DNA damage. In this chapter, I describe chromatin immunoprecipitation (ChIP) experiments I have performed to validate the association of Upf1 with selective gene loci. These results confirm that Upf1 does indeed associate with specific gene loci and in particular with highly transcribed regions. In addition, the association of Upf1 with specific gene loci is shown to be RNA-dependent in this Chapter. Therefore, it is possible that the increased potential DNA damage in *upf1Δ* might be caused by the lack of an important function of Upf1 at transcription sites.

In the second part of this chapter, I report on my investigation on whether Upf1 affects RNA polymerase II function at those genes to which it is bound. To address this question, I performed RNA polymerase II ChIP-sequencing (ChIP-seq) to investigate its genome-wide binding both in wild type and in an *upf1* mutant. In parallel, I performed Upf1 ChIP-sequencing (ChIP-seq) in wild type to investigate its genome-wide binding. I obtained the raw ChIP-seq data, however, did not finish the analysis, since the data would be analysed by other lab members through the cooperation.

4.2 Results

4.2.1 Endogenously FLAG tagged Upf1 is functional in NMD and partly functional in HU resistance

The C terminal region of endogenous Upf1 was tagged with FLAG in *S. pombe* using a PCR-based gene targeting strategy (Bahler et al., 1998). To check that the tag was added at the correct position, the C terminal region of upf1 including the tag was amplified by PCR and sequenced. The sequencing results showed the correct tagging of Upf1 (See Appendix VI, sequencing result). The expression of Upf1-FLAG was verified by western blot, using an anti-FLAG monoclonal antibody (Figure 13A). To check whether Upf1-FLAG is functional, a spot growth assay and Northern blotting were carried out. Consistent with my previous observation (Figure 8A in Chapter 3), *upf1Δ* was hyper-sensitive to 12 mM HU at 37 ℃ when compared to wild type (Figure 13B). However, the *upf1-flag* strain was able to partially complement this defect (Figure 13B), suggesting that Upf1-FLAG is not completely functional. Next, I tested whether Upf1-FLAG is able to elicit NMD using Northern blotting. The results showed that NMD of the reporter mRNA (carrying a PTC at position 6) in the *upf1-flag* strain is comparable to that seen in wild type (lane 1 vs. lane 5, upper panel in Figure 13C). The mRNA level of the NMD reporter in *upf1Δ* was on average 68% of the PTC-less control. In conclusion, Upf1-FLAG is similarly functional in terms of HU resistance and completely functional in NMD.

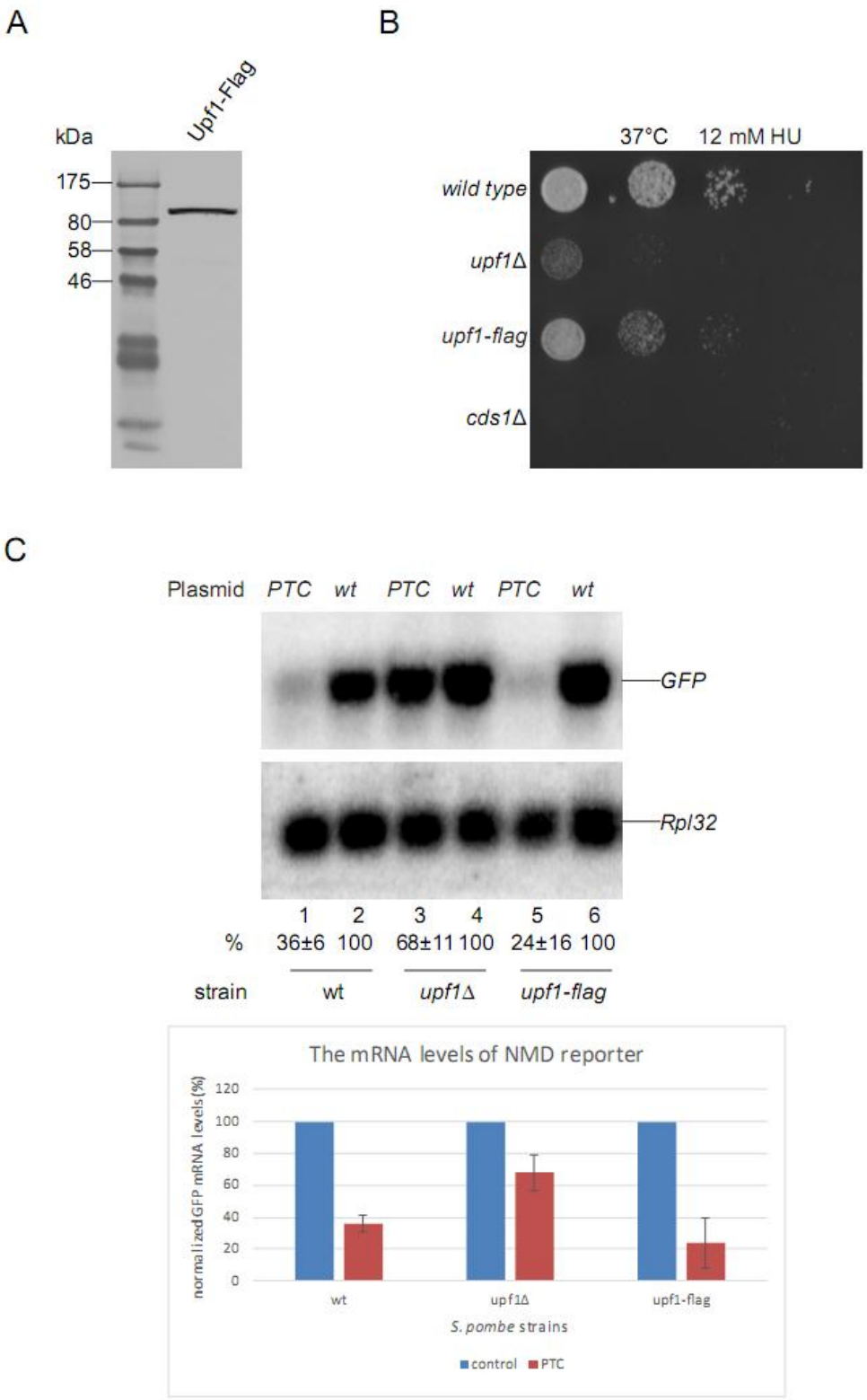
A
kDa
Upf1-Flag
175
80
58
46
B
37°C
12 mM HU
wild type
upf1Δ
upf1-flag
cds1Δ
C
Plasmid PTC wt PTC wt PTC wt
GFP
Rpl32
1 2 3 4 5 6
% 36±6 100 68±11 100 24±16 100
strain wt upf1Δ upf1-flag
The mRNA levels of NMD reporter
normalized GFP mRNA levels (%)
120
100
80
60
40
20
0
wt
upf1Δ
upf1-flag
S. pombe strains
control
PTC

Figure 13. Upf1-FLAG functionality. (A) Western blotting detection of the expression of endogenously tagged Upf1-FLAG from total protein extract. (B) *upf1-flag* strain is less sensitive to 12 mM HU at 37 ℃. Spot growth assay on YES media plates containing 12 mM HU. Exponentially growing cultures of wild type, *upf1Δ*, *upf1-flag* and *cds1Δ* strains were grown on rich medium（YES）at 30 ℃, approximately 10^4, 10^3, 10^2, and 10 cells were spotted and grown for 4 days at 37 ℃. This experiment was not repeated. (C) Nonsense mRNA produced from the NMD reporters in *upf1-flag* strain was degraded to the same extent as in wild type. Northern blotting of mRNA levels of NMD reporter in wild type, *upf1Δ*, *upf1-flag* strains. Bottom blot shows RpL32 mRNA as a loading control. Quantification is as described in Figure 5A in Chapter 3, based on three independent biological repeats (bottom graph). Error bars show the standard deviation (SD).

4.2.2 Upf1 binds both protein-coding and non-protein coding genes

In mammalian cells, Upf1 has been shown to directly bind chromatin and to maintain genome stability (Azzalin and Lingner, 2006). Before investigating whether Upf1 has a similar function in *S. pombe*, I wanted to repeat previous Upf1 chromatin immunoprecipitation (ChIP) experiments performed by Dr. Sandip De in this lab. This ChIP was performed with an HA tagged Upf1, and had indicated that Upf1 associates with many gene loci (unpublished data). I first optimized the ChIP protocol (see Material and Methods) to determine optimal DNA sonication conditions and then used these (Figure 14A) to assess the association of FLAG tagged Upf1 with genes that were identified previously as binding Upf1-HA. I found that Upf1-FLAG associates with the *gpd3* gene (glyceraldehyde 3-phosphate dehydrogenase Gpd3), *tf2* gene repeats (retrotransposable element/transposon Tf2-type) and the *pma1* gene (P-type proton ATPase, P3-type Pma1). The DNA enrichment was about 2 , 3 and 4 fold relative to an intergenic region to which Upf1 is not expected to bind (Figure 14B). In addition, Upf1 appears to bind also at rDNA, $tRNA^{met}$, and telomeric regions (Figure 14C) which are highly transcribed but are non-protein coding genes. In particular, Upf1 association is highest at rDNA repeats (Figure 14C). In conclusion, endogenously FLAG tagged Upf1 appears to bind to protein-coding and highly transcribed non-protein coding genes; these results are consistent with previous ChIP results using Upf1-HA. Upf1 might directly bind to these genes and regulate the replication of them as in mamallian cells (Chawla et al., 2011). It may also likely that Upf1 bind to these genes through nasent RNA and thus have some unknowm funcitons at these loci due to its RNA binding nature (Czaplinski et al., 1995).

A

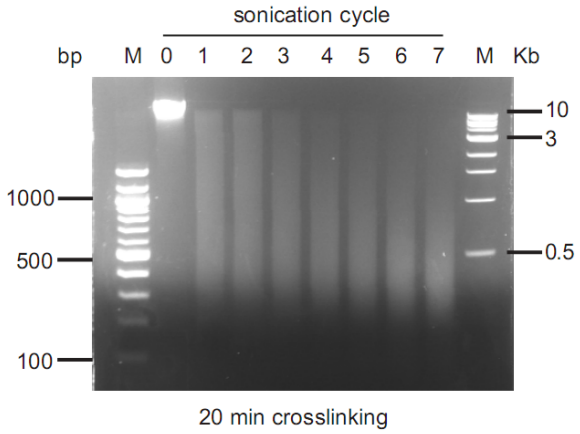

20 min crosslinking

B

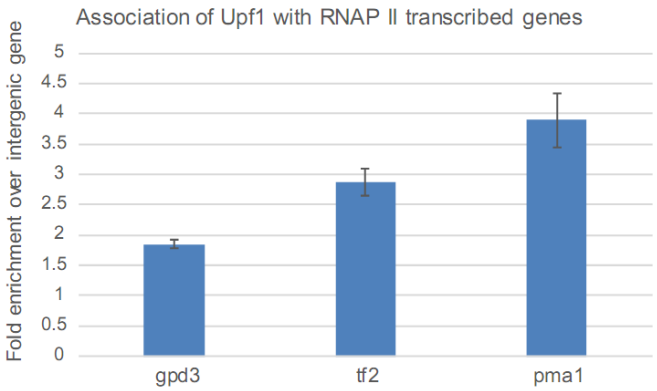

C

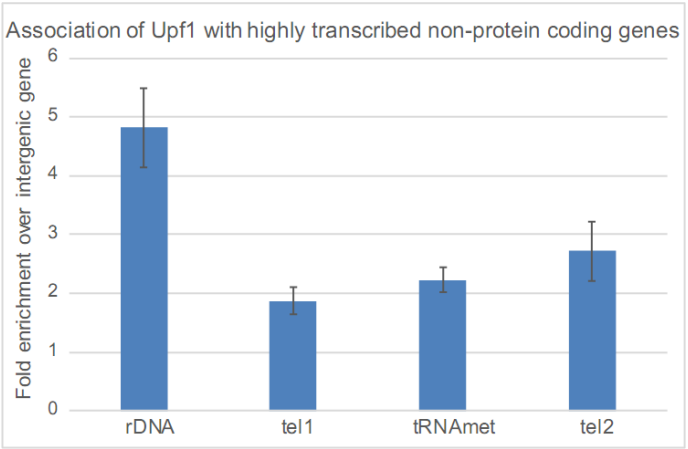

Figure 14. Upf1 associates with various gene loci (A) Optimization of DNA fragmentation. Exponentially growing cultures of *upf1-flag* strain (JM94) in YES media at 30℃ were fixed with 1% formaldehyde for 20 min. The extracted chromatin from cell lysis was equally split and sheared with sonication cycles ranging from 0-7. An equal amount of DNA from different aliquots was analysed on a 1% agarose DNA gel. (B) Upf1 associates with RNAP II transcribed genes. Quantitation of the fold enrichment of Upf1 on protein-coding genes. The JM94 strain was used to perform ChIP using the first ChIP protocol as described in Material and Methods. Quantification of qPCR is based on three independent biological repeats. The error bar is the standard deviation (SD). (C) Upf1 associates with highly transcribed non-protein coding genes. Quantitation of the fold enrichment of Upf1 on non-protein coding genes. The sample was the same as that used in (B) but the genes examined were different. tel1 and tel2 denote two different telomeric regions that were studied. The error bar is the standard deviation (SD). The fold enrichment of the target genes was normalized to the internal reference (intergenic region). The primers used for the study were T67/T68, J64/J65, J82/J83, P2-pma1-F/P2-pma1-R, J84/J85, J100/J101 and J118/J119, J130/J131. The details of the primers are listed in Appendix II, p173.

4.2.3 The association of Upf1 with chromatin is RNA dependent

To confirm whether the association of Upf1 with chromatin is RNase sensitive, I firstly optimized a ChIP in which RNase was used to distinguish between RNA-dependent and RNA-independent association (Abruzzi et al., 2004; Schroder and Moore, 2005). This protocol requires only 5 min formaldehyde treatment, yet, I found that the shorter fixation time had little effect on the fragmentation of the DNA (Figure 14A vs. 15A). To test the ability of this ChIP protocol to identify the association of proteins bound to nascent RNA, I performed an initial ChIP experiment with HA tagged Cbc2, which is the *S. pombe* homologue of cap binding protein Cbp20, that binds the 5' cap of nascent RNA. ChIP assessment of the association of Cbc2 at the highly transcribed *pma1* gene shows a 30 fold enrichment without RNase treatment (Figure 15B). However, when the chromatin sample was treated with RNase A/T1, there is only 1.5-fold enrichment of Cbc2 at the *pma1* gene (Figure 15B). Therefore, the optimized protocol was proven to be able to investigate nascent RNA binding proteins. To assess whether the association of Upf1 with chromatin is via nascent RNA, similar ChIP experiments were performed with Upf1-FLAG. These showed that Upf1 associates with both protein-coding (*pma1*, *gpd3* and *tf2*) and non-protein coding genes (tRNA genes). Among the tested genes, Upf1 had the highest enrichment at rDNA, more than 25 fold (Figure 15C and 15D). There was a significantly higher enrichment of Upf1 at rDNA when using the shorter fixation protocol; the reasons for this are unknown. Unlike mammalian Upf1, the binding of *S. pombe* Upf1 to the chromatin at both protein-coding and non-protein coding genes was in an RNase sensitive manner, since the association was abolished after RNase A/T1 treatment (Figure 15C and 15D). In conclusion, the association of Upf1 to chromatin is dependent on nascent RNA.

A

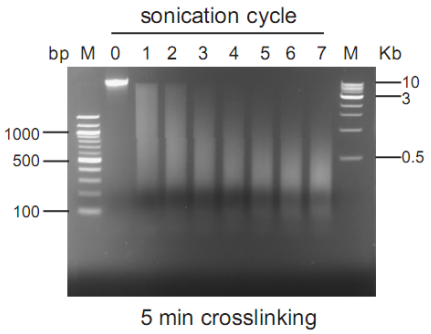
sonication cycle
bp M 0 1 2 3 4 5 6 7 M Kb
1000
500
100
10
3
0.5
5 min crosslinking

B

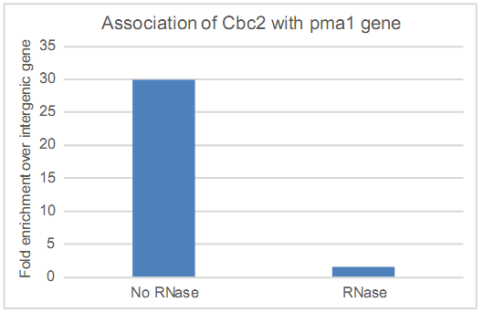
Association of Cbc2 with pma1 gene
Fold enrichment over intergenic gene
35
30
25
20
15
10
5
0
No RNase
RNase

C

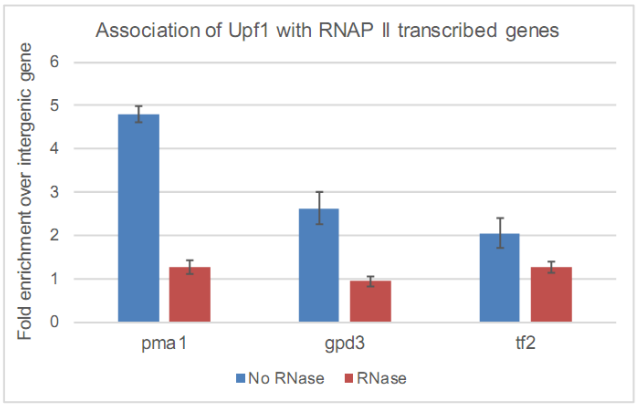
Association of Upf1 with RNAP II transcribed genes
Fold enrichment over intergenic gene
6
5
4
3
2
1
0
pma1
gpd3
tf2
No RNase
RNase

D

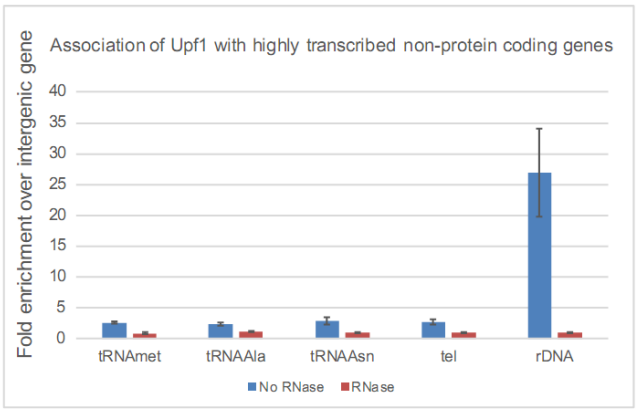
Association of Upf1 with highly transcribed non-protein coding genes
Fold enrichment over intergenic gene
40
35
30
25
20
15
10
5
0
tRNAmet
tRNAAla
tRNAAsn
tel
rDNA
No RNase
RNase

Figure 15. The association of Upf1 to chromatin is nascent RNA dependent. (A) Agarose gel electrophoresis showing DNA fragmentation after a different number of sonication cycles. The optimization procedures are the same as those described in Figure 14A except for the use of 5 min fixation time (B) The enrichment of HA-tagged Cbc2 at the *pma1* gene, with or without RNase treatment. The second ChIP protocol in Material and Methods was used to prepare ChIP DNA from a *cbc2-HA* strain. qPCR was used to examine the enrichment of Cbc2 on *pma1*. (C-D): The enrichment of Flag-tagged Upf1 on protein-coding genes (C) and non-protein coding genes (D) with or without RNase treatment. These experiments were performed as in B except using the JM94 strain. The genes tested are listed at the bottom of the graph. Quantitation is based on three independent biological repeats. The error bar denotes the standard deviation (SD). The fold enrichment of the target genes was normalized to the internal reference (intergenic region). The details of the primers are listed in Appendix II, p173.

4.2.4 Deletion of *upf1* increases the level of specific RNAs

Since Upf1 binds specific transcription sites, it may affect their transcription. To assess this hypothesis, I quantified steady state RNA levels of *pma1*, *tf2* and 25S rDNA in wild type and the *upf1Δ* mutant, using qRT-PCR. I did not observe a significant difference in the levels of *pma1* mRNA between wild type and *upf1Δ* with or without HU treatment (Figure 16A). However, an almost two-fold increase in the level of *tf2* mRNA was observed in the *upf1Δ* strain compared to that in wild type either in the absence or presence of HU (Figure 16B). The *upf1Δ* strain had at least 50% more 25S rRNA than wild type cells before HU treatment. Unlike *pma1* mRNA and *tf2* mRNA, HU treatment dramatically increased the level of 25S rRNA up to 3 fold compared to wild type (Figure 16C). In conclusion, significantly higher levels of *tf2* mRNA and 25S rRNA were observed in the *upf1Δ* strain than in the wild type strain. The difference in 25S rRNA was particularly apparent after HU treatment (Figure 16C).

A

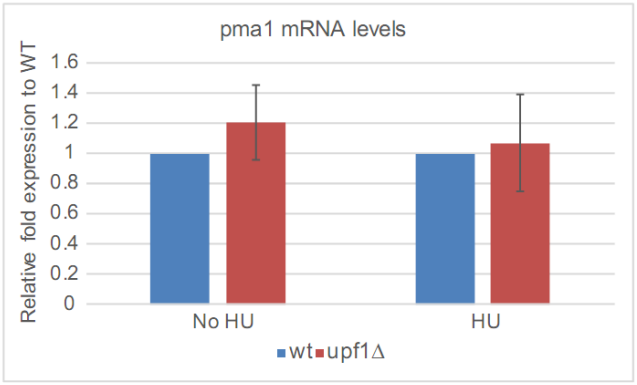
pma1 mRNA levels
Relative fold expression to WT
1.6
1.4
1.2
1
0.8
0.6
0.4
0.2
0
No HU
HU
wt
upf1Δ

B

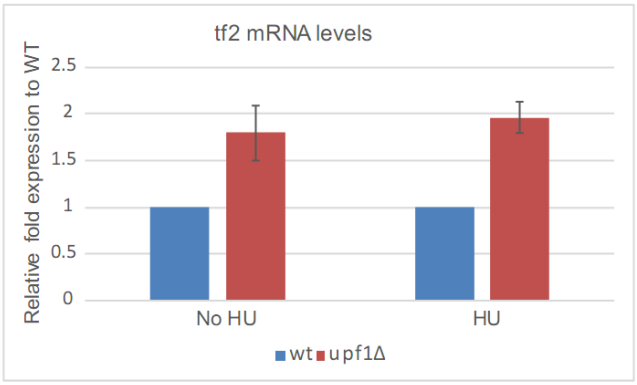
tf2 mRNA levels
Relative fold expression to WT
2.5
2
1.5
1
0.5
0
No HU
HU
wt
upf1Δ

C

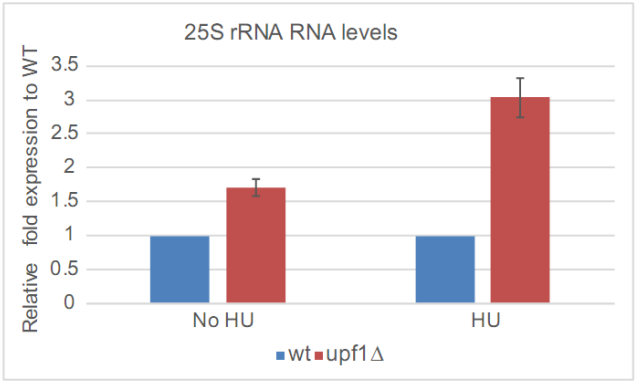
25S rRNA RNA levels
Relative fold expression to WT
3.5
3
2.5
2
1.5
1
0.5
0
No HU
HU
wt
upf1Δ

Figure 16. Deletion of *upf1* increases the level of selected RNAs. (A-C): Quantitation of the levels of *pma1* mRNA (A), *tf2* mRNA (B) and 25S rRNA (C) in wild type and *upf1Δ* strains with or without HU treatment. Exponentially growing cultures of wild type and *upf1Δ S. pombe* were incubated with or without 12mM HU for 4 h. Total RNA was extracted, and the transcripts were quantified by qRT-PCR. Endogenous *act1* mRNA was used as internal reference. The quantitation is based on three independent biological repeats. The error bars denote the standard deviation (SD).

4.2.5 Deletion of *upf1* from the strain where RNA polymerase II subunit 3 (*rpb3*) is endogenously FLAG tagged

Before investigating whether Upf1 affects RNA polymerase II (RNAP II) transcription, the *upf1* gene firstly needs to be deleted from a strain (JM121) where *rpb3* is endogenously FLAG tagged. To achieve this I used a PCR-based approach (Bahler et al., 1998). Each constructed strain was validated using two sets of primers: *upf1* gene specific primers (J15/J16) which were used to examine the presence of the *upf1* gene, and primers J50 and J12 which were used to check the replacement of upf1 with deletion cassette (hphMX6) (Figure 17A). Deletion of *upf1* was confirmed by PCR (lane 3 and 5 in Figure 17B). The results showed that the *upf1* gene was deleted from colonies 1 and 3 (lane 3 and 5 in Figure 17B) whereas *upf1* was still present in colony 2 (lane 4 in Figure 17B). The expression of FLAG tagged Rpb3 from cultures grown from colonies 1 and 3 was further confirmed by Western blotting (lane 2 and 3 in Figure 17C). Therefore, the deletion of *upf1* gene and the expression of FLAG tagged Rpb3 was confirmed in 2 out of 3 constructed strains. The stain from colony 3 was named JM131.

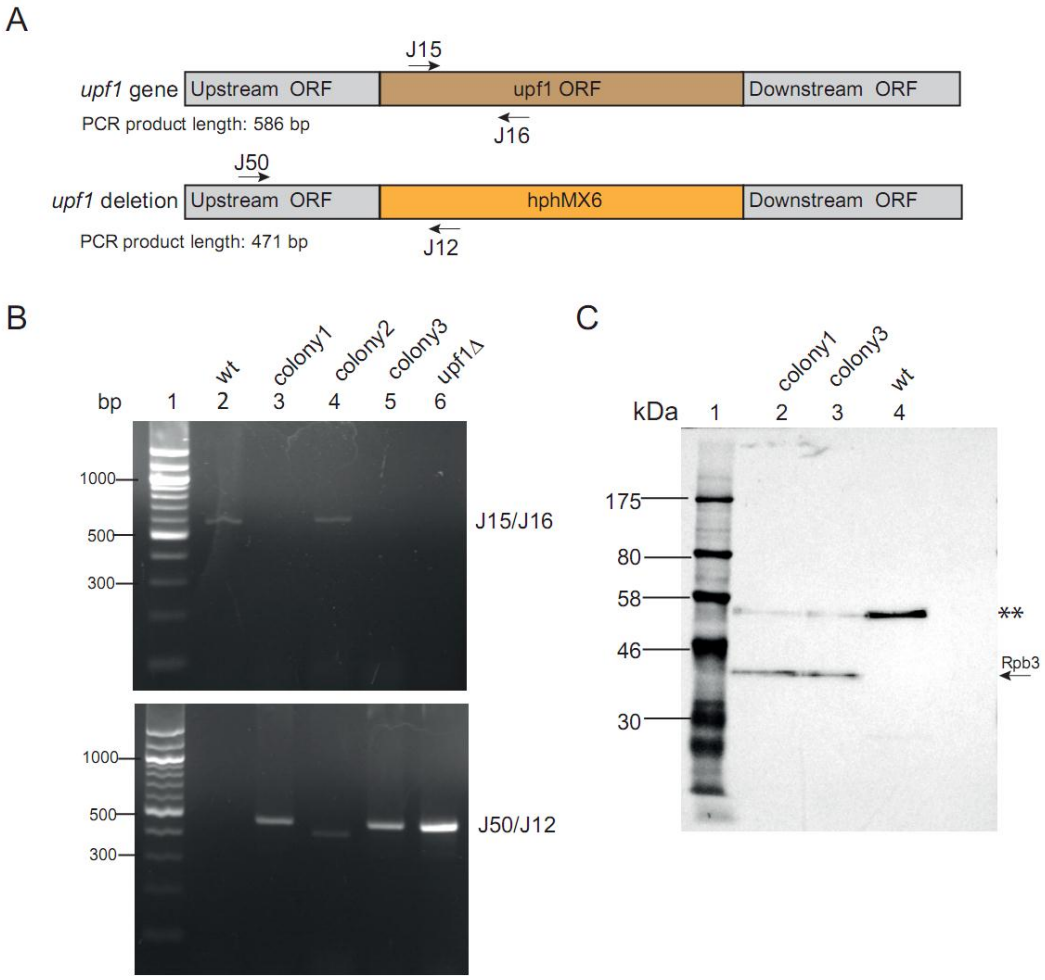

Figure 17. Verification of the deletion of upf1 gene from JM121 strain where *rpb3* was flag tagged. (A) Diagram of the positions of the primers used for validation of *upf1* gene deletion. The primer sequences are listed in Appendix II (B) Confirmation of *upf1* deletion from JM121 by colony PCR. Three individual colonies of potentially constructed strains in lanes 3-5 were checked by colony PCR using primers J15/J16 (upper panel) and J50/J12 (bottom panel). In parallel, the wild type strain was used as a negative control (lane 2), while *upf1Δ* (JM85) (lane 6) was used as positive control. (C) Western blotting detection of FLAG tagged Rpb3 from total protein extract. Total proteins were extracted using the NaOH method as described in Material and Methods. Lanes 2 and 3 were from colonies 1 and 3 respectively; wild type in lane 4 was used as

negative control. A nonspecific band is indicated by asterisks; the arrow indicates the FLAG tagged Rpb3.

4.2.6 Deletion of *upf1* changes the distribution of RNAPII along the genes

To investigate whether the transcription of *pma1* and *gpd3* is affected by the knockout of *upf1*, the association of endogenously FLAG tagged Rpb3 with these genes was examined in wild type (JM121) and *upf1Δ* (JM131) strains by ChIP. In parallel, the *tdh1* gene (glyceraldehyde-3-phosphate dehydrogenase Tdh1) was used as negative control, since it is not bound by Upf1 (Sandip De Ph.D. thesis, 2011). The results showed that Rpb3 loading on *pma1* and *gpd3* genes is increased in the *upf1Δ* mutant, particularly at the 3' end of *pma1*, which shows more than a 2 fold increase (Figure 18A and 18B). However, at the *tdh1* gene, which does not associate with Upf1, deletion of *upf1* shows the opposite effect, resulting in an apparent decrease in RNAPII loading (Figure 18C). Therefore, there was more RNAP II enriched at *pma1* and *gpd3*, but not *tdh1* which is not bound by Upf1.

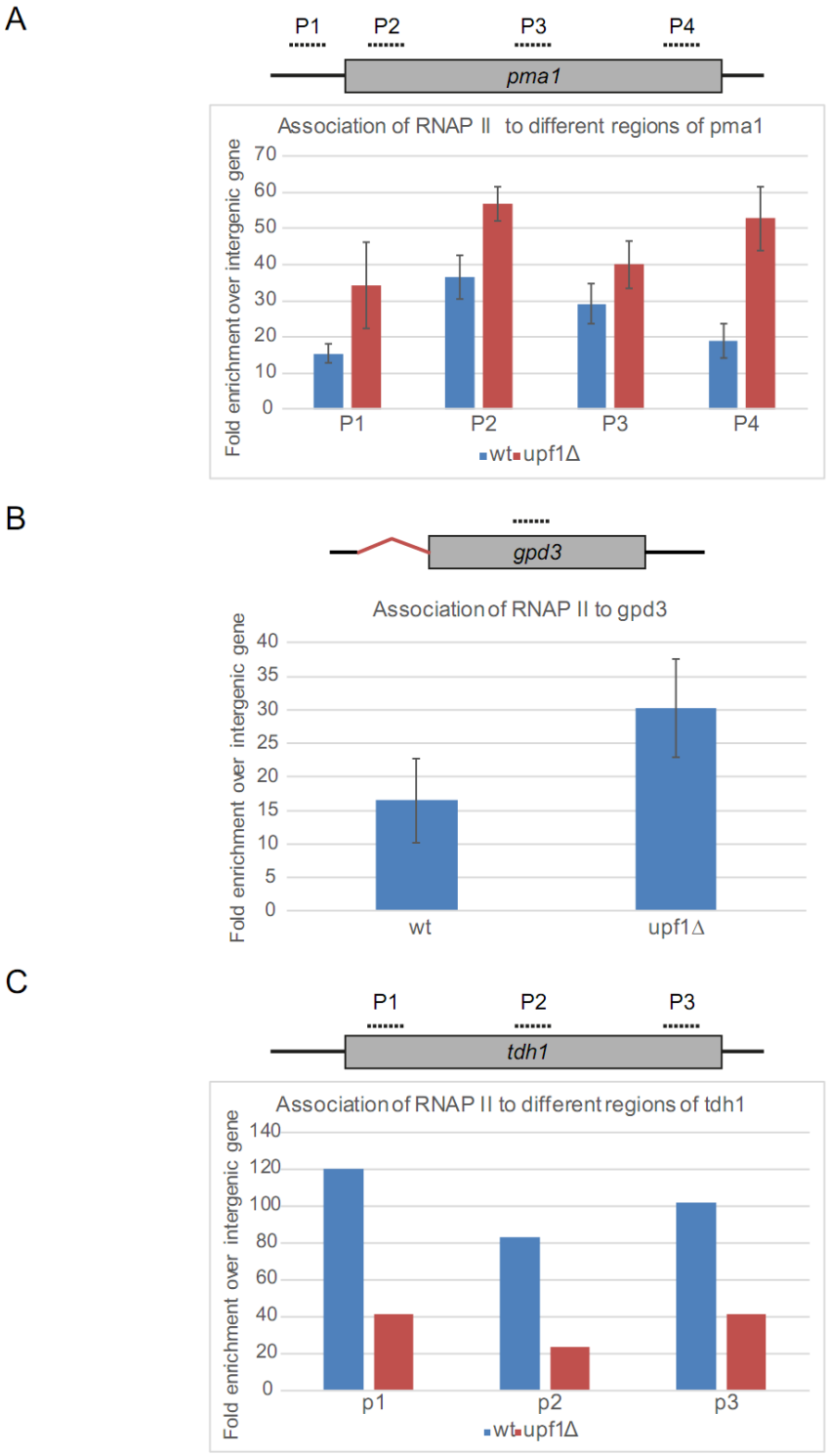

Figure 18. Deletion of *upf1* changes the distribution of RNAPII along the genes. (A-C): The enrichment of RNAPII on *pma1* (A), *gpd3* (B) and *tdh1* (C). The second ChIP protocol in Material and Methods was used to prepare ChIP DNA from JM121 (*flag-*

rpb3) and JM131 (*flag-rpb3*, *upf1Δ*) strains. qPCR was used to examine the enrichment of RNAPII at the tested genes. The positions of the primers are indicated above each gene. Grey box represents the open reading frame; solid black line is the 5' and 3' UTRs; the red solid line denotes the intron. The results are from three independent biological repeats for *pma1* and *gpd3* genes, and once for *tdh1* gene. The error bar denotes the standard deviation (SD). The fold enrichment of the target genes was normalized to the internal reference (intergenic region). The details of the primers are listed in Appendix II, p173.

4.2.7 Optimization of ChIP-Sequencing (ChIP-seq)

As the ChIP protocol used so far yielded little amount of IP DNA, which was not enough for any analysis of genes bound by Rpb3 across the *S. pombe* genome, I used another protocol which was developed by the Bähler lab. This new protocol requires double the amounts of cells (details in Material and Methods). I firstly optimized the DNA sonication cycles, and found the optimal cycle (cycle 7 and 8 in Figure 19A): most of sheared DNA from both cycles is between 200 and 1000 bp, with the average size being around 500 bp. This meets the requirement of ChIP-seq for the size range of sheared DNA. In the new protocol, I also optimized the amount of sheared chromatin used for doing IP and found that using 5 mg of sheared chromatin produces sufficient amount of IP DNA (>10ng in 30 µl purified water), and is not excessive for the fixed amount of anti-FLAG antibody used (Figure 19B). An intergenic region, rDNA, and *nmt1* (4-amino-5-hydroxymethyl-2-methylpyrimidine phosphate synthase Nmt1) are used as negative control, since they are either not transcribed by RNAPII or transcriptionally repressed in YES (thiamine present) (Emmerth et al., 2010; Marguerat et al., 2012). On the other hand, *pma1* is highly transcribed and was therefore used as positive control (Marguerat et al., 2012). For the different amounts of chromatin tested (2 mg, 5 mg. 8.3 mg), there was no enrichment of RNAPII on rDNA, and a little more enrichment on *nmt1* (Figure 19B). However, around a two-fold enrichment of Rpb3 was observed at the intergenic region compared to *nmt1*, suggesting low level transcription of this region (Figure 19B). As expected, RNAPII was enriched most at the *pma1* gene, with about 24-fold enrichment for all of the tested amounts of chromatin when comparing to rDNA (Figure 19B). This indicates that even 8 mg chromatin was not excessive for the antibody. On the other hand, increasing the amount of chromatin resulted in an increase in the total amount of immunoprecipitated nonspecific DNA as

illustrated by analysis of rDNA (Figure 19B). Considering the balance between the yield and specificity of the amount of IP DNA, 5mg chromatin was used for ChIP in the new optimized protocol. In addition, the specificity of the antibody was assessed. In this experiment, rDNA served as negative control, whereas the highly transcribed 60S ribosomal protein gene *rpl1001* was the positive control (Marguerat et al., 2012). In the no-tag strain and *flag-rpb3* (JM121), similar and background levels of rDNA were immunoprecipitated using an anti-FLAG antibody (Figure 19C). Compared to the no-tag strain, there was approximately a 25-fold enrichment of Rpb3 on *rpl1001*, demonstrating the specificity of the antibody in this study (Figure 19C). The finalized ChIP protocol for sequencing the genes bound by Rpb3 across *S. pombe* genome is outlined in the Material and Methods (ChIP protocol number 3).

A

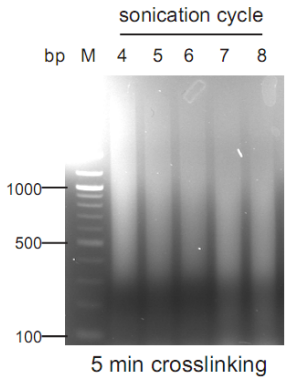
sonication cycle
bp M 4 5 6 7 8
1000
500
100
5 min crosslinking

C

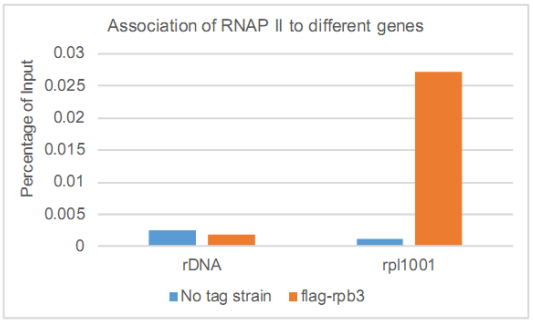
Association of RNAP II to different genes
Percentage of Input
0.03
0.025
0.02
0.015
0.01
0.005
0
rDNA
rpl1001
No tag strain
flag-rpb3

B

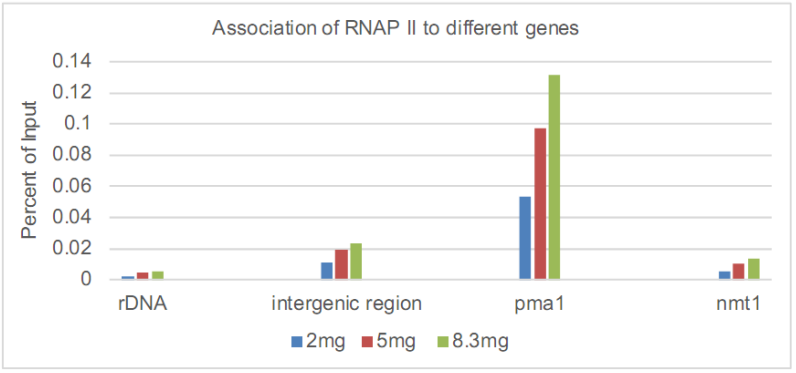
Association of RNAP II to different genes
Percent of Input
0.14
0.12
0.1
0.08
0.06
0.04
0.02
0
rDNA
intergenic region
pma1
nmt1
2mg
5mg
8.3mg

Figure 19. Optimization of ChIP-Seq protocol. (A) Optimization of chromatin fragmentation. 200 ml of an exponentially growing culture of JM121 (*flag-rpb3*) was fixed with 1% formaldehyde for 5 min at 30 ℃. The extracted chromatin was sheared with sonication cycles ranging from 4 to 8. An equal amount of sheared chromatin from each cycle was taken for DNA purification using the phenol-chloroform method as described in Material and Methods. The purified DNA was resolved on a 1.5% agarose gel. (B) Optimization of the amount of chromatin used for ChIP. The extracted chromatin prepared from JM121 was sheared with 8 sonication cycles. 2 mg, 5 mg and 8.3 mg of sheared chromatin was incubated individually with 10 mg of anti-FLAG antibody (Sigma, F1804). The enrichment of Rpb3 at rDNA, an intergenic region, *pma1* and *nmt1* regions was accessed by real-time PCR. The enrichment in the IP sample was normalized to the same Input sample. The experiment was carried out once. (C) Validation of the specificity of the anti-FLAG antibody (Sigma, F1804) used in ChIP-seq. ChIP was performed using the optimized protocol. The enrichment of Rpb3 on rDNA and *rpl1001* either in the wild type strain (No FLAG tag), or in JM121, was assessed by real-time PCR. The enrichment in the IP sample was normalized to the Input sample. The experiment was done once. The details of the primers including for the intergenic region are listed in Appendix II, p173.

4.2.8 Validation of the quality of ChIP samples used for sequencing

Using the newly optimized ChIP protocol, the ChIP samples from JM121 (*flag-rpb3*), JM131 (*flag-rpb3, upf1⊿*), JM94 (*upf1-flag*) and an untagged control strain (JM1) were prepared. The ChIP samples from JM121 and JM131were used to investigate whether the transcription of some genes from RNAP II is affected by the deletion of Upf1; the ChIP sample from JM94 was used to investigate the genome-wide gene binding loci of Upf1; the ChIP sample from untagged strain was used as negative control. To evaluate the quality of these samples which were to be used for sequencing, the enrichment of Rpb3 in JM121 and JM131 at rDNA, *pma1* and *nmt1* were assessed. The enrichment of Upf1 in JM94 on rDNA, *pma1* and *nmt1* was also investigated. The greatest enrichment of Rpb3 on *pma1* in both JM121 and JM131 was observed, with a ratio of 0.34 for JM121 and 0.3 for JM131 (Figure 20A). Rpb3 had around 4-fold less accumulation on nmt1 than *pma1* in both JM121 and JM131 (Figure 20A). As expected, little enrichment of Rpb3 at rDNA was detected in both JM121 (0.012) and JM131 (0.009) as shown in Figure 20A. These results are consistent with the high level of transcription of *pma1* and the repression of *nmt1* transcription (Wood et al., 2012), thus the same ChIP samples can be used for sequencing. However, unlike previous observed more enrichment of Rpb3 on *pma1* in *upf1⊿* (JM131) than in wild type (JM121) studied using P4 primers, no difference was detected using the new optimized protocol in both strains (Figure 18A vs. Figure 20A).

The quality of ChIP samples from the *upf1-flag* strain was also examined. The results showed 2-fold enrichment of Upf1 on rDNA, *pma1* and *nmt1* (Figure 20B). However, using the new protocol and new normalization method, I detected a significantly lower enrichment at all tested genes (Figure 20B vs. Figure 15C and 15D). In summary, analysis of the ChIP results confirmed the expected Pol II enrichment, and although to

a lesser extent, the association of Upf1 with tested genes. I therefore proceeded with high-throughput sequencing of these samples (sequencing was performed but the analysis is in progress).

A

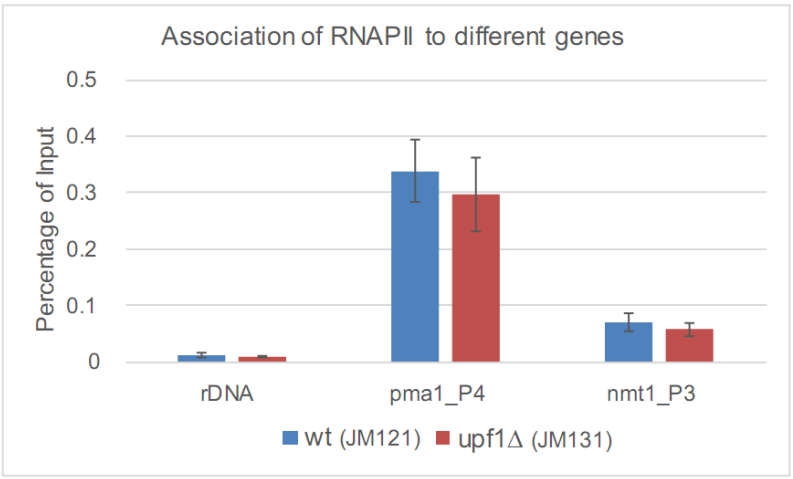

B

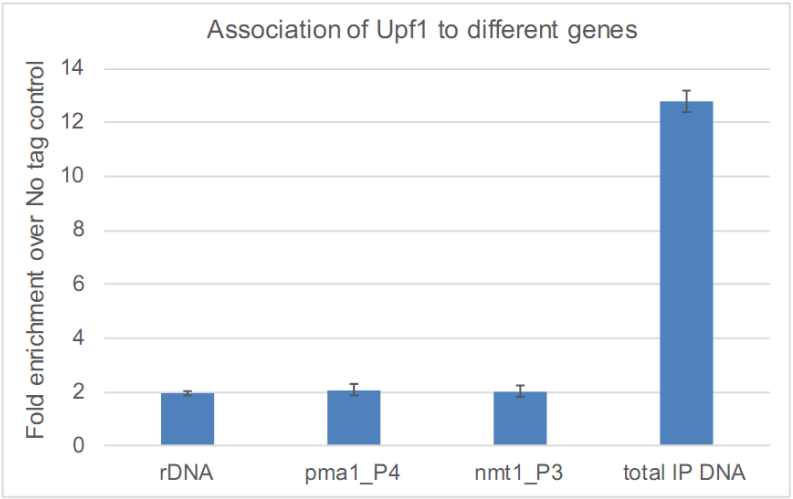

Figure 20. Validation of the quality of ChIP samples used for sequencing. (A) The enrichment of RNAPII on the tested genes. The ChIP DNA from both JM121 (*flag-rpb3*) and JM131 (*flag-rpb3*, *upf1Δ*) strains was prepared following the third ChIP protocol in Material and Methods. The enrichment of RNAPII on rDNA, *pma1* and *nmt1* was assessed by real-time PCR. The enrichment in the IP sample was normalized to the Input sample. The results were based on two independent biological repeats; the error bar shows the SE (standard error). (B) The fold enrichment of Upf1 on the tested genes and the fold enrichment of total IP DNA from *upf1-flag* strain over that from no

tag control strain. The ChIP DNA from both JM94 and the no-tag strain (JM1) were prepared using the same protocol as in (A). The enrichment of Upf1 on rDNA, *pma1* and *nmt1* in JM94 and JM1 was firstly quantified as in (A).The fold enrichment of Upf1 on the tested genes and the total amount of IP DNA from JM94 (*upf1-flag*) was then normalized to that in the no-tag control strain (JM1). The results were based on two independent biological repeats; the error bar is the SE (standard error).

4.3 Discussion

In this Chapter, I described the generation and characterization of a strain expressing Upf1-FLAG. I determined that this tagged Upf1 is functional and therefore used this strain to analyse the association of Upf1 with different genes by ChIP. The functionality is demonstrated by persistence of NMD in the strain (Figure 13C). Using ChIP I found that Upf1-FLAG binds not only protein-coding genes but also non-protein coding genes, including RNA polymerase I transcribed 25S rDNA and RNA polymerase III transcribed tRNA gene loci (Figure 14B and 14C). Unlike the direct binding of human Upf1 to chromatin, the binding of Upf1-FLAG to the chromatin in *S. pombe* is in an RNase sensitive manner, suggesting the binding is through nascent RNA (Figure 15C and 15D) (Azzalin and Lingner, 2006). It is feasible that Upf1 has a direct role in regulating transcription at gene loci at which it is found. To test this hypothesis, the steady state levels of the RNAP II transcribed *tf2* and *pma1* mRNAs, plus RNAP I transcribed 25S rRNA, were quantified in wild type and *upf1Δ*. The levels of *tf2* mRNA and 25S rRNA were increased in *upf1Δ*, whereas the levels of *pma1* mRNA did not significantly change (Figure 16A-16C).

To directly test the hypothesis that Upf1 affects transcription by RNAP II, the *upf1* gene was deleted and RNAP II loading on the genes was assessed by ChIP of a functionally tagged Rpb3 Pol II subunit. My preliminary data suggest that Upf1 might affect the transcription of the genes where it binds (Figure 18C).

To further investigate which genes across the *S. pombe* genome are bound by Upf1 and the transcription of which genes are possibly regulated by Upf1, I prepared the ChIP samples for genome-wide sequencing sequenced. Sequencing has been carried out but the data is yet to be analysed.

Chapter 5

5.0 Genome-wide screening of *upf1* interacting genes

5.1 Summary

As shown in Chapter 3, Upf1 might be involved in maintaining fission yeast genome stability, which is independent of its role in NMD. To further investigate whether Upf1 has additional roles in the nucleus, I used a genome-wide genetic screen to identify genes that have genetic interactions with *upf1* in an attempt to explain why absence of the protein is potentially linked to DNA damage.

The screen required mating an *upf1* deletion strain with a library of deletion mutants in which non-essential genes were knocked out using the kanamycin resistance cassette, KanMX6. To perform the screen, I generated an *upf1* knockout strain (*upf1Δ*) carrying a hygromycin B resistance marker. After mating and sporulation, the strains were plated on double selective media so that only those with both selection markers, the double mutants, could grow. Their growth was compared with that of parental library mutants in order to identify the *upf1* genetic interacting genes. In total, 166 putative *upf1*-interacting genes were identified. Proteins encoded by these genes are involved in various biological functions including translation, transcription, lipid metabolism, vesicle mediated transport and signalling, which indirectly suggests the role of Upf1 in these pathways. In particular, two genes (*air1* and *ppn1*) were chosen from the list to further confirm their synthetic sick with *upf1*, because they are the representatives of genes involved in non-coding RNA (ncRNA) catabolic processes and in mRNA metabolic processes, respectively.

5.2 Results

5.2.1 Marker switch of *upf1Δ* from KanMX6 to HphMX6 cassette

Before carrying out the genetic screen, the standard antibiotic resistant marker in the *upf1* mutant strain needed to be changed from the KanMX6 cassette to a different antibiotic resistance cassette (HphMX6) (Sato et al., 2005). The KanMX6 cassette confers the resistance to the antibiotic Geneticin (G418) in fission yeast, whereas HphMX6 confers resistance to the antibiotic hygromycin B (Sato et al., 2005). Homologous recombination was used to achieve this as described in Materials and Methods. Firstly, the DNA fragment of KanMX6 was amplified by PCR using primers MD1 and MD2 (Figure 21A). Purified DNA was then introduced into the strain JM10 (see Appendix) using *S. pombe* transformation method as described in Materials and Methods. The replacement of KanMX6 with HphMX6 in the newly constructed *upf1* deletion strain was verified by colony PCR (Figure 21B). The constructed hygromycin B-resistant *upf1Δ* was named as JM85.

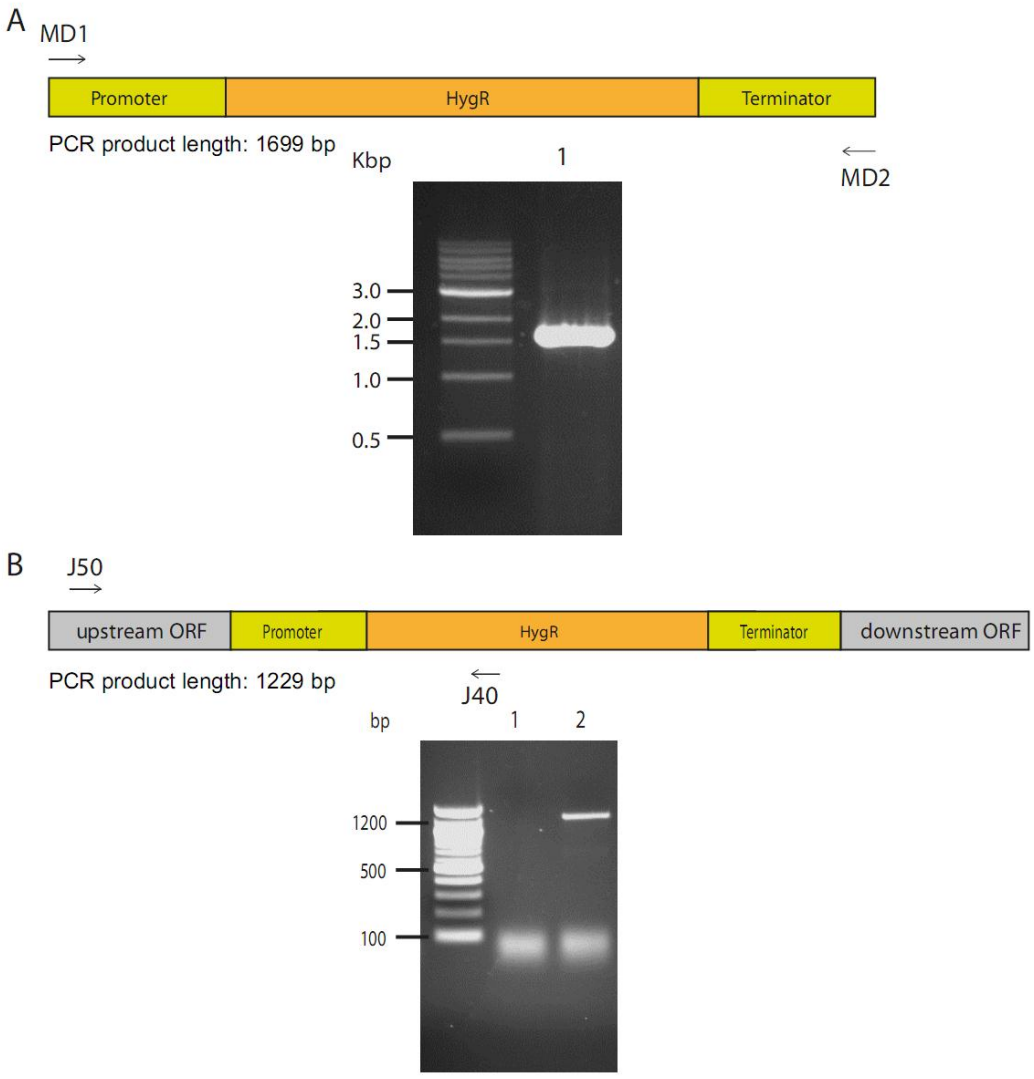

Figure 21. Construction of *upf1* deletion strain with HphMX6 cassette. (A) Amplification of the HphMX6 cassette by PCR. The HphMX6 cassette was amplified by PCR from plasmid DNA pFa6a-hphMX6 using primers MD1 and MD2 (Sato et al., 2005). Top panel illustrates the positions of the primers on the plasmid while the bottom panel shows the corresponding PCR product analysed by agarose gel electrophoresis. (B) Verification of the constructed *upf1* deletion mutant (JM85) by PCR. The JM85 strain was made by the marker swap method and verified by colony PCR as described in Materials and Methods. The primers and their corresponding positions are illustrated

in the upper panel; the lower panel shows the PCR verification result: lane 1 was the negative control (wild type); lane 2 was the JM85 mutant.

5.2.2 Genetic screening to identify potential *upf1* interacting genes

To identify *upf1* interacting genes, JM85 (*upf1Δ*) was mated with an *S. pombe* genome-wide deletion library. The library covers 3400 haploid single deletion mutants. The ORF in each mutant in the library was replaced with the antibiotic resistant cassette KanMX4, which confers resistance to the antibiotic Geneticin (G418) in fission yeast, similar to the KanMX6 cassette used above (Figure 22). After mating, spores were first grown in YES media and then spotted on selective plates (Figure 23A). Their growth was then compared to the parental library single mutants. Four categories were used to describe the results: no genetic interaction- colony size of the potential double mutants is similar to the single mutants; synthetic lethal- no colony of the potential double mutant is formed, when compared to the growth of the single mutants; synthetic sick- colony size of the putative double mutants is smaller than the single mutants; synthetic rescue- colony size of the putative double mutants is larger than the single mutants (Figure 23B). In total, 2747 out of 3308 library mutants were screened, corresponding to 83% of the library strains. The screening procedure was repeated. In total, 166 putative genetic interacting genes or gene products were identified, among which 18 showed synthetic rescue, 11 were synthetic lethal and 137 were synthetic sick with the *upf1* mutant (See appendix V).

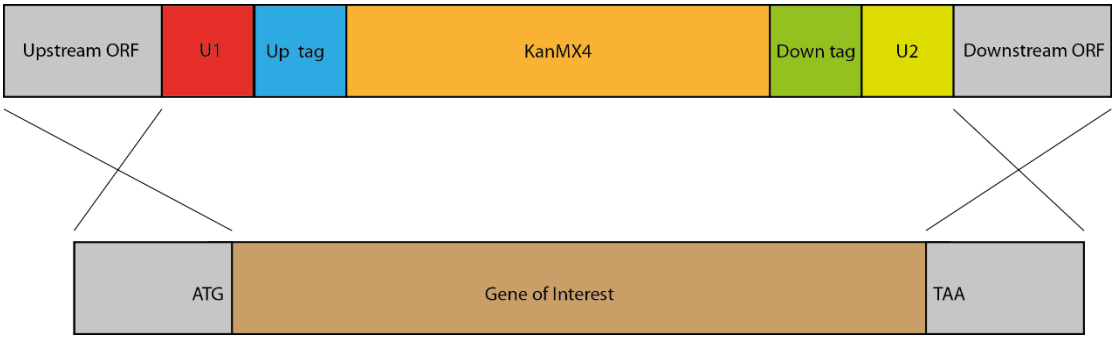

Figure 22. Illustration of the KanMX4 cassette in the Bioneer library. The open reading frame (ORF) of each deleted gene in the library was replaced with the KanMX4 cassette by homologous recombination. Picture was modified from the Bioneer website (http://pombe.bioneer.com/technic_infomation/construction.jsp).

A

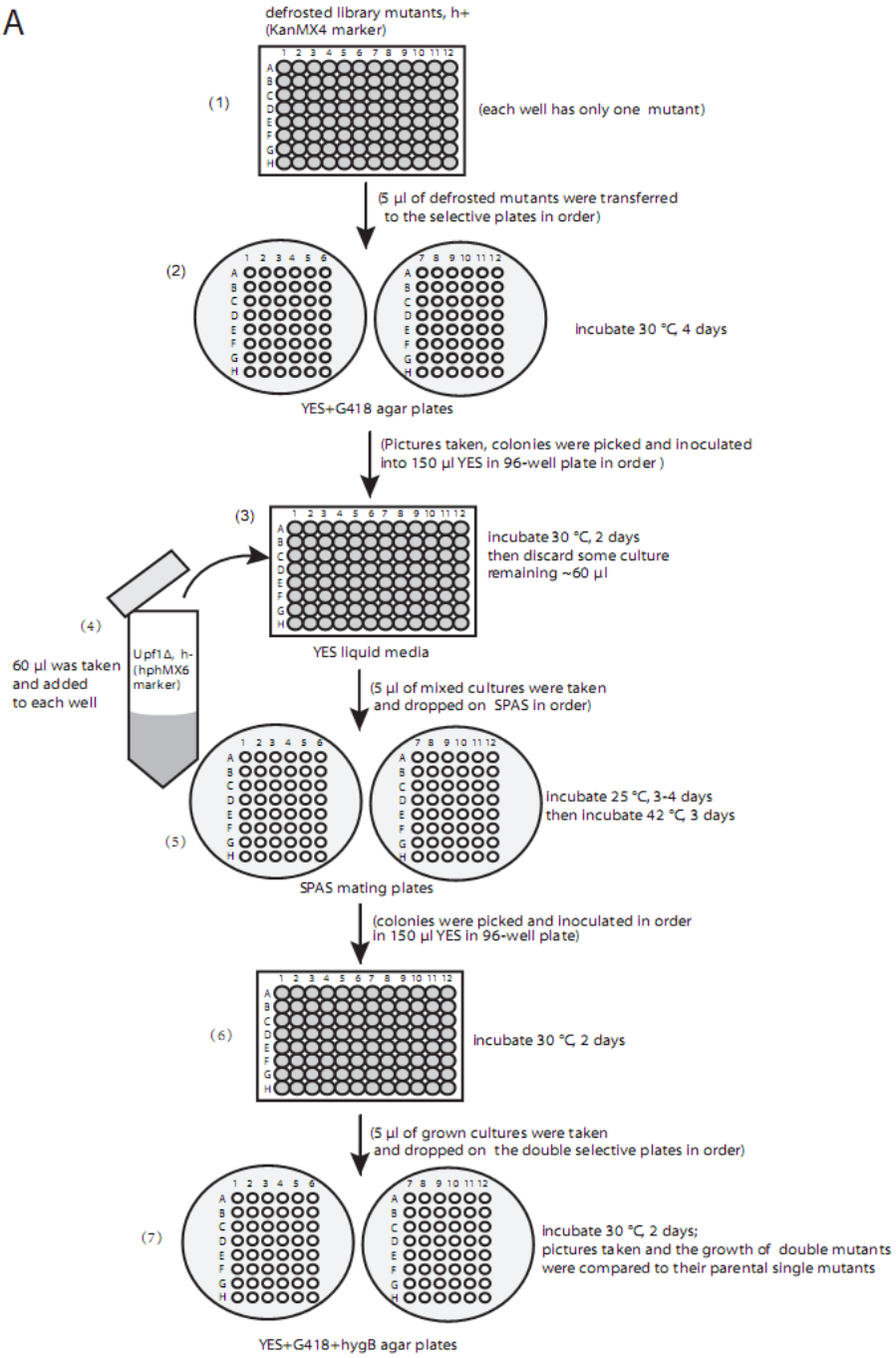
defrosted library mutants, h+
(KanMX4 marker)
(1)
(each well has only one mutant)
(5 µl of defrosted mutants were transferred
to the selective plates in order)
(2)
incubate 30 °C, 4 days
YES+G418 agar plates
(Pictures taken, colonies were picked and inoculated
into 150 µl YES in 96-well plate in order)
(3)
incubate 30 °C, 2 days
then discard some culture
remaining ~60 µl
YES liquid media
(4)
60 µl was taken
and added
to each well
Upf1Δ, h-
(hphMX6
marker)
(5 µl of mixed cultures were taken
and dropped on SPAS in order)
(5)
incubate 25 °C, 3-4 days
then incubate 42 °C, 3 days
SPAS mating plates
(colonies were picked and inoculated in order
in 150 µl YES in 96-well plate)
(6)
incubate 30 °C, 2 days
(5 µl of grown cultures were taken
and dropped on the double selective plates in order)
(7)
incubate 30 °C, 2 days;
pictures taken and the growth of double mutants
were compared to their parental single mutants
YES+G418+hygB agar plates

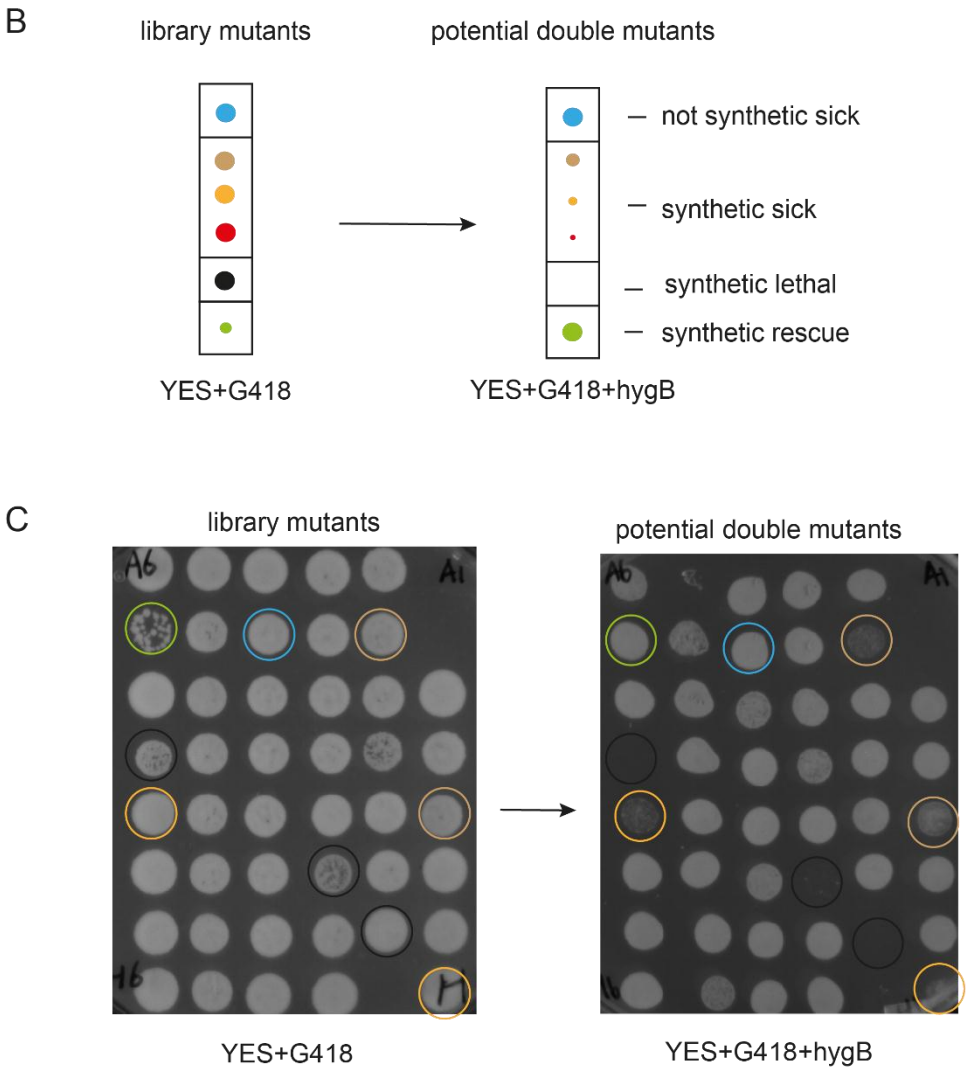

Figure 23. Genome-wide screening of *upf1* putative interacting genes against Bioneer Library. (A) Outline of the systematic genetic screening method. Details are described in Materials and Methods. (B) Illustration of the criteria for evaluating the screening results. After screening, the colony size of the potential double mutants grown on antibiotic plates containing G418 and hygromycin B was compared to their corresponding single mutants grown on YES agar plates containing G418. Blue dot means no genetic interaction; brown, orange and red colour dots stand for synthetic sick; black dot represents synthetic lethal whereas green dot means synthetic rescue. (C) Example of one of the screening results. The coloured circles used here correspond to those used in (B).

5.2.3 Verification of library deletion mutants

The *S. pombe* scientific community has flagged up a number of strains in the Bioneer library that are not those denoted in the database, therefore before drawing any conclusions, the strains which showed putative interactions with *upf1* were checked by colony PCR. Two primer pairs were designed for each mutant, one pair was to check the absence of the gene of interest, whereas another pair was to confirm the integration of the KanMX4 at the position of the gene of interest. For instance, *ste7 (*encoding for arrestin family meiotic suppressor protein, SPAC23E2.03c) and *pab1 (encoding* mRNA export shuttling protein 1, SPAC57A7.04c) showed a synthetic sick phenotype with the *upf1* mutant based on the screening results (See Appendix V). The gene *ste7* was deleted (Figure 24A). I realized that the deletion of the *pab1* in the Bioneer library mutant cannot be verified by colony PCR because of the inappropriate positions of the primers (Figure 27B). The primer position of LP277 is 2614 bp upstream of the start codon of *ste7* gene. The expected PCR product size by LP277 and J12 is 2776 bp. However, the extension time of colony PCR used was only 1 min. It may be not long enough to amplify 2776-bp fragment. In addition, the reverse primer of LP278 is 2248 bp upstream of start codon of *pab1* gene. It is not within the ORF region. Therefore, the primers of LP277 and LP278 cannot be used to verify the presence of *pab1*.

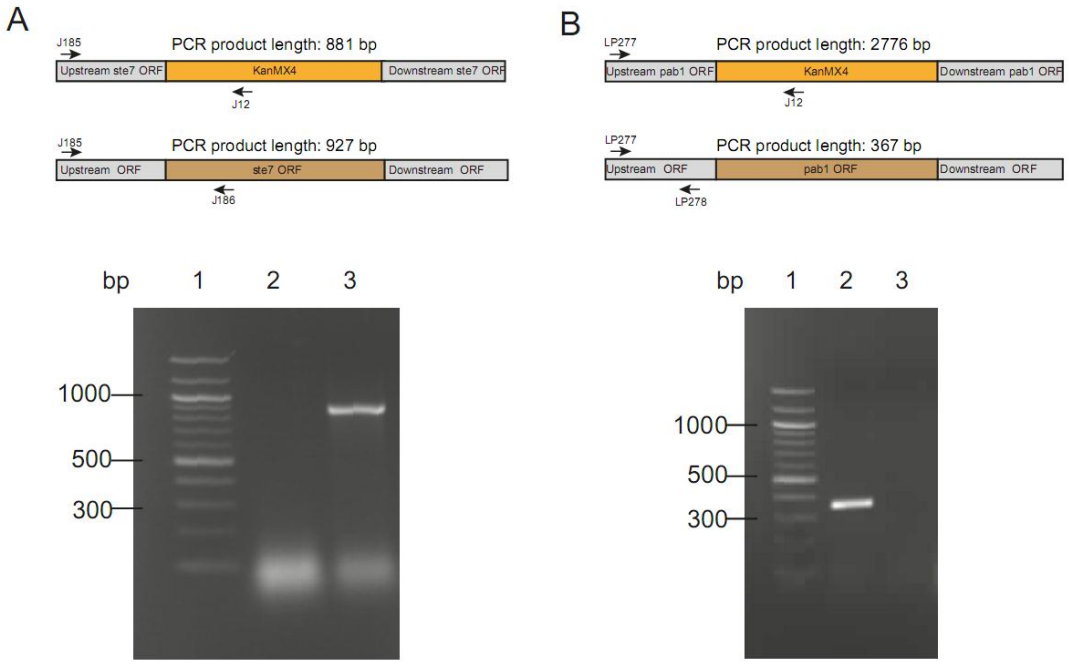

Figure 24. *ste7* is deleted in the Bioneer mutant library. (A) Confirmation of the deletion of *ste7* in library mutant by colony PCR. Deletion of *ste7* gene was verified by PCR using KanMX4 specific primers, J185 and J12 (lane 3) and *ste7* gene specific primers, J185 and J186 (lane 2). (B) Deletion of the *pab1* in the Bioneer library mutant was not confirmed by colony PCR because of the inappropriate positions of the primers. The position of LP277 is 2614 bp upstream of the start codon of *pab1* gene. The gene specific reverse primer LP278 is 2248 bp upstream of the start codon of *pab1* gene. The confirmation primers were of the KanMX4 specific (LP277 and J12, lane 3) and within the 5' untranslated region of *pab1* gene specific (LP277 and LP278, lane 2). Primer positions were indicated on top panel.

5.2.4 Putative *upf1* interacting genes are involved in different biological processes

It is more likely to identify the real *upf1*-intercatig genes from the double mutants which showed a synthetic lethal or strong sick interaction with the *upf1Δ* strain, therefore 27 strains with these representative phenotypes were picked from screening results and checked by colony PCR and 23 of these were correct (Table 1). Two of the genes (*byr1* and *coq3*) showed a synthetic lethal interaction with the *upf1* gene while the remaining showed a synthetic sick interaction with the *upf1* gene (Table 1). These *upf1* interacting genes are involved in different biological processes including translation, transcription, signaling (Table 1). Among those candidates, *ppn1* (SPCC74.02c), *air1* (SPBP35G2.08c), *spt6* (SPAC1F7.01c) are particularly interesting for understanding the potential functions of Upf1 in the regulation of transcription, because they were suggested to have roles in heterochromatin silencing (Buhler et al., 2007; Ivanovska et al., 2011; Kiely et al., 2011; Vanoosthuyse et al., 2014).

Table 1. Library mutants that were verified by colony PCR and showed genetic interaction with the *upf1* mutant

Genetic interaction	Systemic ID	Gene description	*S. pombe* Process Annotations
synthetic lethal	SPAC1D4.13	MAP kinase kinase Byr1	Signaling / Phosphorylation
synthetic lethal	SPCC162.05	hexaprenyldihydroxybenzoate methyltransferase Coq3	Other
synthetic sick	SPAC6B12.15	RACK1 ortholog Cpc2	Translation
synthetic sick	SPBP22H7.08	40S ribosomal protein S10 (predicted)	Ribosome Biogenesis / ncRNA Processing
synthetic sick	SPCC16C4.11	Pho85/PhoA-like cyclin-dependent kinase Pef1	Signaling / Phosphorylation
synthetic sick	SPAC3A11.10c	dipeptidyl peptidase (predicted)	Other
synthetic sick	SPAC4G8.05	serine/threonine protein kinase Ppk14 (predicted)	Signaling / Phosphorylation
synthetic sick	SPBC21C3.13	40S ribosomal protein S19 (predicted)	Translation
synthetic sick	SPAC1F7.01c	nucleosome remodeling protein Spt6	Chromatin / Transcription
synthetic sick	SPAC23E2.03c	arrestin family meiotic suppressor protein Ste7	Signaling / Phosphorylation
synthetic sick	SPBC24C6.06	G-protein alpha subunit	Signaling / Phosphorylation
synthetic sick	SPBP35G2.08c	zinc knuckle TRAMP complex subunit Air1	Ribosome Biogenesis / ncRNA Processing
synthetic sick	SPCC74.02c	mRNA cleavage and polyadenylation specificity factor complex associated protein Ppn1	mRNA Processing
synthetic sick	SPCC31H12.05c	serine/threonine protein phosphatase Sds21	Ribosome Biogenesis / ncRNA Processing
synthetic sick	SPAC31G5.09c	MAP kinase Spk1	Signaling / Phosphorylation
synthetic sick	SPBC14C8.17c	SAGA complex subunit Spt8	Chromatin / Transcription
synthetic sick	SPCC1442.01	guanyl-nucleotide exchange factor Ste6	Signaling / Phosphorylation
synthetic sick	SPAC1565.04c	adaptor protein Ste4	Signaling / Phosphorylation
synthetic sick	SPAC4G8.10	SNARE Gos1 (predicted)	Vesicle Mediated Transport
synthetic sick	SPBC1271.12	oxysterol binding protein (predicted)	Lipid Metabolism
synthetic sick	SPAC25B8.18	mitochondrial thioredoxin-related protein (predicted)	Unknown
synthetic sick	SPAC521.05	40S ribosomal protein S8 (predicted)	Translation
synthetic sick	SPBC365.03c	60S ribosomal protein L21 (predicted)	Translation

5.2.5 Validation of synthetic sick between *ppn1* and *upf1*

From the screening results, *air1* (zinc knuckle TRAMP complex subunit) and *ppn1* (mRNA cleavage and polyadenylation specificity factor complex associated protein) were selected for further confirmation of their synthetic sick with *upf1*, since they were suggested to be involved in heterochromatin silencing and negative regulation of condensin-mediated chromosome condensation, respectively, in *S. pombe* (Buhler et al., 2007; Vanoosthuyse et al., 2014). Spores containing the *upf1Δair1Δ* and *upf1Δppn1Δ* double deletion mutants were isolated by tetrad dissection and verified by colony PCR (Figure 25A and B). The growth assay was then performed to confirm the synthetic sick of *air1* and *ppn1* with *upf1*, and whether overexpression of Upf1 from a plasmid under the control of the *nmt1* promoter could rescue the synthetic sick phenotype of the double mutants. Upf1 from the constructed plasmid was well expressed compared to the negative control (Figure 25C, lane2 and 3). Although the expression of Upf1 under *nmt1* promoter was regulated by thiamine (Figure 25D, lane 3 and 4), its expression was not completely inhibited in the presence of 60 μM thiamine (Figure 25D, lane 3 and 4). Since the leaky expression of Upf1 was also observed when using YES media (Figure 25D, lane 2), the growth assay was done using YES media. Unexpectedly, the *upf1Δair1Δ* mutant did not have any growth defects compared to the growth of *upf1Δ* and *air1Δ* single mutant (Figure 25E) when the YES agar plate was kept at 30°C for 3 days. In comparison, a growth defect of the *upf1Δppn1Δ* double mutant was observed compared to its parental strain (Figure 25F). As expected, the growth defect of the double mutant was rescued in the presence of overexpressed Upf1. In conclusion, under the growth conditions used here, the *ppn1* mutant showed synthetic sick phenotype together with the *upf1* mutation whereas the *air1* mutant did not.

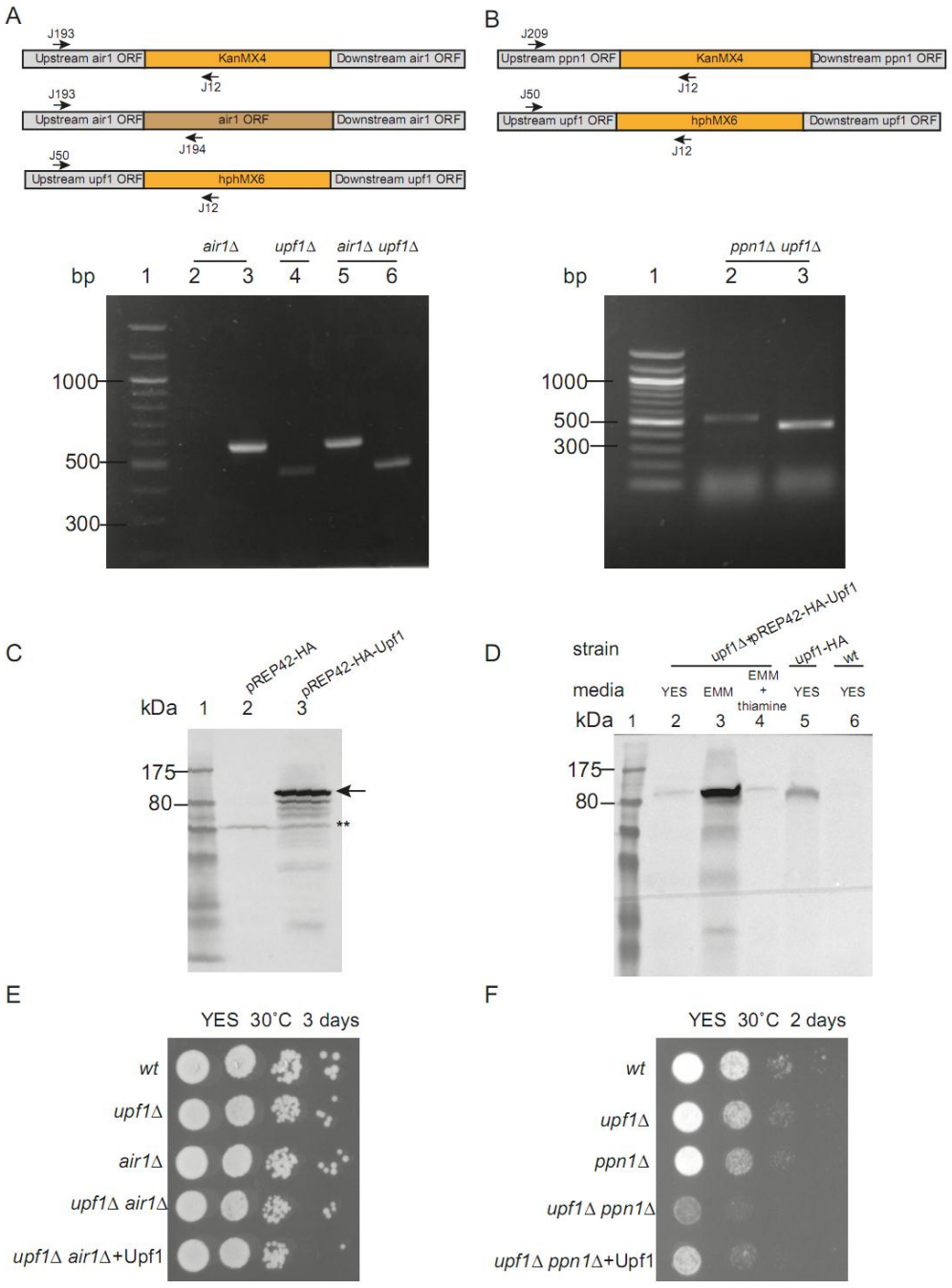

Figure 25. Confirmation of synthetic sick between *ppn1* and *upf1*. (A) Verification of the single *air1Δ, upf1Δ* mutants and the double *upf1Δair1Δ* mutant by colony PCR. The *air1Δ* strain was verified by primers J193 and J194 in lane 2, J193 and J12 in lane 3, respectively; *upf1Δ was* verified by primers J50 and J12 (lane 4) while the double mutant was verified using primers J193 and J12 (lane 5), and J50 and J12 (lane 6). The primer position is indicated in the top panel. (B) Verification of the *ppn1Δupf1Δ* double

mutant by PCR. Primers J209 and J12 were used to confirm the *ppn1* deletion (lane 2), while J50 and J12 were used to validate *upf1* deletion (lane 3). The primer positions are illustrated in the top panel. (C) Detection of the transiently expressed Upf1 by Western blotting. The *upf1Δ* strain JM85 was transformed with either pREP42-HA-Upf1 or the control plasmid pREP42-HA. HA tagged Upf1 was detected from total protein extracts using an anti-HA antibody (12CA5). The HA-Upf1 band is indicated with an arrow in lane 3, while the nonspecific band is indicated by asterisks. Other bands may be the degraded products of HA-Upf1. (D) Expression of HA tagged Upf1 in the *upf1Δ* strain JM85 in different media. HA-Upf1 was assayed by Western blotting as in (C). Samples in lanes 3 and 4 were grown in EMM medium. The medium for sample in lane 4 contained in addition 60 μM thiamine. Endogenously expressed HA-Upf1 (lane 5) was used as a positive control, whereas the wild type strain SPJK002 (lane 6) was used as a negative control. (E-F) *upf1* is not synthetic sick with *air1* (E) but with *ppn1* (F). The strains indicated in the figures were grown in YES until reaching exponential phase. The serially diluted strains were spotted on YES and incubated at 30°C for 3 days (E) or 2 days (F).

5.2.6 The *air1* and *upf1* synthetic sick phenotype is enhanced at low temperature and by DNA replication stress

The slight growth difference between the *upf1Δair1Δ* strain JM140, *upf1Δ* mutant JM85 and *air1Δ* mutant JM139 might be because of their non-related biological function under general growth conditions (30°C on YES). It is likely that the genetic interaction can be observed under temperature stress, as the observation of the genetic interaction between *upf1* and kinetochore protein *mis18* at a higher temperature of 36°C (Hayashi et al., 2014). To test whether the *upf1Δair1Δ* strain JM140 is more sensitive than the parental mutants to temperature stress, a growth assay was carried out at different temperatures including both higher (37°C) and lower temperature (25°C) with or without different concentrations of the replication inhibitor-hydroxyurea (HU). The results showed that the *upf1Δair1Δ* mutant strain grows slower than the wild type SPJK002, *upf1Δ* and *air1Δ* mutant strains at 25°C. The slower growth of the *upf1Δ air1Δ* mutant was recovered to a level comparable to that of *air1Δ* by introducing exogenous Upf1 (Figure 26). *upf1* and *ppn1* deletion also showed a synthetic sick phenotype, which was rescued by overexpressed Upf1 at 25°C (Figure 26). Consistent with the previous observation (Figure 25E and 25F), *upf1Δair1Δ* did not show a synthetic sick phenotype, while *upf1Δppn1Δ* did, at 30°C on YES medium (Figure 26). In the presence of 5 mM HU, *upf1Δair1Δ* was more sensitive than both *upf1Δ* and *air1Δ* individually. Unexpectedly, the synthetic growth defect of *upf1Δair1Δ* in the presence of 5mM HU at 30°C was not rescued when exogenous Upf1 was present (Figure 26). At 37°C, in the presence of 12mM HU, the *upf1Δ* strain was much more sensitive than the wild type, *air1Δ* and *upf1Δ* strains. Overexpression of Upf1 rescued the growth defect of *upf1Δppn1Δ* but not *upf1Δair1Δ* in the presence of 12mM HU at 37°C due to unknown reasons (Figure 26). In conclusion, the synthetic sick phenotype between the

upf1Δ and *ppn1Δ* strains was also observed at 25°C; the *upf1Δ* and *air1Δ* mutants showed only slight synthetic sick phenotype at 25°C. And overexpression of HA tagged Upf1 complements these phenotypes.

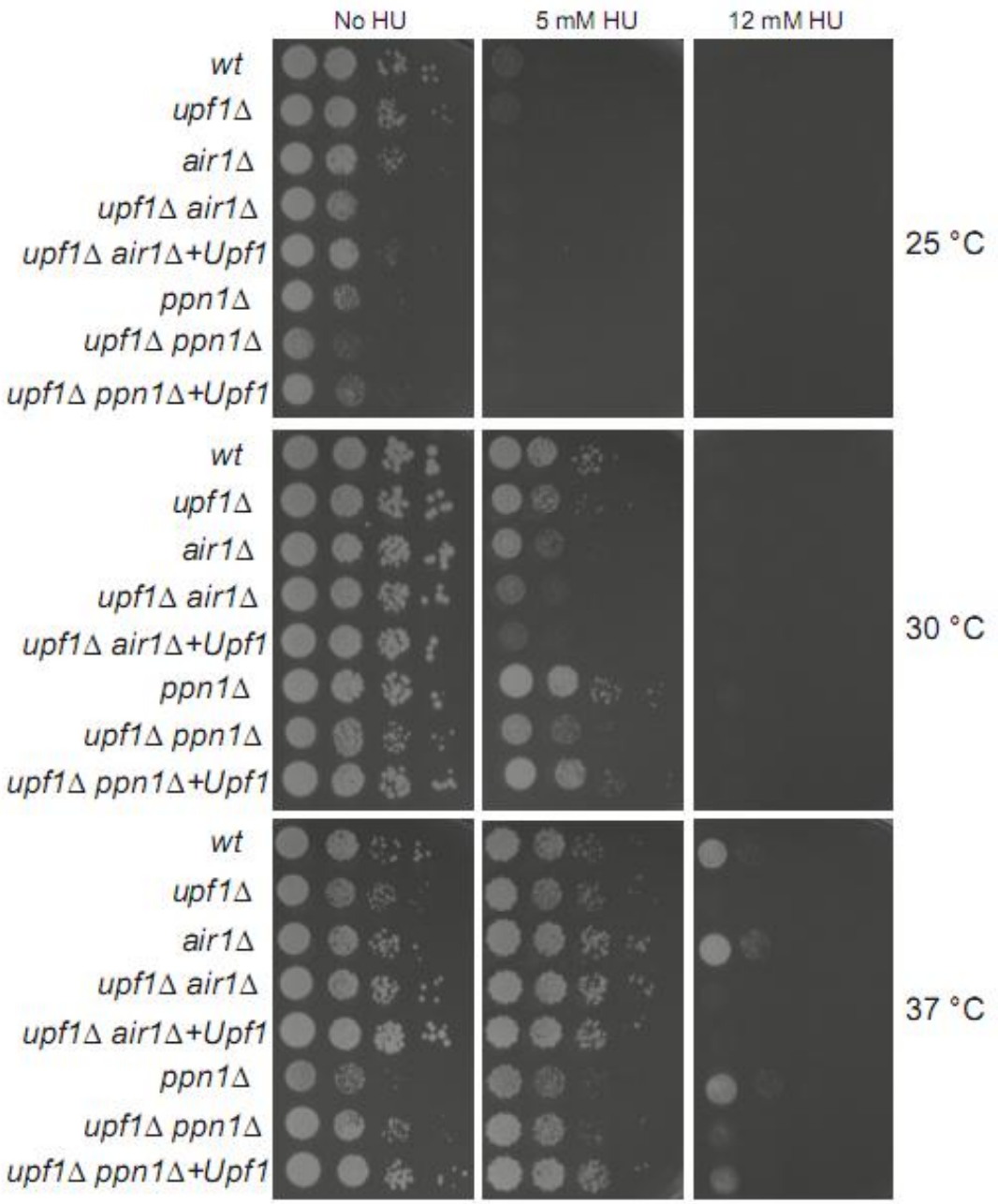

Figure 26. *upf1Δ air1Δ* shows synthetic growth defect at 25°C. The strains with listed genotypes were exponentially grown in YES media at 30°C, and then serially diluted and spotted on YES agar plates with or without different concentrations of HU as indicated in the figure. The plates were kept for 4 days at 25°C, 30°C and 37°C, respectively. Exogenous Upf1 was expressed from the constructed pREP42-HA-Upf1 plasmid. The spot growth assay was done as described in Material and Methods.

5.2.7 Integrating HA tag at the endogenous C terminal of air1 and ppn1

To investigate whether Air1 and Ppn1 physically interact with Upf1 using co-immuoprecipitation (CO-IP) method, I set out to tag the C terminal of Air1 and Ppn1 proteins with HA in a wild type strain, using a highly efficient PCR-based gene targeting method (Krawchuk and Wahls, 1999). This strategy uses plasmid pFA6a-3HA-KanMX6 as a PCR template and increases the length of the flanking sequences homologous to target genes in the genome in order to increase the homologous integration efficiencies (Krawchuk and Wahls, 1999). Two potential *air1*-HA strains were obtained and confirmed by colony PCR (Figure 27A). As expected, the length of the PCR products amplified from HA tagged *air1* strains by primers J310 and J12 was 780 bp (Figure 27A, lanes 5 and 7). In contrast, no PCR products from wild type strain were obtained by the same primers (Figure 27A, lane 3). I also used primers J310 and J311 to further confirm the absence of wild type copy of *air1* gene in the HA tagged *air1* strains. As expected, the 780-bp PCR products were not detected in tagged strains compared to in wild type control (Figure 27A, lanes 4 and 6 vs. lane 2). The expected 2475-bp PCR products by primers J310 and J311 were not detected in tagged strains (Figure 27A, lanes 4 and 6). This might be that the 1-min extension time of colony PCR is not long enough to amplify such large fragments. Based on the colony PCR assays, I obtained two HA-tagged Air strains. However, the expression of HA tagged Air1 was not detected (Figure 27B, lane 2 and 3) by Western blotting compared to the positive control (Figure 27B, lane 5). This may be due to the much lower protein expression level. Indeed, in the vegetative growth stage of *S. pombe*, the average number of Air1 protein is 482.78 molecules per cell which is about 6 times less than that of Upf1 (3387.85 molecules per cell) (Marguerat et al., 2012).

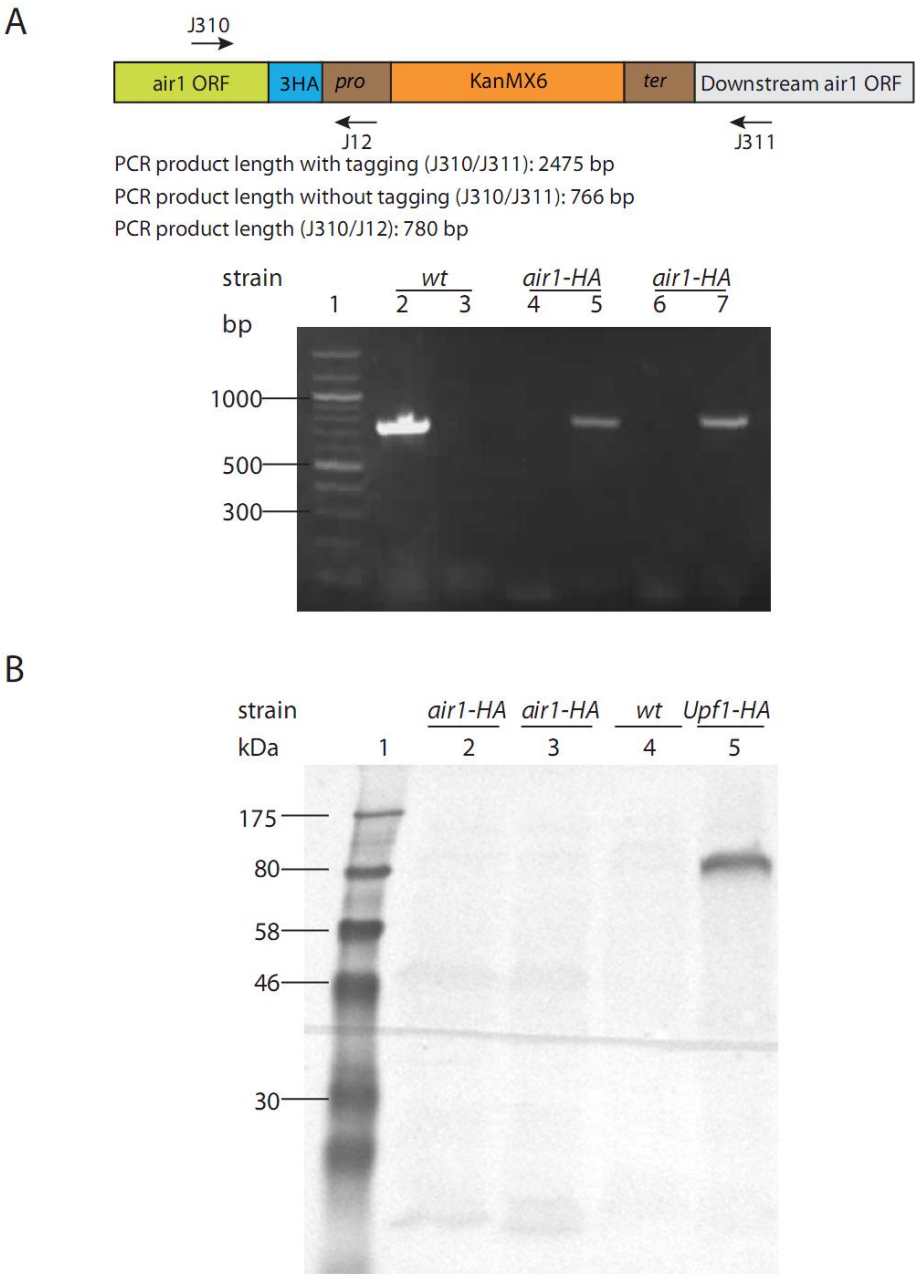

Figure 27. C terminal tagging of endogenous air1 with HA. (A) Verification of HA tagged *air1* by colony PCR. Top panel shows the schematic map of C terminal HA tagging of *air1* and the position of verification primers. Bottom panel shows the PCR verification result. Two potential *air1*-HA strains, labeled on the top of the lanes (lane 4, 5 and lane 6, 7), were confirmed using primers J310 and J311 (lane 4, 6) and primer pair J310 and J12 (lane 5, 7). The wild type strain served as a negative control, checked with primers J310 and J311 (lane2) and primer pair J310 and J12 (lane3). (B)

Verification of Air1-HA expression by Western blotting. Two potential air1-HA strains (A) were examined (lane 2 and 3); wild type was used as a negative control (lane4) whereas Upf1-HA strain was used as a positive control (lane 5).

5.3 Discussion

More *upf1* interacting genes were identified compared to a previous study

In total, 2747 out of 3308 library mutants were screened to identify potential *upf1* interacting genes. This study revealed 166 genes, which may genetically interact with *upf1*, although only 23 mutants were verified by PCR. In contrast, 47 genes were identified as genetically interacting with *upf1* by Ryan and co-workers, when screening 953 mutants (Ryan et al., 2012). The high-throughput screening was carried out using a Singer RoToR station, and the genetic interaction was evaluated using a software toolbox (Ryan et al., 2012). In comparison, the screening in my study relied on manual labour, and the genetic interaction was judged by manually scoring the fitness of the potential double mutants. However, only 7 genes were shared between those identified by Ryan *et al* and my screening results. It is possible that Ryan and co-workers used different criteria for scoring the interaction (Ryan et al., 2012). Both results need to be further confirmed by comparing the growth of the wild type, *upf1* mutant, identified library mutants and their double mutants. Since our screening was not carried out under particular stress such as temperature, and chemical drugs, it is very likely that more genes would be revealed to have a genetic interaction with *upf1*, if selective conditions were applied. One example is that the predicted RNA exonuclease rex2, did not show a genetic interaction with *upf1* unless in the presence of hydrogen peroxide (Matia-Gonzalez et al., 2013). Another example is that the genetic interaction between *upf1* and kinetochore protein *mis18* was more obvious when growing at a higher temperature of 36°C instead of 33°C (Hayashi et al., 2014).

Upf1 might be involved in different biological processes

The genetic interaction between the *upf1* mutant and the 23 library mutants (See Table 1) suggests that Upf1 may be involved in different biological processes. Two genes

from these screening results showed a synthetic lethal phenotype with Upf1: MAP kinase Byr1 and hexaprenyldihydroxybenzoate methyltransferase Coq3 (Table 1). However, it is possible that these synthetic lethalities were not accurate simply because the byr1 mutant was defective in conjugation and sporulation and deletion of coq3 impaired mating efficiency (Nadin-Davis and Nasim, 1988; Sun et al., 2013), therefore, they cannot generate double mutants with the *upf1* mutant. In addition, the synthetic sick results (Table 1) suggest that Upf1 may be involved in translation, signaling, lipid metabolism, vesicle mediated transport, chromatin organization, transcription, mRNA processing, ribosome biogenesis, ncRNA processing and other functions. Upf1 genetically interacted with three genes encoding different 40S ribosomal proteins and one gene encoding the 60S ribosomal protein L21, suggesting a potential role in translation. Physical interaction of Upf1 with ribosome 40S subunit Rps26 in budding yeast was demonstrated by a yeast two-hybrid analysis, also suggesting its role in translation, possibly in the dissociation of the premature termination complex (Min et al., 2013). The potential role of Upf1 in other biological functions, including transcription, revealed by both my screening results and Ryan *et al* may be due to its direct or indirect regulation of RNA expression of identified genes involved in these functions (Ryan et al., 2012). For example, Upf1 in fission yeast not only showed a genetic interaction with RNA exonuclease rex2 but also regulated its transcription, as investigated by a microarray (Rodriguez-Gabriel et al., 2006). However, expression of the genes identified by our genetic screening was not identified in the list of genes whose expression was affected by deletion of *upf1* gene (Rodriguez-Gabriel et al., 2006), suggesting the direct role of Upf1 in the regulation of those process.

upf1 genetically interacts with *air1* and *ppn1*

Air1 is one of the components of the zinc knuckle TRAMP complex which plays a key

role in heterochromatin silencing in *S. pombe*, via recruiting the exosome and/or RNAi machinery (Buhler et al., 2007). Ppn1 is a component of the Cleavage and Polyadenylation Factor (CPF), and negatively regulates condensin-mediated chromosome condensation in *S. pombe*, thus affecting transcription (Vanoosthuyse et al., 2014). The genetic interaction of *upf1* with *air1* and *ppn1* was further confirmed by comparing the growth of their single mutants to that of the double mutants. The *air1 upf1* double mutant did not display a growth defect when grown at 30°C but showed reduced growth than the parental single mutants when at a lower temperature of 25°C, or in the presence of 5mM HU at 30°C (Figure 25E and 26). It is possible that the functional correlation between Upf1 and Air1 was more important under selective conditions such as lower temperature and replication inhibition due to unknown reasons. Unexpectedly, overexpression of Upf1 did not suppress the higher sensitivity of *upf1Δair1Δ* in the presence of HU at both 30°C and 37°C (Figure 26). Since the overexpression plasmid contains a selective leucine marker, it may have been lost when transformants were grown in rich media containing leucine (YES media). The *upf1Δppn1Δ* mutant showed a synthetic sick phenotype which was rescued by overexpression of Upf1 at both 25°C and 30°C (Figure 25F and 26). However, the growth of the *upf1Δppn1Δ* mutant was slightly better at 37°C without or with 5 mM HU than that of *ppn1Δ* (Figure 25F and 26). This could be due to a technical problem or the synthetic sick phenotype of the *upf1Δppn1Δ* strain could somehow be rescued by temperature stress, such as a higher temperature of 37°C. In conclusion, the genetic interaction of Upf1 with Air1 and Ppn1 suggested it has either a direct or indirect role in regulating transcription.

Chapter 6

6.0 Discussion and Conclusions

6.1 Discussion

6.1.1 NMD mutants potentially show increased DNA damage

The sensitivity of all the NMD mutants to HU and MMS initially suggested that NMD directly or indirectly regulates the expression of factors involved in DNA replication or repair (Figure 6 and 8 in Chapter 3). However, none of the known NMD targets have a direct role in DNA replication or repair in *S. pombe* (Matia-Gonzalez et al., 2013). NMD was proposed to regulate the levels of specific mRNAs, which corresponding proteins are important for telomere maintenance due to the observation of the telomere-associated defects in *upf1Δ*, *upf2Δ* and *upf3Δ* in *S. cerevisiae* (Lew et al., 1998). However, these NMD targets that are allegedly important for telomere functions were not identified (Lew et al., 1998). It is possible that NMD has a direct role in DNA replication or repair. The different sensitivity of NMD mutants to HU and MMS treatment may indicate NMD factors may also play different roles in HU and MMS caused DNA damages. Likewise, although there were 201, 48, and 187 genes upregulated in *upf1Δ*, *upf2Δ* and *upf3Δ* strains, respectively, only 10 genes were upregulated in all three NMD mutants, suggesting that the NMD factors also have different roles to one another that are not related to NMD in *S. pombe* (Matia-Gonzalez et al., 2013). HU and MMS treatment stalls DNA replication forks although through different mechanisms. The HU arrests DNA replication by deleting the dNTP pool (Poli et al., 2012), while MMS methylates DNA and thus blocks replication fork movement (Groth et al., 2010; Kumar and Huberman, 2009). In my experiments all strains were sicker at higher temperature (37 ℃) than at lower temperature (30 ℃) in the presence of

the same concentration of MMS (bottom two panels in Figure 6 and Figure 8B in Chapter 3). This may be because of more DNA damage was induced when the cells were treated with MMS at higher temperature (Lundin et al., 2005). The opposite was observed with HU: all of the strains I have tested grew better at higher temperature at the same concentration of HU (top two panels in Figure 6 and Figure 8A in Chapter 3). Although the reason for this is unclear, the damaged DNA might be repaired more efficiently at higher temperature due to the activation of heat shock proteins or it may be partly due to the fact that the HU is more unstable at 37 ℃ than 30 ℃ (Heeney et al., 2004; Velichko et al., 2012).

Although *upf1Δ, upf2Δ* mutants appear to be more sensitive to the chronic DNA replication stress produced by HU or MMS treatment, deletion of these genes did not affect the normal growth of these mutants as the doubling time of these mutants growing in liquid culture and the size of the colonies growing on YES plates differ little from wild type (Figure S3, Figure 6 and 8A and 8B in Chapter 3). In addition, short time HU treatments did not result in dramatic reduction in the viability of the *upf1Δ* mutant (Figure S1 in Appendix). Short-time HU treatment might not lead to DNA damage or the damaged DNA could be repaired by relevant DNA repair pathways.

6.1.2 *upf3Δ* accumulates more ubiquitinated PCNA

Ubiquitination of proliferating cell nuclear antigen (PCNA) interacts with a variety of proteins involved in DNA replication and repair, therefore plays an important role in response to DNA damage in eukaryotes (Frampton et al., 2006). In *S. pombe*, mono and poly-ubiquitination of PCNA was also observed when cells were treated with different DNA damaging agents including ionizing radiation, HU and MMS (Frampton et al., 2006). I investigated the ubiquitination of PCNA in NMD mutants at 30 ℃ and 37 ℃.

At 30 ℃ there was little modified PCNA in wild type and *upf1Δ* strains, and possibly a small amount of ubiquitinated PCNA in a *upf3Δ* strain (lane 1-4 in Figure 9 in Chapter 3) suggesting that few PCNA-related DNA damages were produced in all the strains at 30 ℃. However, the increase in the levels of ubiquitinated PCNA in NMD mutants at 37 ℃ suggested more heat-induced DNA damage in these mutants (lane 6-8 in Figure 9 in Chapter 3). In particular, the significant increase in the amount of ubiquitination of PCNA in the *upf3Δ* strain suggests more DNA damage produced in this mutant (lane 8 in Figure 9 in Chapter 3). However, spot growth assay showed that the *upf3Δ* strain is less sensitive to 12 mM HU, 0.004% and 0.006% MMS than *upf1Δ* and *upf2Δ* mutants (Figure 8A and 8B in Chapter 3). It is possible that the increased levels of ubiquitinated PCNA confers the *upf3Δ* strain the ability to maintain genome stability at 37 ℃. The slight different behaviour of the *upf3Δ* strain compared to the *upf1Δ* and *upf2Δ* strains suggest the possibility that the DNA damage phenotype is not solely due to lack of NMD, as all these mutants show a similar NMD phenotype (Figure 8A and 8B in Chapter3).

6.1.3 NMD mutants display a slow S-phase

Since NMD mutants are more sensitive to MMS and HU as discussed above, they may have DNA replication associated problems. In that case, the resulting damaged DNA will activate checkpoint mechanisms. FACS was used to analyse cell cycle progression in *upf1Δ*, *upf2Δ* and *upf3Δ* mutants. Consistent with expectations, the exponentially growing wild type cells showed a major 2C peak with a smaller 4C peak (Right panel in Figure 10A in Chapter 3). As for the NMD mutants, there was no obvious 4C peak, and more cells with DNA content between 2C and 4C compared to wild type, indicating that cells have delayed S phase and replication problems. This result further confirmed the sensitivity of NMD mutants to chronic HU treatment. Wild type and NMD mutants

were arrested by 4h HU treatment in the early stage of S phase which displays one single Peak (Figure 10B in Chapter 3) suggesting that NMD mutants are not defective in intra S phase checkpoint. However, 4h HU treatment did not completely inhibit *cds1Δ* replication (Figure 10B in Chapter 3), which is defective in intra S-phase checkpoint and would continue DNA replication under replication stress (Sabatinos et al., 2012). The delayed S phase in NMD mutants were further illustrated by FACS after 2.5 h release into fresh media (Figure 10B in Chapter 3).

6.1.4 Rad52 is required to repair the DNA damage occurred in NMD mutants

Since Pku70 and Rad52 are involved in nonhomologous end-joining (NHEJ) and homologous recombination (HR) pathways, respectively. The hypersensitivity of *rad52Δ* than *pku70Δ* to HU suggests that HR pathway is more important in repairing HU caused DNA damage (upper panel in Figure 12A vs. upper panel in Figure 12B in Chapter 3). This is consistent to previous research which showed that HR deletion mutants but not *pku70Δ* showed extreme sensitivity to DNA damaging agents (Manolis et al., 2001). According to the genetic interaction interpretation (Mani et al., 2008), the synthetic sick phenotype of NMD mutants with *rad52Δ* (Figure 12A) might indicate either they act in compensatory pathways or the formation of protein complexes among them. However, there are no published results showing that Rad52 physically interacts with NMD proteins(Wood et al., 2012). It is very likely that lack of NMD proteins results in double strand DNA breaks, and HR is responsible to repair the damaged DNA. Notably, the reduced sensitivity of *upf3Δ rad52Δ* compared to either *upf1Δ rad52Δ* or *upf2Δ rad52Δ* mutants growing on YES at 37℃ (lower panel in Figure 12A in Chapter 3) or in the presence of 1 mM HU at both 30℃ and 37℃ may also indicate the independent function of NMD proteins on maintaining genome stability from their classic roles in NMD surveillance pathway in *S. pombe*.

6.1.5 Upf1 binds chromatin through nascent RNA

The function of Upf1 in DNA replication or repair might be explained by the selective association of Upf1 to the chromatin (Chapter 4). The specific enrichment of Upf1 to the chromatin in this study is consistent to what Sandip De observed using endogenously HA tagged Upf1 strain (Sandip De Ph.D. thesis, 2011). The binding of Upf1 to chromatin in this study was further shown to be dependent on RNA, suggesting a potential role of Upf1 in transcription regulation. Apart from the binding to protein-coding genes, Upf1 was also shown to bind non-protein coding genes through nascent RNA including both RNAPI and RNAPIII transcribed genes. This is not consistent with the classic role of Upf1 in NMD, which is coupled to mRNAs translation (Brogna and Wen, 2009). Therefore, it is likely that Upf1 has an additional direct or indirect role in transcription regulation. Since the transcripts of the *tf2* gene, 25S rDNA that were shown to be bound by Upf1 were upregulated in *upf1Δ* in this study, Upf1 may have a direct role in repression of the transcription of the genes which it binds to. However, the levels of mRNAs of *pma1*bound by Upf1 was not affected by the deletion of Upf1 suggesting that Upf1 does not regulate the transcription of some of the genes which it binds to (Figure 16A). Another possibility is that the transcripts of *pma1* in the absence of Upf1 were upregulated, but co-transcriptionally degraded by the RNA exosome; consistent with this explanation, the exosome of *Schizosaccharomyces pombe* was shown to co-trancriptionally degrade nascent RNA produced from RNAPII backtracking (Lemay et al., 2014). Based on my data, I propose the following model of Upf1in regulating the transcription and maintaining genome stability: The replisome and RNA transcription machinery are travelling along the same gene in the head-on orientation. At some time point, possibly during transcription termination, Upf1 is directly or via unknown RNA-binding proteins recruited to the nascent transcript,

arrests and disassociates the RNA transcription machinery, thus avoiding the clash between the replisome and RNA transcription machinery.

In addition to these findings in this study, two ChIP-seq experiments were optimized and carried out to uncover the genome-wide Upf1 binding sites and the RNAP II loading pattern with or without Upf1 in order to find out the correlation of the specific chromatin-binding feature of Upf1 and the transcription regulation in *S. pombe*. I obtained the raw ChIP-seq data, however, did not finish the analysis, since the data would be analysed by other lab members through the cooperation.

6.1.6 Unbiased genetic screening method was used to reveal the nuclear function of Upf1

In this study, the genome-wide genetic screening method was used to gather further insights into what the nuclear function of Upf1 in *S. pombe* might be. my data show that *upf1*genetically interacts with *ppn1*. Ppn1, the *S. pombe* homologue of vertebrate PNUTS, was identified as a negative regulator of condensin-mediated chromosome condensation (Vanoosthuyse et al., 2014). The functional relationship between *upf1* and *ppn1* as indicated by the genetic interaction also suggests the important role of Upf1 in genome stability and transcription, since mitotic chromosome condensation plays an essential role in genome integrity and an important role in transcription (Vanoosthuyse et al., 2014). I also observed genetic interaction between *upf1* and *spt6* (Suppressor of Ty 6), a conserved RNA polymerase II-interacting histone H3–H4 chaperone that is required for nucleosome restoration in highly transcribed gene loci in *S. cerevisiae* and for heterochromatic silencing in *S. pombe* via regulating several processes including transcription, indicating that Upf1 acts in parallel with Spt6 to regulate transcription and thereby maintain heterochromatin (Ivanovska et al., 2011; Kiely et al., 2011). These results suggest the function of Upf1 in the maintenance of genome stability and in

transcription regulation in *S. pombe*. Additionally, the screening results suggest other roles of Upf1 in cell cycle regulation, translation and signaling.

There are three possible explanations for the possible function of Upf1 in these biological activities. The first one is that these identified *upf1* interacting genes may be a NMD target. However, only the levels of *pef1* (Pho85/PhoA-like cyclin-dependent kinase) mRNAs were found to be upregulated in *upf1Δ* in previous study (Rodriguez-Gabriel et al., 2006). In comparison, the mRNA levels of another *upf1* interacting gene (*SPAC25B8.18*) mRNA levels was downregualted in *upf1Δ* (Rodriguez-Gabriel et al., 2006). The second explanation is that Upf1 protein may physically interact with the protein products of these interacting genes. From the screening results, 40S ribosomal proteins S8, S10 and S19 were shown to genetically interact with Upf1 in this study; they may physically interact with Upf1 just like Rps26 of the 40S ribosomal subunit in budding yeast was demonstrated to specifically associate with Upf1 (Min et al., 2013). The physical interaction between Upf1 protein and the screened gene products need to be verified by either Co-Immunoprecipitation (Co-IP) or yeast two-hybrid assay. The last explanation is that Upf1 may regulate the mRNA levels of specific genes that are important for these screened genes. In other words, loss of Upf1 could indirectly affects the functions of these genes.

Although the genetic screening method used in this study aids to understanding of the comprehensive function of Upf1 in *S. pombe*, these are still several disadvantages. Firstly, the mutant library does not include all the non-essential protein coding genes including *rad52* which has been shown to genetically interact with *upf1* in Chapter 3 in this study. Secondly, the essential genes cannot be tested using this method. Finally, the *upf1* interacting genes that are required for responses to particular environmental growth stresses such as addition of replication drugs, oxidative chemicals, changes of

growing temperature were not identified under normal growth condition in this study (Anver et al., 2014; Hayashi et al., 2014; Matia-Gonzalez et al., 2013; Rodriguez-Gabriel et al., 2006). To address the problems as mentioned above, many more protein coding genes that are not included in the library should be studied; conditional strains like temperature-sensitive mutants of the essential genes could be used in the screening; different types of growth conditions should be applied to the screening.

6.2 Conclusions

My data demonstrate that the NMD key factors Upf1, Upf2 and Upf3 are required for *S. pombe* genome stability. This observations cannot fully explained by their classic role in NMD, because the three NMD mutants do not have the same DNA damage phenotypes. The observations I presented here, together with those previously made in the lab, suggest instead that DNA damage might be a consequence of lack of these proteins at transcription sites. The conclusion is based on our extensive evidence of specific RNA-dependent association of Upf1 with different transcription sites, encoding both protein-coding genes and con-coding RNAs. ChIP-seq experiments are being performed to test whether the occupancy of RNA polymerase II at these loci is affected by the absence of Upf1. The results of these experiments would allow to test the prediction that Upf1 has a role in regulating transcription of the genes that it binds to, and therefore maintain the genome stability by coordination of the replication and transcription at these gene loci in *S. pombe*.

References

Abruzzi, K.C., Lacadie, S., and Rosbash, M. (2004). Biochemical analysis of TREX complex recruitment to intronless and intron-containing yeast genes. EMBO J *23*, 2620-2631.

Aguilera, A., and Gomez-Gonzalez, B. (2008). Genome instability: a mechanistic view of its causes and consequences. Nat Rev Genet *9*, 204-217.

Amrani, N., Ganesan, R., Kervestin, S., Mangus, D.A., Ghosh, S., and Jacobson, A. (2004). A faux 3'-UTR promotes aberrant termination and triggers nonsense-mediated mRNA decay. Nature *432*, 112-118.

Anders, K.R., Grimson, A., and Anderson, P. (2003). SMG-5, required for C.elegans nonsense-mediated mRNA decay, associates with SMG-2 and protein phosphatase 2A. EMBO J *22*, 641-650.

Anver, S., Roguev, A., Zofall, M., Krogan, N.J., Grewal, S.I., and Harmer, S.L. (2014). Yeast X-chromosome-associated protein 5 (Xap5) functions with H2A.Z to suppress aberrant transcripts. EMBO Rep *15*, 894-902.

Applequist, S.E., Selg, M., Raman, C., and Jack, H.M. (1997). Cloning and characterization of HUPF1, a human homolog of the Saccharomyces cerevisiae nonsense mRNA-reducing UPF1 protein. Nucleic Acids Res *25*, 814-821.

Aronoff, R., Baran, R., and Hodgkin, J. (2001). Molecular identification of smg-4, required for mRNA surveillance in C. elegans. Gene *268*, 153-164.

Atkin, A.L., Altamura, N., Leeds, P., and Culbertson, M.R. (1995). The majority of yeast UPF1 co-localizes with polyribosomes in the cytoplasm. Mol Biol Cell *6*, 611-625.

Azzalin, C.M., and Lingner, J. (2006). The human RNA surveillance factor UPF1 is required for S phase progression and genome stability. Curr Biol *16*, 433-439.

Azzalin, C.M., Reichenbach, P., Khoriauli, L., Giulotto, E., and Lingner, J. (2007). Telomeric repeat containing RNA and RNA surveillance factors at mammalian chromosome ends. Science *318*, 798-801.

Bahler, J., Wu, J.Q., Longtine, M.S., Shah, N.G., McKenzie, A., 3rd, Steever, A.B., Wach, A., Philippsen, P., and Pringle, J.R. (1998). Heterologous modules for efficient and versatile PCR-based gene targeting in Schizosaccharomyces pombe. Yeast *14*, 943-951.

Bentley, D.L. (2014). Coupling mRNA processing with transcription in time and space. Nat Rev Genet *15*, 163-175.

Bhattacharya, A., Czaplinski, K., Trifillis, P., He, F., Jacobson, A., and Peltz, S.W. (2000). Characterization of the biochemical properties of the human Upf1 gene product that is involved in nonsense-mediated mRNA decay. RNA *6*, 1226-1235.

Brogna, S., and Wen, J. (2009). Nonsense-mediated mRNA decay (NMD) mechanisms. Nat Struct Mol Biol *16*, 107-113.

Brognard, J., Niederst, M., Reyes, G., Warfel, N., and Newton, A.C. (2009). Common polymorphism in the phosphatase PHLPP2 results in reduced regulation of Akt and protein kinase C. J Biol Chem *284*, 15215-15223.

Buhler, M., Haas, W., Gygi, S.P., and Moazed, D. (2007). RNAi-dependent and -independent RNA turnover mechanisms contribute to heterochromatic gene silencing. Cell *129*, 707-721.

Buschini, A., Carboni, P., Martino, A., Poli, P., and Rossi, C. (2003). Effects of temperature on baseline and genotoxicant-induced DNA damage in haemocytes of Dreissena polymorpha. Mutat Res *537*, 81-92.

Cali, B.M., Kuchma, S.L., Latham, J., and Anderson, P. (1999). smg-7 is required for mRNA surveillance in Caenorhabditis elegans. Genetics *151*, 605-616.

Carastro, L.M., Tan, C.K., Selg, M., Jack, H.M., So, A.G., and Downey, K.M. (2002). Identification of delta helicase as the bovine homolog of HUPF1: demonstration of an interaction with the third subunit of DNA polymerase delta. Nucleic Acids Res *30*, 2232-2243.

Carlson, C.R., Grallert, B., Stokke, T., and Boye, E. (1999). Regulation of the start of DNA replication in Schizosaccharomyces pombe. J Cell Sci *112 (Pt 6)*, 939-946.

Carmody, S.R., and Wente, S.R. (2009). mRNA nuclear export at a glance. J Cell Sci *122*, 1933-1937.

Celik, A., Kervestin, S., and Jacobson, A. (2015). NMD: At the crossroads between translation termination and ribosome recycling. Biochimie *114*, 2-9.

Chan, W.K., Bhalla, A.D., Le Hir, H., Nguyen, L.S., Huang, L., Gecz, J., and Wilkinson, M.F. (2009). A UPF3-mediated regulatory switch that maintains RNA surveillance. Nat Struct Mol Biol *16*, 747-753.

Chawla, R., Redon, S., Raftopoulou, C., Wischnewski, H., Gagos, S., and Azzalin, C.M. (2011). Human UPF1 interacts with TPP1 and telomerase and sustains telomere leading-strand replication. EMBO J *30*, 4047-4058.

Chiu, S.Y., Serin, G., Ohara, O., and Maquat, L.E. (2003). Characterization of human Smg5/7a: a protein with similarities to Caenorhabditis elegans SMG5 and SMG7 that functions in the dephosphorylation of Upf1. RNA *9*, 77-87.

Cho, H., Park, O.H., Park, J., Ryu, I., Kim, J., Ko, J., and Kim, Y.K. (2015). Glucocorticoid receptor interacts with PNRC2 in a ligand-dependent manner to recruit UPF1 for rapid mRNA degradation. Proc Natl Acad Sci U S A *112*, E1540-1549.

Choe, J., Ahn, S.H., and Kim, Y.K. (2014). The mRNP remodeling mediated by UPF1 promotes rapid degradation of replication-dependent histone mRNA. Nucleic Acids Res *42*, 9334-9349.

Collart, M.A., and Oliviero, S. (2001). Preparation of yeast RNA. Curr Protoc Mol Biol *Chapter 13*, Unit13 12.

Cooper, G.M. (2000). The cell : a molecular approach, 2nd edn (Washington, D.C.Sunderland, Mass.: ASM Press ;Sinauer Associates).

Cui, Y., Hagan, K.W., Zhang, S., and Peltz, S.W. (1995). Identification and characterization of genes that are required for the accelerated degradation of mRNAs containing a premature translational termination codon. Genes Dev *9*, 423-436.

Culbertson, M.R., and Neeno-Eckwall, E. (2005). Transcript selection and the recruitment of mRNA decay factors for NMD in Saccharomyces cerevisiae. RNA *11*, 1333-1339.

Cusack, B.P., Arndt, P.F., Duret, L., and Roest Crollius, H. (2011). Preventing dangerous nonsense: selection for robustness to transcriptional error in human genes. PLoS Genet *7*, e1002276.

Czaplinski, K., Weng, Y., Hagan, K.W., and Peltz, S.W. (1995). Purification and characterization of the Upf1 protein: a factor involved in translation and mRNA degradation. RNA *1*, 610-623.

Dixon, S.J., Fedyshyn, Y., Koh, J.L., Prasad, T.S., Chahwan, C., Chua, G., Toufighi, K., Baryshnikova, A., Hayles, J., Hoe, K.L., *et al.* (2008). Significant conservation of synthetic lethal genetic interaction networks between distantly related eukaryotes. Proc Natl Acad Sci U S A *105*, 16653-16658.

Durand, S., and Lykke-Andersen, J. (2013). Nonsense-mediated mRNA decay occurs during eIF4F-dependent translation in human cells. Nat Struct Mol Biol *20*, 702-709.

Eberle, A.B., Herrmann, K., Jack, H.M., and Muhlemann, O. (2009). Equal transcription rates of productively and nonproductively rearranged immunoglobulin mu heavy chain alleles in a pro-B cell line. RNA *15*, 1021-1028.

Emmerth, S., Schober, H., Gaidatzis, D., Roloff, T., Jacobeit, K., and Buhler, M. (2010). Nuclear retention of fission yeast dicer is a prerequisite for RNAi-mediated heterochromatin assembly. Dev Cell *18*, 102-113.

Ferreira, M.G., and Cooper, J.P. (2004). Two modes of DNA double-strand break repair are reciprocally regulated through the fission yeast cell cycle. Genes Dev *18*, 2249-2254.

Fiorini, F., Bagchi, D., Le Hir, H., and Croquette, V. (2015). Human Upf1 is a highly processive RNA helicase and translocase with RNP remodelling activities. Nat Commun *6*, 7581.

Fiorini, F., Boudvillain, M., and Le Hir, H. (2013). Tight intramolecular regulation of the human Upf1 helicase by its N- and C-terminal domains. Nucleic Acids Res *41*, 2404-2415.

Forsburg, S.L. (2001). The art and design of genetic screens: yeast. Nat Rev Genet *2*, 659-668.

Forsburg, S.L. (2003a). Growth and manipulation of S. pombe. Curr Protoc Mol Biol *Chapter 13*, Unit 13 16.

Forsburg, S.L. (2003b). Introduction of DNA into S. pombe cells. Curr Protoc Mol Biol *Chapter 13*, Unit 13 17.

Forsburg, S.L. (2003c). Overview of Schizosaccharomyces pombe. Curr Protoc Mol Biol *Chapter 13*, Unit 13 14.

Forsburg, S.L. (2003d). S. pombe strain maintenance and media. Curr Protoc Mol Biol *Chapter 13*, Unit 13 15.

Forsburg, S.L., and Rhind, N. (2006). Basic methods for fission yeast. Yeast *23*, 173-183.

Frampton, J., Irmisch, A., Green, C.M., Neiss, A., Trickey, M., Ulrich, H.D., Furuya, K., Watts, F.Z., Carr, A.M., and Lehmann, A.R. (2006). Postreplication repair and PCNA modification in Schizosaccharomyces pombe. Mol Biol Cell *17*, 2976-2985.

Gaba, A., Jacobson, A., and Sachs, M.S. (2005). Ribosome occupancy of the yeast CPA1 upstream open reading frame termination codon modulates nonsense-mediated mRNA decay. Mol Cell *20*, 449-460.

Gao, Q., Das, B., Sherman, F., and Maquat, L.E. (2005). Cap-binding protein 1-mediated and eukaryotic translation initiation factor 4E-mediated pioneer rounds of translation in yeast. Proc Natl Acad Sci U S A *102*, 4258-4263.

Gatfield, D., Unterholzner, L., Ciccarelli, F.D., Bork, P., and Izaurralde, E. (2003). Nonsense-mediated mRNA decay in Drosophila: at the intersection of the yeast and mammalian pathways. EMBO J *22*, 3960-3970.

Gehring, N.H., Neu-Yilik, G., Schell, T., Hentze, M.W., and Kulozik, A.E. (2003). Y14 and hUpf3b form an NMD-activating complex. Mol Cell *11*, 939-949.

Gong, C., and Maquat, L.E. (2011). lncRNAs transactivate STAU1-mediated mRNA decay by duplexing with 3' UTRs via Alu elements. Nature *470*, 284-288.

Gonzalez, C.I., Bhattacharya, A., Wang, W., and Peltz, S.W. (2001). Nonsense-mediated mRNA decay in Saccharomyces cerevisiae. Gene *274*, 15-25.

Green, M.R., Sambrook, J., and Sambrook, J. (2012). Molecular cloning : a laboratory manual, 4th edn (Cold Spring Harbor, N.Y.: Cold Spring Harbor Laboratory Press).

Grimson, A., O'Connor, S., Newman, C.L., and Anderson, P. (2004). SMG-1 is a phosphatidylinositol kinase-related protein kinase required for nonsense-mediated mRNA Decay in Caenorhabditis elegans. Mol Cell Biol *24*, 7483-7490.

Groth, P., Auslander, S., Majumder, M.M., Schultz, N., Johansson, F., Petermann, E., and Helleday, T. (2010). Methylated DNA causes a physical block to replication forks independently of damage signalling, O(6)-methylguanine or DNA single-strand breaks and results in DNA damage. J Mol Biol *402*, 70-82.

Gudikote, J.P., and Wilkinson, M.F. (2002). T-cell receptor sequences that elicit strong down-regulation of premature termination codon-bearing transcripts. EMBO J *21*, 125-134.

Hayashi, T., Ebe, M., Nagao, K., Kokubu, A., Sajiki, K., and Yanagida, M. (2014). Schizosaccharomyces pombe centromere protein Mis19 links Mis16 and Mis18 to recruit CENP-A through interacting with NMD factors and the SWI/SNF complex. Genes Cells *19*, 541-554.

He, F., Brown, A.H., and Jacobson, A. (1996). Interaction between Nmd2p and Upf1p is required for activity but not for dominant-negative inhibition of the nonsense-mediated mRNA decay pathway in yeast. RNA *2*, 153-170.

He, F., Brown, A.H., and Jacobson, A. (1997). Upf1p, Nmd2p, and Upf3p are interacting components of the yeast nonsense-mediated mRNA decay pathway. Mol Cell Biol *17*, 1580-1594.

He, F., and Jacobson, A. (1995). Identification of a novel component of the nonsense-mediated mRNA decay pathway by use of an interacting protein screen. Genes Dev *9*, 437-454.

He, F., Peltz, S.W., Donahue, J.L., Rosbash, M., and Jacobson, A. (1993). Stabilization and ribosome association of unspliced pre-mRNAs in a yeast upf1- mutant. Proc Natl Acad Sci U S A *90*, 7034-7038.

Heeney, M.M., Whorton, M.R., Howard, T.A., Johnson, C.A., and Ware, R.E. (2004). Chemical and functional analysis of hydroxyurea oral solutions. J Pediatr Hematol Oncol *26*, 179-184.

Hodgkin, J., Papp, A., Pulak, R., Ambros, V., and Anderson, P. (1989). A new kind of informational suppression in the nematode Caenorhabditis elegans. Genetics *123*, 301-313.

Holla, O.L., Kulseth, M.A., Berge, K.E., Leren, T.P., and Ranheim, T. (2009). Nonsense-mediated decay of human LDL receptor mRNA. Scand J Clin Lab Invest *69*, 409-417.

Hosoda, N., Kim, Y.K., Lejeune, F., and Maquat, L.E. (2005). CBP80 promotes interaction of Upf1 with Upf2 during nonsense-mediated mRNA decay in mammalian cells. Nat Struct Mol Biol *12*, 893-901.

Imamachi, N., Tani, H., and Akimitsu, N. (2012). Up-frameshift protein 1 (UPF1): multitalented entertainer in RNA decay. Drug Discov Ther *6*, 55-61.

Ishigaki, Y., Li, X., Serin, G., and Maquat, L.E. (2001). Evidence for a pioneer round of mRNA translation: mRNAs subject to nonsense-mediated decay in mammalian cells are bound by CBP80 and CBP20. Cell *106*, 607-617.

Ivanovska, I., Jacques, P.E., Rando, O.J., Robert, F., and Winston, F. (2011). Control of chromatin structure by spt6: different consequences in coding and regulatory regions. Mol Cell Biol *31*, 531-541.

Jacobs, J.Z., Ciccaglione, K.M., Tournier, V., and Zaratiegui, M. (2014). Implementation of the CRISPR-Cas9 system in fission yeast. Nat Commun *5*, 5344.

Kadlec, J., Guilligay, D., Ravelli, R.B., and Cusack, S. (2006). Crystal structure of the UPF2-interacting domain of nonsense-mediated mRNA decay factor UPF1. RNA *12*, 1817-1824.

Kadlec, J., Izaurralde, E., and Cusack, S. (2004). The structural basis for the interaction between nonsense-mediated mRNA decay factors UPF2 and UPF3. Nat Struct Mol Biol *11*, 330-337.

Kaygun, H., and Marzluff, W.F. (2005). Regulated degradation of replication-dependent histone mRNAs requires both ATR and Upf1. Nat Struct Mol Biol *12*, 794-800.

Kiely, C.M., Marguerat, S., Garcia, J.F., Madhani, H.D., Bahler, J., and Winston, F. (2011). Spt6 is required for heterochromatic silencing in the fission yeast Schizosaccharomyces pombe. Mol Cell Biol *31*, 4193-4204.

Kim, S.H., Koroleva, O.A., Lewandowska, D., Pendle, A.F., Clark, G.P., Simpson, C.G., Shaw, P.J., and Brown, J.W. (2009). Aberrant mRNA transcripts and the nonsense-mediated decay proteins UPF2 and UPF3 are enriched in the Arabidopsis nucleolus. Plant Cell *21*, 2045-2057.

Kim, V.N., Kataoka, N., and Dreyfuss, G. (2001a). Role of the nonsense-mediated decay factor hUpf3 in the splicing-dependent exon-exon junction complex. Science *293*, 1832-1836.

Kim, V.N., Yong, J., Kataoka, N., Abel, L., Diem, M.D., and Dreyfuss, G. (2001b). The Y14 protein communicates to the cytoplasm the position of exon-exon junctions. EMBO J *20*, 2062-2068.

Kim, Y.K., Furic, L., Desgroseillers, L., and Maquat, L.E. (2005). Mammalian Staufen1 recruits Upf1 to specific mRNA 3'UTRs so as to elicit mRNA decay. Cell *120*, 195-208.

Kim, Y.K., Furic, L., Parisien, M., Major, F., DesGroseillers, L., and Maquat, L.E. (2007). Staufen1 regulates diverse classes of mammalian transcripts. EMBO J *26*, 2670-2681.

Knutsen, J.H., Rein, I.D., Rothe, C., Stokke, T., Grallert, B., and Boye, E. (2011). Cell-cycle analysis of fission yeast cells by flow cytometry. PLoS One *6*, e17175.

Koulintchenko, M., Vengrova, S., Eydmann, T., Arumugam, P., and Dalgaard, J.Z. (2012). DNA polymerase alpha (swi7) and the flap endonuclease Fen1 (rad2) act together in the S-phase alkylation damage response in S. pombe. PLoS One *7*, e47091.

Krawchuk, M.D., and Wahls, W.P. (1999). High-efficiency gene targeting in Schizosaccharomyces pombe using a modular, PCR-based approach with long tracts of flanking homology. Yeast *15*, 1419-1427.

Kudo, N., Wolff, B., Sekimoto, T., Schreiner, E.P., Yoneda, Y., Yanagida, M., Horinouchi, S., and Yoshida, M. (1998). Leptomycin B inhibition of signal-mediated nuclear export by direct binding to CRM1. Exp Cell Res *242*, 540-547.

Kumar, S., and Huberman, J.A. (2009). Checkpoint-dependent regulation of origin firing and replication fork movement in response to DNA damage in fission yeast. Mol Cell Biol *29*, 602-611.

Le Hir, H., Gatfield, D., Izaurralde, E., and Moore, M.J. (2001). The exon-exon junction complex provides a binding platform for factors involved in mRNA export and nonsense-mediated mRNA decay. EMBO J *20*, 4987-4997.

Le Hir, H., Izaurralde, E., Maquat, L.E., and Moore, M.J. (2000). The spliceosome deposits multiple proteins 20-24 nucleotides upstream of mRNA exon-exon junctions. EMBO J *19*, 6860-6869.

Leeds, P., Peltz, S.W., Jacobson, A., and Culbertson, M.R. (1991). The product of the yeast UPF1 gene is required for rapid turnover of mRNAs containing a premature translational termination codon. Genes Dev *5*, 2303-2314.

Leeds, P., Wood, J.M., Lee, B.S., and Culbertson, M.R. (1992). Gene products that promote mRNA turnover in Saccharomyces cerevisiae. Mol Cell Biol *12*, 2165-2177.

Lejeune, F., Ishigaki, Y., Li, X., and Maquat, L.E. (2002). The exon junction complex is detected on CBP80-bound but not eIF4E-bound mRNA in mammalian cells: dynamics of mRNP remodeling. EMBO J *21*, 3536-3545.

Lemay, J.F., Larochelle, M., Marguerat, S., Atkinson, S., Bahler, J., and Bachand, F. (2014). The RNA exosome promotes transcription termination of backtracked RNA polymerase II. Nat Struct Mol Biol *21*, 919-926.

Lew, J.E., Enomoto, S., and Berman, J. (1998). Telomere length regulation and telomeric chromatin require the nonsense-mediated mRNA decay pathway. Mol Cell Biol *18*, 6121-6130.

Lewis, B.P., Green, R.E., and Brenner, S.E. (2003). Evidence for the widespread coupling of alternative splicing and nonsense-mediated mRNA decay in humans. Proc Natl Acad Sci U S A *100*, 189-192.

Longman, D., Plasterk, R.H., Johnstone, I.L., and Caceres, J.F. (2007). Mechanistic insights and identification of two novel factors in the C. elegans NMD pathway. Genes Dev *21*, 1075-1085.

Lord, C.J., and Ashworth, A. (2012). The DNA damage response and cancer therapy. Nature *481*, 287-294.

Lundin, C., North, M., Erixon, K., Walters, K., Jenssen, D., Goldman, A.S., and Helleday, T. (2005). Methyl methanesulfonate (MMS) produces heat-labile DNA damage but no detectable in vivo DNA double-strand breaks. Nucleic Acids Res *33*, 3799-3811.

Lykke-Andersen, J., Shu, M.D., and Steitz, J.A. (2000). Human Upf proteins target an mRNA for nonsense-mediated decay when bound downstream of a termination codon. Cell *103*, 1121-1131.

Maderazo, A.B., Belk, J.P., He, F., and Jacobson, A. (2003). Nonsense-containing mRNAs that accumulate in the absence of a functional nonsense-mediated mRNA decay pathway are destabilized rapidly upon its restitution. Mol Cell Biol *23*, 842-851.

Mani, R., St Onge, R.P., Hartman, J.L.t., Giaever, G., and Roth, F.P. (2008). Defining genetic interaction. Proc Natl Acad Sci U S A *105*, 3461-3466.

Manolis, K.G., Nimmo, E.R., Hartsuiker, E., Carr, A.M., Jeggo, P.A., and Allshire, R.C. (2001). Novel functional requirements for non-homologous DNA end joining in Schizosaccharomyces pombe. EMBO J *20*, 210-221.

Marchetti, M.A., Kumar, S., Hartsuiker, E., Maftahi, M., Carr, A.M., Freyer, G.A., Burhans, W.C., and Huberman, J.A. (2002). A single unbranched S-phase DNA damage and replication fork blockage checkpoint pathway. Proc Natl Acad Sci U S A *99*, 7472-7477.

Marguerat, S., Schmidt, A., Codlin, S., Chen, W., Aebersold, R., and Bahler, J. (2012). Quantitative analysis of fission yeast transcriptomes and proteomes in proliferating and quiescent cells. Cell *151*, 671-683.

Martin, F., Schaller, A., Eglite, S., Schumperli, D., and Muller, B. (1997). The gene for histone RNA hairpin binding protein is located on human chromosome 4 and encodes a novel type of RNA binding protein. EMBO J *16*, 769-778.

Marzluff, W.F., Wagner, E.J., and Duronio, R.J. (2008). Metabolism and regulation of canonical histone mRNAs: life without a poly(A) tail. Nat Rev Genet *9*, 843-854.

Matia-Gonzalez, A.M., Hasan, A., Moe, G.H., Mata, J., and Rodriguez-Gabriel, M.A. (2013). Functional characterization of Upf1 targets in Schizosaccharomyces pombe. RNA Biol *10*, 1057-1065.

Matsuo, Y., Asakawa, K., Toda, T., and Katayama, S. (2006). A rapid method for protein extraction from fission yeast. Biosci Biotechnol Biochem *70*, 1992-1994.

Matsuyama, A., Arai, R., Yashiroda, Y., Shirai, A., Kamata, A., Sekido, S., Kobayashi, Y., Hashimoto, A., Hamamoto, M., Hiraoka, Y., *et al.* (2006). ORFeome cloning and global analysis of protein localization in the fission yeast Schizosaccharomyces pombe. Nat Biotechnol *24*, 841-847.

Mendell, J.T., ap Rhys, C.M., and Dietz, H.C. (2002). Separable roles for rent1/hUpf1 in altered splicing and decay of nonsense transcripts. Science *298*, 419-422.

Mendell, J.T., Medghalchi, S.M., Lake, R.G., Noensie, E.N., and Dietz, H.C. (2000). Novel Upf2p orthologues suggest a functional link between translation initiation and nonsense surveillance complexes. Mol Cell Biol *20*, 8944-8957.

Metzstein, M.M., and Krasnow, M.A. (2006). Functions of the nonsense-mediated mRNA decay pathway in Drosophila development. PLoS Genet *2*, e180.

Min, E.E., Roy, B., Amrani, N., He, F., and Jacobson, A. (2013). Yeast Upf1 CH domain interacts with Rps26 of the 40S ribosomal subunit. RNA *19*, 1105-1115.

Mitchell, S.F., Jain, S., She, M., and Parker, R. (2013). Global analysis of yeast mRNPs. Nat Struct Mol Biol *20*, 127-133.

Mortensen, U.H., Lisby, M., and Rothstein, R. (2009). Rad52. Curr Biol *19*, R676-677.

Muhlemann, O., Eberle, A.B., Stalder, L., and Zamudio Orozco, R. (2008). Recognition and elimination of nonsense mRNA. Biochim Biophys Acta *1779*, 538-549.

Muller, B., Blackburn, J., Feijoo, C., Zhao, X., and Smythe, C. (2007). DNA-activated protein kinase functions in a newly observed S phase checkpoint that links histone mRNA abundance with DNA replication. J Cell Biol *179*, 1385-1398.

Nadin-Davis, S.A., and Nasim, A. (1988). A gene which encodes a predicted protein kinase can restore some functions of the ras gene in fission yeast. EMBO J *7*, 985-993.

Nakayashiki, H., Kadotani, N., and Mayama, S. (2006). Evolution and diversification of RNA silencing proteins in fungi. J Mol Evol *63*, 127-135.

Nasmyth, K.A. (1977). Temperature-sensitive lethal mutants in the structural gene for DNA ligase in the yeast Schizosaccharomyces pombe. Cell *12*, 1109-1120.

Ninio, J. (1991). Transient mutators: a semiquantitative analysis of the influence of translation and transcription errors on mutation rates. Genetics *129*, 957-962.

Noguchi, C., Garabedian, M.V., Malik, M., and Noguchi, E. (2008). A vector system for genomic FLAG epitope-tagging in Schizosaccharomyces pombe. Biotechnol J *3*, 1280-1285.

Noguchi, E., Ansbach, A.B., Noguchi, C., and Russell, P. (2009). Assays used to study the DNA replication checkpoint in fission yeast. Methods Mol Biol *521*, 493-507.

Ohnishi, T., Yamashita, A., Kashima, I., Schell, T., Anders, K.R., Grimson, A., Hachiya, T., Hentze, M.W., Anderson, P., and Ohno, S. (2003). Phosphorylation of hUPF1 induces formation of mRNA surveillance complexes containing hSMG-5 and hSMG-7. Mol Cell *12*, 1187-1200.

Page, M.F., Carr, B., Anders, K.R., Grimson, A., and Anderson, P. (1999). SMG-2 is a phosphorylated protein required for mRNA surveillance in Caenorhabditis elegans and related to Upf1p of yeast. Mol Cell Biol *19*, 5943-5951.

Papamichos-Chronakis, M., and Peterson, C.L. (2013). Chromatin and the genome integrity network. Nat Rev Genet *14*, 62-75.

Park, E., Gleghorn, M.L., and Maquat, L.E. (2013). Staufen2 functions in Staufen1-mediated mRNA decay by binding to itself and its paralog and promoting UPF1 helicase but not ATPase activity. Proc Natl Acad Sci U S A *110*, 405-412.

Park, E., and Maquat, L.E. (2013). Staufen-mediated mRNA decay. Wiley Interdiscip Rev RNA *4*, 423-435.

Petermann, E., Orta, M.L., Issaeva, N., Schultz, N., and Helleday, T. (2010). Hydroxyurea-stalled replication forks become progressively inactivated and require two different RAD51-mediated pathways for restart and repair. Mol Cell *37*, 492-502.

Pfeifer, G.P., and Besaratinia, A. (2012). UV wavelength-dependent DNA damage and human non-melanoma and melanoma skin cancer. Photochem Photobiol Sci *11*, 90-97.

Poli, J., Tsaponina, O., Crabbe, L., Keszthelyi, A., Pantesco, V., Chabes, A., Lengronne, A., and Pasero, P. (2012). dNTP pools determine fork progression and origin usage under replication stress. EMBO J *31*, 883-894.

Pulak, R., and Anderson, P. (1993). mRNA surveillance by the Caenorhabditis elegans smg genes. Genes Dev *7*, 1885-1897.

Raji, H., and Hartsuiker, E. (2006). Double-strand break repair and homologous recombination in Schizosaccharomyces pombe. Yeast *23*, 963-976.

Rodriguez-Gabriel, M.A., Watt, S., Bahler, J., and Russell, P. (2006). Upf1, an RNA helicase required for nonsense-mediated mRNA decay, modulates the transcriptional response to oxidative stress in fission yeast. Mol Cell Biol *26*, 6347-6356.

Rufener, S.C., and Muhlemann, O. (2013). eIF4E-bound mRNPs are substrates for nonsense-mediated mRNA decay in mammalian cells. Nat Struct Mol Biol *20*, 710-717.

Ryan, C.J., Roguev, A., Patrick, K., Xu, J., Jahari, H., Tong, Z., Beltrao, P., Shales, M., Qu, H., Collins, S.R., *et al.* (2012). Hierarchical modularity and the evolution of genetic interactomes across species. Mol Cell *46*, 691-704.

Sabatinos, S.A., and Forsburg, S.L. (2009). Measuring DNA content by flow cytometry in fission yeast. Methods Mol Biol *521*, 449-461.

Sabatinos, S.A., Green, M.D., and Forsburg, S.L. (2012). Continued DNA synthesis in replication checkpoint mutants leads to fork collapse. Mol Cell Biol *32*, 4986-4997.

Sacher, M., Pfander, B., Hoege, C., and Jentsch, S. (2006). Control of Rad52 recombination activity by double-strand break-induced SUMO modification. Nat Cell Biol *8*, 1284-1290.

Sambrook, J., and Russell, D.W. (2001). Molecular cloning : a laboratory manual, 3rd ed. edn (Cold Spring Harbor, N.Y.: Cold Spring Harbor Laboratory Press).

Sato, M., Dhut, S., and Toda, T. (2005). New drug-resistant cassettes for gene disruption and epitope tagging in Schizosaccharomyces pombe. Yeast *22*, 583-591.

Schroder, P.A., and Moore, M.J. (2005). Association of ribosomal proteins with nascent transcripts in S. cerevisiae. RNA *11*, 1521-1529.

Serin, G., Gersappe, A., Black, J.D., Aronoff, R., and Maquat, L.E. (2001). Identification and characterization of human orthologues to Saccharomyces cerevisiae Upf2 protein and Upf3 protein (Caenorhabditis elegans SMG-4). Mol Cell Biol *21*, 209-223.

Shikata, M., Ishikawa, F., and Kanoh, J. (2007). Tel2 is required for activation of the Mrc1-mediated replication checkpoint. J Biol Chem *282*, 5346-5355.

Shirley, R.L., Lelivelt, M.J., Schenkman, L.R., Dahlseid, J.N., and Culbertson, M.R. (1998). A factor required for nonsense-mediated mRNA decay in yeast is exported from the nucleus to the cytoplasm by a nuclear export signal sequence. J Cell Sci *111 (Pt 21)*, 3129-3143.

Siede, W., Friedl, A.A., Dianova, I., Eckardt-Schupp, F., and Friedberg, E.C. (1996). The Saccharomyces cerevisiae Ku autoantigen homologue affects radiosensitivity only in the absence of homologous recombination. Genetics *142*, 91-102.

Sinha, R.P., and Hader, D.P. (2002). UV-induced DNA damage and repair: a review. Photochem Photobiol Sci *1*, 225-236.

Su, Y., Meador, J.A., Geard, C.R., and Balajee, A.S. (2010). Analysis of ionizing radiation-induced DNA damage and repair in three-dimensional human skin model system. Exp Dermatol *19*, e16-22.

Sun, L.L., Li, M., Suo, F., Liu, X.M., Shen, E.Z., Yang, B., Dong, M.Q., He, W.Z., and Du, L.L. (2013). Global analysis of fission yeast mating genes reveals new autophagy factors. PLoS Genet *9*, e1003715.

Vanoosthuyse, V., Legros, P., van der Sar, S.J., Yvert, G., Toda, K., Le Bihan, T., Watanabe, Y., Hardwick, K., and Bernard, P. (2014). CPF-associated phosphatase activity opposes condensin-mediated chromosome condensation. PLoS Genet *10*, e1004415.

Velichko, A.K., Petrova, N.V., Kantidze, O.L., and Razin, S.V. (2012). Dual effect of heat shock on DNA replication and genome integrity. Mol Biol Cell *23*, 3450-3460.

Wang, W., Cajigas, I.J., Peltz, S.W., Wilkinson, M.F., and Gonzalez, C.I. (2006). Role for Upf2p phosphorylation in Saccharomyces cerevisiae nonsense-mediated mRNA decay. Mol Cell Biol *26*, 3390-3400.

Wang, Z.F., Whitfield, M.L., Ingledue, T.C., 3rd, Dominski, Z., and Marzluff, W.F. (1996). The protein that binds the 3' end of histone mRNA: a novel RNA-binding protein required for histone pre-mRNA processing. Genes Dev *10*, 3028-3040.

Wen, J., and Brogna, S. (2010). Splicing-dependent NMD does not require the EJC in Schizosaccharomyces pombe. EMBO J *29*, 1537-1551.

Weng, Y., Czaplinski, K., and Peltz, S.W. (1996). Genetic and biochemical characterization of mutations in the ATPase and helicase regions of the Upf1 protein. Mol Cell Biol *16*, 5477-5490.

Wood, V., Gwilliam, R., Rajandream, M.A., Lyne, M., Lyne, R., Stewart, A., Sgouros, J., Peat, N., Hayles, J., Baker, S., *et al.* (2002). The genome sequence of Schizosaccharomyces pombe. Nature *415*, 871-880.

Wood, V., Harris, M.A., McDowall, M.D., Rutherford, K., Vaughan, B.W., Staines, D.M., Aslett, M., Lock, A., Bahler, J., Kersey, P.J., *et al.* (2012). PomBase: a comprehensive online resource for fission yeast. Nucleic Acids Res *40*, D695-699.

Xiao, W. (2006). Yeast protocols, 2nd edn (Totowa, N.J.: Humana Press).

Yamashita, A., Izumi, N., Kashima, I., Ohnishi, T., Saari, B., Katsuhata, Y., Muramatsu, R., Morita, T., Iwamatsu, A., Hachiya, T., *et al.* (2009). SMG-8 and SMG-9, two novel subunits of the SMG-1 complex, regulate remodeling of the mRNA surveillance complex during nonsense-mediated mRNA decay. Genes Dev *23*, 1091-1105.

Yamashita, A., Ohnishi, T., Kashima, I., Taya, Y., and Ohno, S. (2001). Human SMG-1, a novel phosphatidylinositol 3-kinase-related protein kinase, associates with components of the mRNA surveillance complex and is involved in the regulation of nonsense-mediated mRNA decay. Genes Dev *15*, 2215-2228.

Yang, H., McLeese, J., Weisbart, M., Dionne, J.L., Lemaire, I., and Aubin, R.A. (1993). Simplified high throughput protocol for northern hybridization. Nucleic Acids Res *21*, 3337-3338.

Yoshida, S.H., Al-Amodi, H., Nakamura, T., McInerny, C.J., and Shimoda, C. (2003). The Schizosaccharomyces pombe cdt2(+) gene, a target of G1-S phase-specific transcription factor complex DSC1, is required for mitotic and premeiotic DNA replication. Genetics *164*, 881-893.

Zund, D., Gruber, A.R., Zavolan, M., and Muhlemann, O. (2013). Translation-dependent displacement of UPF1 from coding sequences causes its enrichment in 3' UTRs. Nat Struct Mol Biol *20*, 936-943.

Appendixes

Appendix I-detailed protocols

Materials

1. Equipment

ABI PRISM 7000 Sequence Detection System

Accumet Research AR15 pH Meter

Beckman J2-MC Centrifuge

Bioruptor Plus Sonicator

Eppendorf Centrifuge 5415R

Flow cytometer (BD FACSCalibur)

GeneQuant pro RNA/DNA Calculator

Innova 44 Incubator Shaker (New Brunswick)

Misonix XL2020 Sonicator

NanoDrop ND-1000 Spectrophotometer

Qubit 2.0 Fluorometer

Sigma 3-16K Centrifuge

Syngene G:Box (GE)

PMI Personal Molecular Imager (Bio-Rad)

2. Chemicals

Amersham ECL Prime (Western Blotting Detection Reagent)

dsDNA HS Assay Kit (Qubit)

MinElute PCR Purification Kit (QIAGEN)

Ponceau S Staining Solution (Sigma)

qScript cDNA Synthesis Kit (Quanta BioSciences)

SensiFAST SYBR Hi ROX Kit (Bioline)

3. Buffers

ChIP solutions and buffers

FA Lysis buffer

- 50 mM HEPES-KOH pH 7.5
- 150 mM NaCl
- 1 mM EDTA
- 1% Triton X-100
- 0.1% Na Deoxycholate

When using with PMSF/protease inhibitor cocktail, add 25 µl of 0.2 M PMSF and half a tablet of protease inhibitor cocktail to 5 ml FA lysis buffer.

TE

- 10 mM Tris-HCl pH 8.0
- 1 mM EDTA

Wash Buffer 1

- FA lysis buffer
- 0.1% SDS
- 275 mM NaCl

Wash Buffer 2

- FA lysis buffer
- 0.1% SDS
- 500 mM NaCl

Wash Buffer 3

- 10 mM Tris-HCl pH 8.0
- 0.25 mM LiCl
- 1 mM EDTA

- 0.5% NP-40
- 0.5% Igepal CA-630

Elution buffer

- 50 mM Tris-HCl pH 7.5
- 10 mM EDTA
- 1% SDS

TES Buffer

- 10mM Tris-HCl pH8
- 1mM EDTA
- 1% SDS.

Northern blot buffers:

1×Northern running buffer (1 L):

- 100 ml 10×MOPS
- 20 ml 37% formaldehyde (Sigma)
- Add DEPC-treated H_2O up to 1L

10×MOPS, pH 7.0 (0.2 M MOPS, 50 mM NaAc and 10 mM EDTA)

20×SSC, pH 7.0 (3M NaCl, 300 mM NaAc)

Hybridization solution: (1.5×SSPE, 7% SDS and 10% PEG8000)

20×SSPE (1L):

- 175.2 g NaCl
- 27.6 g $NaH_2PO_4 \cdot H_2O$
- 7.4 g Na_2EDTA in 800 ml H_2O

Adjust pH to 7.4 with NaOH

4. *S. pombe* media

The recipes of media can be found on Forsburg Lab website (http://www-bcf.usc.edu/~forsburg/media.html).

YES (Yeast Extract with Supplements)

- 5 g/L yeast extract
- 30 g/L glucose
- 0.25 g/L SP SUPPLEMENTS (FORMEDIUM)

Solid media is made by adding 2% Oxoid Agar Technical

EMM (Edinburgh minimal medium)

- 12.3 g/L EMM Broth without Dextrose (FORMEDIUM)
- 20 g/L glucose
- 20 ml/L salts
- 1 ml/L vitamins
- 0.1 ml/L minerals
- 225 mg/L supplements (arg, ade, leu, his, lys, ura...) as required.

Solid media is made by adding 2% Oxoid Agar Technical

Small-scale preparation of plasmids

1. Spin 1 ml of bacteria culture in 1.5 ml tube at 16168 ×g for 1 min and discard supernatant.
2. Resuspend pellets with 110 µl of ice cold STET buffer (8% sucrose, 50 mM Tris pH 8.0, 50 mM EDTA pH 8.0, 5% Triton X-100) containing 5 µl of 20 mg/ml lysozyme by pipetting up and down.
3. Boil samples for 20 s and then centrifuge at 16168 ×g for 10 min. Carefully remove pellets by using sterile toothpicks.
4. Add 110 µl of isopropanol to the supernatant, mix and centrifuge at 16168 ×g for 15 min.

5. Discard the supernatant and wash pellet with 70% ethanol. After air-dry pellet, dissolve in 40 µl TE (10 mM Tris-Cl, pH 8.0, 1 mM EDTA, pH 8.0) containing 0.2 µl of 1 mg/ml RNase A stock. Incubate DNA samples at 65 ℃ for 20 min before being stored at -20 ℃.

   If needed, the extra 4 ml of cell culture would be used to extract pure plasmids using Fermentas GeneJET plasmid Miniprep kit.

S. pombe DNA transformation

Rapid procedure:

1. 10 ml exponential phase cultures of *S. pombe* were centrifuged at 3000 rpm for 5 min (Sigma 3-16K Centrifuge, Rotor 11180) at room temperature and the pellet was washed once with 10 ml of sterile water.
2. The cells were centrifuged again under the same conditions and resuspended in 100 µl of sterilized water. An equal volume of LiAc buffer (10 mM Tris-HCl pH 8.0, 1 mM EDTA, and 0.1 M lithium acetate) was added and thoroughly mixed with the resuspended cells (cell density should be above to $5x10^8$).
3. For each transformation, 100 µl of LiAc-resuspended cells was transferred into a 1.5 ml sterile eppendorf tube and kept at room temperature (lower than 28 ℃) for 15-30 min.
4. Then 1 µg of plasmid DNA (episomal expression) and 2 µl of 10 mg/ml ssDNA were mixed with 100 µl of LiAc-treated cells. The mixture was then kept at room temperature for 20-30 min.
5. After that, 220 µl of 50% PEG3350 solution and 40 µl of LiAc buffer were added to the transformation mixture and mixed gently. The sample was kept at 30 ℃ (25 ℃ for ts strain) for 1 h.

6. The sample was heat shocked at 42 ℃ for 15 min and briefly centrifuged at 835 ×g for 1 min.
7. Discard about half of supernatant (about 200 µl), and the pellet was resuspended before being spread on the appropriate selection plate.

Long procedure:

Day1

1. Pick single colony from YES plate, and inoculate into 3 ml YES in 50 ml falcon tube. Grow in a shaking incubator at 30 ℃, 220 rpm and start at about 6pm.

Day2

2. Measure the OD of cells at OD600 at about 5.30pm, then dilute the culture to OD_{600} of 0.02 in 25 ml YES in 250 ml flask, put the culture in a shaking incubator at 30 ℃, 220 rpm and start at about 6pm, grow O/N for about 15 h.

Day3

3. At about 9am, boiling 10 mg/ml ssDNA for 5 min, then immediately put on ice. 20 ml of about 10^7 cells/ml cells were used for each transformation.
4. Pellet cells at 3000 rpm 25 ℃ 5 min (Sigma 3-16K Centrifuge, Rotor 11180), wash once with 10 ml sterilized distilled water. Remove the water, resuspend the cells in 1ml sterilized distilled water and transfer to 1.5 ml sterilized Eppendorf tube.
5. Pellet the cells at 835 ×g 25 ℃ 5 min. Wash the cells with 1ml 0.1 M LiAc/TE. Pellet the cells again at 835 ×g 25 ℃ 5 min. Resuspend the cell pellet in 100 µl 0.1 M LiAc/TE.
6. Add 30 µl PCR product (about 1.2 µg DNA fragment) and 4 µl 10 mg/ml ssDNA to the cells. Mix and put the cells at room temperature for 10 min.
7. Add 220 µl of 50% PEG3350 and 40 µl 0.1 M LiAC to the cells and mix gently.

8. Put the Eppendorf tube in a shaking incubator at 32 ℃ 160 rpm for 1 h.
9. Add 43 μl DMSO to the treated cells, mix gently and heat shock at 42 ℃ for 5 min.
10. Pellet the cells at 835 ×g 25 ℃ 1 min. Discard about half of supernatant (about 200 μl), and the pellet was resuspended before being spread on YES agar plate.
11. Put the plate in 30 ℃ incubator for about 18 h, then replicate the plate onto appropriate selection plate. Put the plate at 30 ℃ incubator for about 3 days until the colonies were formed.

Genomic DNA extraction

Zymolyase digestion based method:

1. 10 ml cell cultures were pelleted by centrifugation at 4000 rpm, 3 min at room temperature (Sigma 3-16K Centrifuge, Rotor 11180).
2. Discard the supernatant, and resuspend pellets with 1ml distilled water before transferring to 1.5 ml Eppendorf tube.
3. Pellet cells at 3341 ×g for 2 min at room temperature, and then discard supernatant.
4. Resuspend pellets with 800 μl 0.1M sodium phosphate buffer (pH7.5) and add 11 μl of 10 mg/ml Zymolyase (20T).
5. Incubate the mixture at 37 ℃ for 1h before centrifugation at 16168 ×g at room temperature for 1 min.
6. Discard supernatant, resuspend cells with 200 FA lysis buffer.
7. Add 200 μl 1:1 phenol: chloroform and invert the Eppendorf tube several times to mix the mixture.
8. Centrifuge the mixture at 16168 ×g for 5 min at room temperature and transfer supernatant (~200 μl) to another new Eppendorf tube.

9. Mix the transferred supernatant with 500 µl 100% ethanol and 20 µl 2.6M sodium acetate (pH5.2) by inverting several times.
10. Put the mixture at -20 ℃ for 1h. After that, centrifuge sample at 16168 ×g at 4 ℃ for 15 min.
11. Discard supernatant and wash the pellet once with 1 ml 70% ethanol.
12. Discard most of the supernatant, spin the remaining liquid at 4 ℃ for 1 min; Remove the residual liquid by using 100 µl pipette.
13. Air dry the pellet for 9 min at room temperature; Dissolve the pellet in 50 µl distilled water, briefly vortex and quickly spin down the DNA sample.
14. Store the dissolved sample at -20 ℃.

Glass beads based method:

1. 10 ml cell cultures were pelleted by centrifugation at 4000 rpm, 3 min at room temperature (Sigma 3-16K Centrifuge, Rotor 11180).
2. Discard the supernatant, and resuspend pellets with 1ml distilled water before transferring to 1.5 ml Eppendorf tube.
3. Pellet cells at 3341 ×g for 2 min at room temperature, and then discard supernatant.
4. Resuspend pellets with 500 µl FA lysis buffer and transfer to 2 ml screw cap tube containing 500 µl acid washed glass beads (425-600 µm, Sigma), screw back the cap.
5. Cells were broken up in a Precellys 24 homogenizer (Bertin Technologies) using the settings: 6500 rpm, 2 x 30 s, 20 s interval, 5 min on ice; The process was repeated for another 5 times until more than 70% of cells were broken up as observed under the microscope.

6. Make three holes in bottom of the 2 ml screw cap tube using orange needle (25G) and place the tube in the middle of the lid of 15 ml falcon tube (with a hole on top of the 15ml tube lid which just fits 2 ml tube); screw back the lid of 15 ml tube with the 2 ml tube to the falcon tube.
7. Centrifuge at 1000 rpm for 1 min at room temperature and wash the beads with 500 µl FA (Sigma 3-16K Centrifuge, Rotor 11180).
8. Discard screw cap tube (sample is now in 15 ml falcon tube), transfer sample to 1.5 ml Eppendorf tube.
9. Centrifuge the sample at 16168 ×g for 20 min at 4 ℃ and resuspend pellets with 200 µl FA lysis buffer.
10. Follow the same DNA extraction steps from step 7 as in Zymolyase digestion based method.

Protein extraction

TCA extraction:

1. Pellet 5 or 6 OD of cells in a 50 ml falcon tube by centrifugation at 4000 rpm, for 3 min at 4 ℃ (Sigma 3-16K Centrifuge, Rotor 11180), resuspend the pellet in 200 µl newly made 20% TCA and transfer into a 1.5 ml screw cap tube, remover supernatant and .
2. Add about 200 µl glass beads (425-600 µm) using 0.2 ml PCR tube.
3. Lyse the cells in Precellys 24 homogenizer (Bertin Technologies) in cold room following the programs below
    - 5500 rpm, 30 s
    - 20 s stop
    - 5500 rpm 30 s
    - 2 min on ice

Repeat this program for another 5 times

4. Check lysis under phase contrast microscope (should have at least 70% broken cells).
5. Make 3 holes in the bottom of screw cap tube using orange needle (25G) and place the tube in a 1.5 ml Eppendorf tube.
6. Spin at 1485×g, 2 min, discard the screw cap tube.
7. Spin 16168×g 5 min at 4 ℃ and remove all supernatant.
8. Add 100 µl of 0.3M NaOH, put on ice for at least 30 min and add 100 µl 2×SDS loading buffer, resuspend the pellet.
9. Keep sample at -20℃.
10. Boil at 95℃ for 5 min, spin down debris before use for 1 min at 16168×g.

Northern blot analysis of RNA samples

Day 1-RNA Gel running and blot transfer

1. RNA gel preparation: Dissolve 1.2 g agarose in 86.25 ml DEPC-treated distilled water in Microwave, add 12 ml 10XMOPS buffer and 21.45 ml 37% formaldehyde. Mix the solutions before pouring into gel tank.
2. RNA sample treatment: Mix 5 or 10 µg RNA sample with 5.5 µl 37% formaldehyde, 15 µl formamide and 3µl 10xMOPS. Incubate mixture at 65℃ for 15 min before quickly putting on ice for 5 min. Meanwhile pre-run RNA gel in 1x MOPS buffer at 80 V for 5 min.
3. Running RNA sample: add 1 µl 10X RNA loading buffer to each sample, mix and briefly spin down at 4℃. Load RNA sample on RNA gel and run the gel at 80 V for about 2.5 h.

4. Wash RNA gel: After gel running, put gel in a plastic container and wash twice with DEPC-treated distilled water for 20 min each. Wash the gel for another time with 20×SSC for 30 min.
5. While the gel is washing, prepare transfer papers and membrane: Cut 1 piece of 3 mm Whatman paper servicing as bridge exactly the same size as the blot transfer apparatus. Cut also 4-5 pieces of 3 mm Whatman paper exactly the same size as the gel. Prepare nylon membrane (Hybond-N, GE Healthcare) 0.5 cm larger than each side of the gel. Cut paper towels exactly the same size as the gel (the height of paper towels should be about 5 cm when stacked).
6. RNA gel transfer: Assembling of RNA gel transfer blot is as standard protocol (Green et al., 2012). After transfer blot being assembled, leave it overnight.

Day 2-UVcrosslinking, membrane pre-hybridization and hybridization

1. UV crosslinking: Remove tower papers and Whatman papers, cur top left corner of the membrane and label the data on top right corner of the membrane. Put the membrane on top of pre-wet 3 mm Whatman paper (DEPC treated distilled water) with RNA side up. Crosslink the membrane with UV light (254 nm) at 0.120J.
2. Stain membrane: After UV crosslinking, wash the membrane once with DEPC-treated distilled water for 5 min, and then stain membrane with methylene blue for 5 min. After that, wash membrane with DEPC-treated distilled water until stained bands can be seen clearly. Take picture of the membrane.
3. Pre-hybridization: Boil 600 μl 10 mg/ml ssDNA for 5 min and put on ice immediately. Leave ssDNA on ice before use. Put membrane into hybridization tube containing 30 ml hybridization solution, and then add 300 μl 10 mg/ml

ssDNA and 30 µl 250 mg/ml heparin. Put the hybridization tube at 68 µl for 3-4 h while rotating.

4. Synthesis of radioisotope labelled probe: Mix 50 ng PCR or gel purified DNA template, 5 µl 5X labelling buffer (Promega) and DEPC-treated distilled water in a total volume of 21 µl in 1.5 ml Eppendorf tube. The mixture was boiled for 3 min and then put on ice for 5 min. Add 1 µl of a premix of three unlabelled dNTPs (dGTP, dCTP, dTTP, each at 125 µM), 0.5 µl of DNA Polymerase I Large (Klenow) Fragment (5000 units/ml, NEB) and 2.5µl of [α-^{32}P]dATP, 250 µCi, 3,000 Ci/mmol (PerkinElmer). Mix gently, and incubate the reaction tube at room temperature for 2-4 h.
5. Purification of radioisotope labelled probe by size exclusion chromatography (optional): Remove the plunger from 1ml syringe and add a small amount of glass wool into the barrel of syringe to block the hole. After that, remove the plunger as it is not required and place the barrel of syringe into a 15ml falcon tube. The Sephadex G-50 was slowly added to the whole barrel to avoid air bubbles. Spin the column for 5 min at 2000 rpm at room temperature followed by washing once with 100 µl STE (Sigma 3-16K Centrifuge, Rotor 11180). Remove syringe and drain off liquid from the 15ml tube. Radioisotope labelled probe was then purified by the column and collected using 1.5 ml screw cap cap tube being placed underneath the barrel by centrifugation for 5 min at 2000 rpm (Sigma 3-16K Centrifuge, Rotor 11180). Boil purified probe for 5 min and put on ice immediately for 5 min.
6. Membrane hybridization: After 3-4 h pre-hybridization, replace pre-hybridization solution in hybridization tube with 20 ml fresh hybridization buffer followed by adding 200 µl 10mg/ml ssDNA, 20 µl 250 mg/ml heparin

and the purified probe. Keep the hybridization tube at 68℃ with rotation overnight.

Day 3-Membrane washing, signal development and quantitative analysis

1. Make 400 ml washing solution containing 2×SSC and 0.1% SDS, and wash membrane at 68℃ for 2 min, 5 min, 30 min and 30 min, respectively, each time with 100 ml of washing solution.
2. Make 100 ml washing solution containing 0.2×SSC and 0.1% SDS, and wash membrane once at 68℃ for 30 min.
3. Develop the membrane: After washing, the membrane wrapped in Saran film. The membrane was exposed to a Kodak phosphorimaging screen and developed by the PMI Personal Molecular Imager (Bio-Rad).
4. The signal intensities were analysed using the Quantity-one program (Bio-Rad).
5. Stripping membrane (optional): Submerge membrane in just boiled 1×SSC (hot) for 1 min and wrap membrane again with Saran film. Use survey meter (Mini-Monitor G-M tube) to confirm removal of probe. If necessary, repeat stripping for another time.

Genome-wide screening of Upf1 putative interacting genes against Bioneer Library

1. Defrosting of Bioneer Deletion Library

Each 96-well plate containing library mutants stored at -80℃ was defrosted in the biosafety cabinet for 15 min. Strains in 96-well plate were resuspended using multichannel micropipet. 5 µl of resuspended culture from each well were applied onto YES agar plate containing 100 µg/ml G418. YES agar plates were dried for 20 min at room temperature and incubated at 30℃ for 4 days. Plates were photographed using GeneSnap viewer to record their growth phenotype

2. Inoculation of library mutants and *upf1* mutant

Add 150 µl of YES liquid media to each well of new 96-well plate. Individual colonies grown on YES + G418 plate were picked and inoculated in order into 96-well plate. This inoculated 96-well plate was then incubated at 30 ℃ for 2 days. At the same time, the *upf1Δ* strain labelled as JM85 was inoculated into 10 ml YES liquid media, and then incubated at 30 ℃ with shaking at 220 rpm for 2 days.

3. Mating

Discard 50 µl of resuspended culture from each well of 96-well plate. The remaining of 2-day cultures were mixed with equal volume of JM85 culture. 5 µl of mixed culture from each well were dropped onto SPAS mating agar plates in order. The mating plates were dried at room temperature and then incubated at 25 ℃ for 3 days.

4. Spores Enrichment

After incubation for 3 days 25 ℃, check whether mated cultures have formed spores. To do this, 5 individual colonies were picked randomly from incubated SPAS mating agar plate and were checked under light phrase microscope at 40X magnification. If one colony was observed to contain less than 3 asci in the vision field, the corresponding SPAS mating agar plate was incubated for at least another day until they formed enough asci. After that, mating plates were incubated at 42 ℃ for 3 days to kill unmated haploid cells and vegetative cells.

5. Double Mutant Selection

After spores enrichment, individual mated colonies grown on SPAS mating agar medium were picked and inoculated into a new 96-well plate containing 150 µl of YES liquid media. This inoculated 96-well plate was then incubated at 30°C for 2 days. 5 µl of resuspended culture from each well was applied onto YES + G418 + hygromycin B double selection agar plates in order. They were then incubated at 30 ℃ for 2 days.

6. Identification of Upf1 putative genetic interacting genes

Colonies grown for 2 days on YES + G418 + hygromycin B agar plates were photographed using GeneSnap viewer to record the growth of the potential double mutants. They were then compared with their parental Bioneer library mutants grown on YES + G418 agar plates to identify putative genetic synthetic rescue genes, synthetic sick genes and synthetic lethal genes. The criterias used for judging screening results was shown in Figure 23B.

The first Chromatin Immunoprecipitation (ChIP) protocol

Preparing Samples

1. Grow 100 ml culture in 500 ml flask to OD 0.7.
2. To the 100 ml culture add 10 ml of 11% HCHO (freshly made from commercial 37% solution) so that the final [HCHO] = 1%. Make the 11% HCHO by adding 3 ml of 37% HCHO to 7 ml diluent (final concentration 0.1 M NaCl, 1 mM EDTA, 50 mM HEPES-KOH, pH 7.5). Incubate 20 min at RT (30 ℃), 70 rpm in a shaking incubator.

Diluent (500 ml):	0.143 M NaCl	14.3 ml 5M NaCl
	1.43 mM EDTA	1.43 ml 0.5M EDTA
	71.43 mM HEPES-KOH	8.51 g HEPES
	Adjust pH with KOH	
	Add Water up to 500 ml autoclave by filtration	

3. Add 13 ml 3 M glycine and return to shaking incubator for a further 5 min.
4. Transfer culture to a 500 ml plastic Nalgene bottle and centrifuge at 4 ℃, 4000rpm, 5 min to pellet cells (Beckman J2-MC centrifuge, Fiberlite F10-6×500 Rotor).
5. Add 50 ml ice cold PBS to resuspend the pellet, transfer the culture to a 50 ml falcon tube, using 1m blue tips to transfer the remaining liquid in the plastic Nalgene bottle,

centrifuge at 4℃, 4000 rpm, 5 min to pellet cells (Sigma 3-16K Centrifuge, Rotor 11180).

6. Discard the media and wash pellet in 50 ml ice cold PBS then centrifuge as previously to pellet. (Firstly gently pour off the media, then briefly invert the tube on tissue paper, to remove most of the media)
7. Resuspend the pellet in 10 ml ice cold FA lysis buffer with 0.5% SDS (firstly using a 1m blue tip to resuspend the pellet and then gently vortex for about 10 s)
8. Centrifuge at 4℃, 3000 rpm, 5 min (Sigma 3-16K Centrifuge, Rotor 11180).
9. Discard supernatant (Firstly gently pour off the media, then briefly invert the tube on tissue paper, to remove most of the media, spin 4℃, 3000 rpm, 5 min (Sigma 3-16K Centrifuge, Rotor 11180), and then remove the supernatant carefully using a 1m blue tip) and resuspend the pellet in 1 ml FA lysis buffer/0.1% SDS with 2 mM PMSF and protease inhibitor.
10. Add 4 scoops of glass beads to each of two 2 ml screw cap tubes, put the screw cap tubes on ice beforehand.
11. Add 600 µl of the lysate to each of the tubes and ensure complete saturation of the beads.
12. Vortex in a Precellys cell lysis machine at 5500 rpm, 13×20 s on, 20 s off, 20 s on, put on ice 2 min in between cycles.
13. Check cells under microscope, should be more than 90% broken up.
14. Make three holes at the bottom of the screw cap tube and one hole in the lid with a gauge needle, and place this tube in the hole of a 15 ml tube lid (the size of the hole in the lid of 15 ml tube can just hold the screw cap tube), close a 15 ml Falcon tube with the lid (In this way, only the lysis from screw cap tube can come to the 15 ml Falcon tube by contrifugation).

15. Collect lysate by centrifuging at 1000 rpm, 1 min, 4 ℃ (Sigma 3-16K Centrifuge, Rotor 11180).
16. Wash remaining lysate from beads with a further 500 µl FA/PMSF and centrifuge again using the same conditions.
17. Resuspend the pellet using the 1ml tip. Then aliquot 500 µl into two 1.5 ml eppendorf tubes.
18. Centrifuge for 30 min, 4 ℃, 16168 ×g, remove supernatant and resuspend pellet in 1 ml FA/PMSF. Centrifuge again and resuspend final pellet in 1 ml FA/PMSF.
19. Make 2 ×500 µl aliquots for sonication.

Sonication

1. Set sonicator XL2020 (Misonix) to level 3 and frequency 10%. Sonicate samples for 6 cycles of 20 s, ensuring at least 1mins on ice in between cycles.
2. After sonication, centrifuge samples 30 min, 16168 ×g, 4 ℃.
3. Transfer supernatant containing chromatin using filter tips to a fresh LoBind eppendorf (should be ~450 µl chromatin from 500 µl sample).
4. Samples can be frozen in liquid nitrogen and stored at -80 ℃ at this stage along with any unused lysate samples.

Preparation of beads

1. Add 50 µl of Protein G Dynabeads (Life Technologies) to 1 ml PBS containing 5 mg/ml BSA.
2. Vortex briefly, then briefly centrifuge to bring down any beads from the top of the tube.
3. Place the tube in a magnetic rack and allow the beads to migrate to the magnetic surface.

4. Rotate the tube 6 times to wash the beads then remove PBS. Repeat a further 3 times with fresh 1 ml PBS/BSA each time.
5. After the final wash, resuspend the beads in 500 µl PBS/BSA.
6. Add 10 µg of antibody to the beads and incubate on a rotator either for 90 min at RT or at 4 ℃ overnight.
7. Spin the tube briefly and place in the magnetic rack.
8. Wash twice with 1 ml PBS/BSA as before to remove any unbound antibody.
9. Resuspend beads in 50 µl FA lysis buffer without 0.1% SDS.

Immunoprecipitation

1. Take 50 µl of antibody coated beads and add 400 µl chromatin (keep 50 µl of chromatin as input, store at -20 ℃).
2. Incubate o/n at 4 ℃.
3. Thaw input samples on ice.
4. Spin immunoprecipitated samples briefly and place tubes into the magnetic rack. Discard the supernatant.
5. Wash the beads once for 5 min on a rotator at room temperature with 1 ml of each of the following (add wash buffer then vortex to ensure beads are released from the side of the tube. After wash on rotator, spin briefly then rotate in magnetic rack as before):-
    - Wash buffer 1 – FA lysis buffer/0.1% SDS/275 mM NaCl
    - Wash buffer 2 – FA lysis buffer/0.1% SDS/500 mM NaCl
    - Wash buffer 3 – 10 mM Tris-HCl, pH 8.0/0.25 mM LiCl, 1 mM EDTA, 0.5% Igepal CA-630, 0.5% Na deoxycholate
    - TE - 10 mM Tris-HCl pH 8.0, 1 mM EDTA

6. To elute the protein-DNA complexes add 100 µl of ChIP elution buffer, pipetting gently to resuspend beads, then incubate in a water bath for 10 min at 65 ℃.
7. Spin briefly and place the tube into the magnetic rack. Transfer the supernatant to a new LoBind tube. The samples were eluted once more as in step 6.
8. Add 150 µl of ChIP elution buffer to the input samples to give an equal volume to the ChIP samples.
9. Add 5 µl of 20 mg/ml Proteinase K to each sample and incubate overnight at 65 ℃.
10. Purify the ChIP and Input DNA with QIAquick PCR Purification Kit (QIAGEN), and elute the DNA in 50 µl purified water. Add 1 µl of 1 mg/ml RNase A, and incubate at 37 ℃ for 1 h.
11. Add 450 µl purified water to each purified ChIP and Input DNA samples.
12. Diluted samples could be kept at -20 ℃.

The third Chromatin immunoprecipitation protocol for Chip-seq

Growing and fixing *S. pombe* cells

1. Grow 400 ml of cells to an OD_{600} of 0.8 in a 2L flask in a shaking incubator at 30 ℃, 220 rpm.
2. Add 11 ml of 37% formaldehyde (1% final), fix for 5min in a shaking incubator at 30 ℃, 70 rpm.
3. Add 20 ml of 2.5M glycine, incubate for 10 min in a shaking incubator at 30 ℃, 70 rpm. Transfer fixed cultures to 500 ml centrifugation tube, spin at 4 ℃, 4000 rpm for 5 min (Beckman J2-MC centrifuge, Fiberlite F10-6×500 Rotor).
4. Wash cells twice in 40 ml ice-cold 1x PBS at 4 ℃, 4000 rpm for 5 min (Sigma 3-16K Centrifuge, Rotor 11180). Resuspend cells in 8 ml ice-cold PBS, split into four 2 ml eppendorf tubes and spin again at 4 ℃, 1485×g for 5 min.
5. Discard supernatant

Cell extracts preparation and chromatin sonication

1. Resuspend pellets in each 2 ml tube with 750 µl of ice-cold FA lysis buffer containing 1 mM PMSF, protease inhibitor (Add 1 Roche Ultra-pure EDTA free tablet to 15 ml FA lysis buffer).
2. Transfer resuspended cells to 4 ice-cold 2 ml screw cap tubes containing 500 µl of acid-washed glass beads (now you have four tubes per sample). Break cells in Precellys cell lysis machine using programme: 6500 rpm, 2 x 20 s with 20 s interval, 5 min on ice. Repeat this for another 12 times. Mix 1 µl of cell lysate with 2 µl of distilled water, visualize in the microscope of cells to estimate the breaking efficiency (should be >90%).
3. Make three holes in the bottom of each 2 ml screw cap tube containing broken cells with a sterile needle (25G) after flaming it and place the tube in the middle of the lid of 15ml falcon tube (there was a hole in the middle of the 15 ml tube lid which just fits 2ml tube); close a 15 ml Falcon tube with the lid (In this way, only the lysis from screw cap tube can come to the 15 ml Falcon tube by contrifugation). Spin for 1 min at 1000 rpm at 4 ℃ to collect the lysate (Sigma 3-16K Centrifuge, Rotor 11180). Wash the glass beads once with 500 µl lysis buffer (withinhibitors), spin and pool with the first flow-through (the additional washing of beads increases yield).
4. Spin the lysate for 30 min 4 ℃ at 16168 ×g, discard the supernatants and wash once more with 800 µl lysis buffer (with inhibitors) (the additional wash increases yield).
5. After the wash, resuspend the pellet with 600 µl of cold Lysis buffer and pool the material from four eppendorf tubes into one 15 ml falcon tube (you're back to 1 tube/ sample). Add PMSF to 1 mM. Briefly vortex and split into 2x1.2 ml

aliquots in 15 ml falcon tube (this is the volume and tubes for which sonication was calibrated)

6. Sonicate 8 x 5 min with 30 s ON/ 30 s OFF at HIGH setting, refill the water bath with ice-cold water (no crushed ice chips!!) after each 5 min interval (Bioruptor plus settings). This will produce chromatin fragments of ~300 bps. The conditions of sonication have typically to be set-up in each lab. The volume and concentration of the extract as well as the duration and strength of the sonication will affect the size of the sheared chromatin.
7. Spin the sonicated material at 16168×g for 30 min at 4℃ and pool the supernatant from two tubes (chromatin extract, CE) into one 15 ml falcon tube. Briefly vortex and then aliquot 550 µl into four 1.5 ml DNA low binding tubes (Eppendorf). The CE was quick frozen with liquid nitrogen and stored at -80 ℃.

Chromatin concentration measurement

Thaw chromatin stored at -80 ℃ on ice (takes about 2h) before measuring chromatin concentration using Bradford assay.

1. Make BSA standard in 50 µl PBS:
    a. 1.4 mg/ml: 14 µl 10 mg/ml BSA+86 µl PBS;
    b. 1 mg/ml: 10 µl 10 mg/ml BSA+90 µl PBS;
    c. 0.5 mg/ml: 10 µl 10 mg/ml BSA+190 µl PBS;
    d. 0.25 mg/ml: 100 µl 0.5 mg/ml BSA+100 µl PBS;
    e. 0mg/ml: no BSA but PBS;

    Put BSA standard on ice.
2. 20 time dilution of chromatin sample by mixing 5 µl chromatin extract with 95 µl PBS and put diluted chromatin on ice.
3. Bring Bradford solution (Sigma, B6916) to room temperature.

4. Prepare 1.5 ml eppendorf tubes, add 1ml Bradford solution to each eppendorf tubes.
5. Add 30 µl either diluted standard BSA or chromatin to 1 ml Bradford solution, vortex briefly.
6. Use 1 ml Bradford solution for blanking.
7. Incubate mixed sample at room temperature for 11 min, then start measuring each sample at OD595 nm (The absorbance of the samples must be recorded within 60 min and within 10 min of each other).
8. Calculate chromatin concentration according to the readings of BSA standard. (I only measured all BSA standard for the first time to test whether readings of different BSA standards are in a linear range. After confirmation of the linear range of BSA standards from 0 mg/ml to 1 mg/ml, I only used 0 mg/ml and 0.5 mg/ml as reference thereafter to calculate chromatin concentration).

Preparation of beads

1. Add 50 µl of Protein G Dynabeads (Life Technologies) to 1 ml PBS containing freshly made 5 mg/ml BSA in 1.5 ml DNA low binding tubes (Eppendorf).
2. Vortex briefly, then briefly centrifuge to bring down any beads from the top of the tube at room temperature, 371 ×g for 3s.
3. Place the tube in a magnetic rack and allow the beads to migrate to the magnetic surface.
4. Rotate the tube 6 times to wash the beads then remove PBS. Repeat a further 3 times with a fresh 1 ml PBS/BSA each time.
5. After the final wash, resuspend the beads in 500 µl PBS/BSA.
6. Add 10 µg of monoclonal anti-FLAG® M2 antibody (F1804, sigma) to the beads and incubate on a rotator for 90 min at room temperature at 12 rpm.

7. Spin the tube briefly and place in the magnetic rack.
8. Wash 2×with 1 ml PBS/BSA as before to remove any unbound antibody.
9. Resuspend beads in 50 µl FA lysis buffer without 0.1% SDS.

Immunoprecipitation

1. Mix 50 µl of antibody coated beads with 5mg chromatin and adjust final volume of mixture in the tube with FA lysis buffer to a final volume of 500 µl (keep 50 µl of chromatin as input, store at -20 ℃. As different initial chromatin samples have slightly different concentrations, the same amount of chromatin was taken as input referring to 50 µl).
2. Incubate overnight at 4 ℃, 12 rpm on a rotator.
3. Thaw input samples on ice.
4. Spin immunoprecipitated samples briefly at room temperature, 371 ×g for 3 s and place tubes into the magnetic rack. Discard the supernatant.
5. Wash beads once for 5 min on a rotator at room temperature with 1 ml of each of the following (invert tube several times to ensure beads are released from the side of the tube. After wash on rotator, spin briefly then rotate in magnetic rack as before):
    a. Wash buffer 1 – FA lysis buffer/0.1% SDS/275 mM NaCl
    b. Wash buffer 2 – FA lysis buffer/0.1% SDS/500 mM NaCl
    c. Wash buffer 3 – 10 mM Tris-HCl, pH 8.0/0.25 mM LiCl, 1 mM EDTA, 0.5% Igepal CA-630, 0.5% Na deoxycholate
    d. TE – 10 mM Tris-HCl pH 8.0, 1 mM EDTA
6. To elute the protein-DNA complexes add 100 µl of ChIP elution buffer, pipetting gently to resuspend beads, then incubate in heat block for 10 min at 65 ℃ (For ChiP-seq IP DNA preparation, three 5 mg chromatin aliquots were used to

performed IP in parallel, so at first elution step after washing beads, combine beads in 100 µl of ChIP elution buffer in one 1.5 ml DNA low binding tube from three aliquots).

7. Spin briefly and place the tube into the magnetic rack. Transfer the supernatant to a new 1.5 ml DNA low binding tube. Elute beads another time with 100 µl of ChIP elution buffer, then transfer the supernatant to the previous eluted sample (you have 200 µl eluted chromatin per sample).
8. Add 150 µl of TES buffer to the input samples to give an equal volume to the ChIP samples.
9. Incubate eluted chromatin together with input overnight at 65 ℃.

Purifying ChIP and Input DNA

1. Digest proteins and RNA. Add 200 µl TE, 2.5 µl of DNase-free RNase (1 mg/ml), incubate at 37 ℃ for 30 min. Then add 7 µl proteinase K (20 mg/ml), incubate at 55 ℃ for 2 h.
2. DNA purification. MinElute PCR Purification Kit (QIAGEN) was used to purify chromatin. DNA was eluted twice, each time with 20 µl sterile distilled water.
3. Measure DNA concentration using Qubit 2.0.

   Take 3 µl of Input DNA and dilute to 200 pg/µl with sterile distilled water; Dilute 3 µl of ChiP DNA with 147 µl sterile distilled water. Check enrichment of genes of interest by quantitative PCR (SensiFAST™ Real-Time PCR Kit, Bioline).
4. 10 ng of ChIP and Input DNA can be used as starting material for ChIP-seq library preparation and sequencing.

Appendix II-primer sequences

RT-qPCR primer sequences			
Primer name	Other name	Sequence	Comments
J1	tf2-F	AGAACAGCCTCGTATGGTAA	
J2	tf2-R	GGTAGGCAGTTTATGTGCTC	targeting to tf2 retrotransponson element ORF region
J5	act1-F	ATTGGTGGATCCATTCTTGC	
J6	act1-R	CACTTACGGTAAACGATACCA	targeting to act1 ORF region
J56	rad52-F	CATTTAGCAGTAGCAGAGGACACAGC	
J57	rad52-R	GTGGAACAGCGACAGGATAGGT	targeting to rad52 ORF region
J64	25s rDNA-F	CGATGGTTGATGAAACGGAAGTGTT	from 3324-3348 bp of 28s rDNA
J65	25s rDNA-R	CGTAACAACAAGGCTACTCTACTGC	from 3437-3461 bp of 28s rDNA
P2-pma1-F	P2-PMAC1-F	GTCTTCGTGATTGGGTCGAT	detect pma1 gene coding region
P2-pma1-R	P2-PMAC1-R	GGGGTCACCATAGTGCTTGT	

strain verification primer sequences			
Primer name	Other name	Sequence	Comments
J12	kan inP1r	TATTCTGGGCCTCCATGTC	check KanMX6 cassette
J15	upf1F	TGAAGAACACTGTGCCTATTGCC	120 bp downstream of the starting site of upf11 ORF
J16	upf1R	AGCCTCCGCTTGAATGAGCG	686 bp downstream of the starting site of upf1 ORF
J17	upf2F	TCCTGAAATTACCGCCGCCATCG	228 bp downstream of the starting site of upf2 ORF
J18	upf2R	TGGCAGACTCACTCCTTTCGCCT	1098 bp downstream of the starting site of upf2 ORF
J23	upf3F	AAACGAGTATAAACGCACGA	upf3 deletion verification with J12
J25	upf3sen	ATTACCATGCAAAGTCCTCG	27 bp downstream of the starting site of upf3 ORF
J26	upf3rev	AAGCGTAGCTTTTTCTTAGC	532 bp downstream of the starting site of upf3 ORF
J37	MD1	CGGATCCCCGGGTTAATTAAGGCG	hphMX6,natMX6 and KanMX6 cloning Marker switch
J38	MD2	GAATTCGAGCTCGTTTAAACACTGGATGGCGGC	hphMX6,natMX6 and KanMX6 cloning Marker switch
J40	hph_R	ATTGACCGATTCCTTGCGGT	413bp downstream of hph ORF
J50	upf1 F2	TTACATGGTCTCAGCAACCGT	upf1 deletion verification with J12
J52	upf2 F2	TTGTACCAATGCACAAACCTCC	upf2 deletion verification with J12
J143	cbp2F2	CGACGAATTATCATGGGCGT	with J12 for checking the HA c terminnal tagging
J185	12F6 ste7 F	ATGGAGCAAAGCCCAGGTAT	730bp upstream of ATG of ste7
J186	12F6 ste7 R	CATCGGAATCGGAGGCAGAA	180bp downstream of ATG of ste7
J193	13H7 air1 F	CCTTGAAGAGTCGGGAAGGT	450bp upstream of ATG of air1
J194	13H7 air1 R	TGAGGGATCTGACCCGAAGT	290bp downstream of ATG of air1
J209	14D5 Ppn1 F	TGATCCGATCTAAAAACGGTGA	360bp upsteam of ATG of ppn1
J210	14D5 Ppn1 R	ACAGAGGTGACTGGGAGTGT	380bp downstream of ATG of ppn1
J310	verify Air1-3HA tag F	GCACTGCATTTTGTGAAGCG	305bp upstream TAA
J311	verify Air1-3HA tag R	CCTGGTGGTAAGGCTCTTCA	460bp downstream TAA
w16	upf1ch.sens	CCGCTAAGCACCACATAA	combine with Kan inp1r, give 750 bp bands
w17	upf2ch.sens	TCATACTGGAAAGGCTGCTA	combine with Kan inp1r, give 750 bp bands
w19	kan inP1r, J12	TATTCTGGGCCTCCATGTC	check KanMX6 cassette
LP277	pabp F	GGAAGAATGAATGGGGGAAT	mRNA export shuttling protein pabp
LP278	pabp R	TGTCAAGTGACCCATCTCCA	mRNA export shuttling protein pabp
upf1-flag-con(F)		CCT TAA CCC TTA CTC CTC CTC AG	verifcation of upf1 C terminal flag tagging with primer w19

primer sequences used for Northern Blotting			
Primer name	Other name	Sequence	Comments
w22	rpl32-sens	GGCTGCTGTCAATATCAT	
w23	rpl32-for	GTGACCTTTACACCGAGA	rpl32 as the Northern blot control
w27	gfp rev	AAG GAA GGA TCC TTA GCA GCC AGA TCC TTT GTA TAG	
w28	gfp sens	CGGGA CAT ATG GCT AGC AAA GGA GAA GAA C	gfp as the Northern blotting template
primer sequences used for gene deletion and tagging			
Primer name	Other name	Sequence	Comments
J141	cbc2F1	TTATTCGTGCAGATTTGGATCATGG	326 bp upstream of cbc2 stop codon
J142	cbc2R1	AGTAAGCTAGGATGGGATGGCT	with J141 for C terminal HA tagging
Upf1-hph-flag-F	Upf1-Kan-HA-F	GAAGACTTTAGAAGTCAGGTTGGTGATGATGAAAGCAAGTTCGACGAACCTACTAGGTTC CGG ATC CCC GGG TTA ATT AA	
Upf1-hph-flag-R	Upf1-Kan-HA-R	TCAACAAATAAAAGATATGTTGGCATTCGTAATTACAAGTAAGCAAATACTTATTAACTA GAA TTC GAG CTC GTT TAA AC	upf1 gene C terminal flag tagging
Upf1-kanmx6 F		TGTTACAATTATTTACACTTTGCAAATTGACGGCTTAATAACATATCAAGTTGTCTTTCC CGG ATC CCC GGG TTAATTAA	
Upf1-kanmx6 R		ATATCAACAAATAAAAGATATGTTGGCATTCGTAATTACAAGTAAGCAAATACTTATTA GAA TTC GAG CTC GTTTAAAC	upf1 gene deletion
J301	Air1 w(Forward)	GAGGCGAGAGCAGAATCGAA	250bp upstream TAA of air1
J302	Air1_3HA_1R	GGG GAT CCG TCG ACC TGC AGC GTA CGACCATTTTCGTTTACGATTTT	TAA of air1
J303	Air1_3HA_2F	GTTTAAACGAGCTCGAATTCATCGATTTCATGTGCTGGTATTATT	TAAof air1
J305	Air1 z (Reverse)	TGGTTTACTCCGTTATCATAGCTT	250bp downstream TAA of air1

ChiP primer sequences			
Primer name	Other name	Sequence	Comments
J1	tf2-F	AGAACAGCCTCGTATGGTAA	
J2	tf2-R	GGTAGGCAGTTTATGTGCTC	targeting to tf2 retrotransponson element ORF region
J64	25s rDNA-F	CGATGGTTGATGAAACGGAAGTGTT	from 3324-3348 bp of 28s rDNA
J65	25s rDNA-R	CGTAACAACAAGGCTACTCTACTGC	from 3437-3461 bp of 28s rDNA
J82	gpd3-F	CAAGCGTGTCATCATCTCTGCTCCT	
J83	gpd3-R	GTGCAAGAGGCGTTGGAGATAACC	detect gpd3 gene coding region
J84	tel1F	TATTTCTTTATTCAACTTACCGCACTTC	
J85	tel1R	CAGTAGTGCAGTGTATTATGATAATTAAAATGG	detect telomeric region, from Claus
J100	tRNA Met-F	AAAAGAAAACGGTCAGGGAGG	Pebernard, 2008; SPBTRNAMET.05
J101	tRNA Met-R	GAGCCTCACCAGGAGCATTATAG	Pebernard, 2008; SPBTRNAMET.05
J102	tRNA Ala-R	CCTGCAAACGTATGTTACGTAAGG	Pebernard, 2008
J103	tRNA Ala-F	TCCAATTATTAAGTGAATGCTCTCG	Pebernard, 2008
J104	tRNA Asn-F	GGTCGGGTAGCATAGTTGGTT	SPBTRNAASN.01
J105	tRNA Asn-R	AGAAAACGGTCAGGGAGGGA	SPBTRNAASN.01
J118	tel2F	TCA AAG TTG GCG ACG TTG CTG ATG	detect telomeric region; Rozenzhak S, 2010
J119	tel2R	AAG CAA TGT GTG GAG CAA CAG TGG	detect telomeric region; Rozenzhak S, 2011
J130	tf2-4F	ACACCAACACAAACCCAAGCGA	from 2035-2056 bp 0f ORF of tf2-1
J131	tf2-4R	ACGGCTCCTACAGCGACATCT	from 2165-2145 bp 0f ORF of tf2-1
J203	PMA1 P4F2	TGCAACGGTCCCTTCTGGTCT	
J204	PMA1 P4R2	TGACCACCCTTGAACCAACCGA	detect pma1 gene coding region
T67	T67SpIntF	AGAGGCACATAGTAGGGGAACT	
T68	T68SpIntR	TCCCATCTCCCACTGTTAATTGA	detect intergenic gene region
T105	P1-tdh1-F	CCGTAACGCTTTGGTCGCTA	Pombe tdh1 For primer 5' ORF
T106	P1-tdh1-R	CCGTGGGTAGAGTCGTACTTG	Pombe tdh1 Rev primer 5' ORF
T107	P2-tdh1-F	CACTGTCCACGCTACCACTG	Pombe tdh1 For primer mid ORF
T108	P2-tdh1-R	GAGGAGGGGATGATGTTGGC	Pombe tdh1 Rev primer mid ORF
T109	P3-tdh1-F	GCCAAGCCTACCAACTACGA	Pombe tdh1 For primer 3' ORF
T110	P3-tdh1-R	TGTCACCGCAGAAGTCAGTG	Pombe tdh1 Rev primer 3' ORF
P1-pma1-F	P1-PMA1Pro F	CTCTAGAACATACGTTATTTAATCTCGA	
P1-pma1-R	P1-PMA1Pro R	GTATTACCGACAATAGAAAAGGGG	detect pma1 gene promoter region
P2-pma1-F	P2-PMAC1-F	GTCTTCGTGATTGGGTCGAT	
P2-pma1-R	P2-PMAC1-R	GGGGTCACCATAGTGCTTGT	detect pma1 gene coding region
P3-pma1-F	P3-PMAC2-F	ATCCCGTTTCCAAGAAGGTT	
P3-pma1-R	P3-PMAC2-R	GAGGATCGGAACAAGGCATA	detect pma1 gene coding region
P4-pma1-F	P4-PMAC3-F	GTCTTTCCACCGTCATTGGT	
P4-pma1-R	P4-PMAC3-R	ACGGAGAACGGCAACAATAG	detect pma1 gene coding region

Appendix III-strains

Stock	Strain name	Genotype	Source
JM1	py114	h+ ade6-210 leu1-32 ura4DS/E arg3D his3D	Dr Janet F. Partridge (janet.partrigde@stjude.org)(Petrie et al., 2005)
SPJK002	py115	h- ade6-210 leu1-32 ura4DS/E arg3D his3D	Dr Janet F. Partridge (janet.partrigde@stjude.org)(Petrie et al., 2005)
JM2	upf1Δ	h+ ade6- upf1::KanMX6,his3D leu1-32 ura4D18? arg?	this study (made by back crossing SPJK030 twice to JM1)
JM3	upf2Δ	h+ ade6- upf2::KanMX6,his3D leu1-32 ura4D18? arg?	this study (made by back crossing SPJK031 twice to JM1)
JM10	upf1Δ	h- ade6- upf1::KanMX6,his3D leu1-32 ura4D18? arg?	this study (made by back crossing SPJK030 twice to JM1)
JM11	upf2Δ	h- ade6- upf2::KanMX6,his3D leu1-32 ura4D18? arg?	this study (made by back crossing SPJK031 twice to JM1)
JM15	cdc17-K42	not clear	Antony Carr
JM24	upf1 Δ upf2Δ	h- ade- upf1::KanMX6, upf2::KanMX6, arg3D his3D leu-32 ura4D18?	this study (made by crossing SPJK032 to JM1)
JM26	upf3Δ	h+ ade6- upf3::KanMX4, arg3D his3D leu-32 ura4D18?	this study
JM37	cds1Δ	h+ cds1::KanMX4 ura4-D18 leu1-32	Position V3-P36-52 in bioneer library M-3030H Version 2.0
JM38	upf3-gfp	h+ ade6-210 upf3:gfp:hphMX6 arg3D his3D leu1-32 ura4DS/E	this study (made using two-step PCR and JM1)
JM40	upf3-flag	h+ ade6-210 upf3:5FLAG:hphMX6 arg3D his3D leu1-32 ura4DS/E	this study (made using two-step PCR and JM1)
JM60	SAL424	h- cdc25-22 ade6-704 leu1-32 ura4-D18	Antony Carr
JM70	upf1Δ cdc25-22	h+ ade6- upf1::KanMX6 cdc25-22 leu-32 ura4D arg3D? his3D?	this study (made by crossing JM60 to JM2)
JM72	MCW1285	h+ rad22::ura4+ ura4-D18 leu1-32 his3-D1 arg3-D4	Osman et al,2005; Requested from Matthew C. Whitby
JM73	JCF728	h+ pku70::kanMX, ura4-D18 leu1-32	Julia Copper
JM83	upf1Δ	h+ upf1::hphMX6,his3D leu1-32 ura4D18 arg3D?	this study; (made by using marker swap method and strain JM2)
JM85	upf1Δ	upf1::hphMX6,his3D leu1-32 ura4D18 arg?;h-	this study (made by using marker swap method and strain JM10)
JM89	upf2Δ pku70Δ	upf2::KanMX6 pku70::KanMX6 ura4D leu1-32 arg3D? his3D?	this study (made by crossing JM73 with JM11)
JM90	upf3Δ pku70Δ	upf3::KanMX6 pku70::KanMX6 ura4D leu1-32 arg3D? his3D?	this study (made by crossing JM73 with JM25)
JM91	rad52Δ upf1Δ	rad52::ura4+ upf1::KanMX6 ura4- his3D arg3D leu1-32	this study (made by crossing JM72 with JM10)
JM92	rad52Δ upf2Δ	rad52::ura4+ upf2::KanMX6 ura4- his3D arg3D leu1-32	this study (made by crossing JM72 with JM11)
JM93	rad52Δ upf3Δ	rad52::ura4+ upf3::KanMX6 ura4- his3D arg3D leu1-32	this study (made by crossing JM72 with JM25)

Stock	Strain name	Genotype	Source
JM94	upf1:flag	h+ ade6-210 arg3D his3D leu1-32 ura4DS/E upf1:5flag::hphMX6	this study (made using one step PCR and JM1)
JM109	Δupf1 Δpku70	pku70::KanMX6 upf1::hphMX6 ura4D leu1-32 arg3D? his3D?	this study (made by crossing JM73 with JM85)
JM111	146	h+ 975	Dr. Clause Azzalin (ETH Zurich)
JM115	cbp20-HA	h+ ade6-210 leu1-32 ura4DS/E arg3D his3D cbc2:HA:KanMX6	this study (made using one step PCR and JM1)
JM117	cbp20-HA upf1Δ	h+ upf1::hphMX6, cbc2:HA:KanMX6 his3D leu1-32 ura4D18 arg3D?	this study (made using one step PCR in JM83)
JM121	JY741/FLAG-Rpb3	h- flag-rpb3 ade6-M216 ura4-D18 leu1	from Japanese National BioResource Project--Yeast
JM131	upf1Δ FLAG-Rpb3	h- flag-rpb3 ade6-M216 ura4-D18 leu1 upf1::hphMX6	upf1 was deletion by PCR based method
JM138	JM85+pREP42-HA-Upf1		JM85 strain was transformed with pREP42-HA-Upf1 plasmid
JM139	air1Δ	h+ air1:: KanMX4 ade6-M216 ura4-D18 leu1-32	Position V3-P13-91 in bioneer library M-3030H Version 2.0
JM140	upf1Δ air1Δ	upf1::hphMX6 air1:: kanMX4	this study (made by crossing of JM85 and JM139)
JM142	upf1Δair1Δ+ pREP42-HA-Upf1		JM140 strain was transformed with pREP42-HA-Upf1 plasmid
JM143	ppn1Δ	h+ ppn1:: KanMX4 ade6-M216 ura4-D18 leu1-32	Position V3-P14-41 in bioneer library M-3030H Version 2.0
JM144	upf1Δ ppn1Δ	upf1::hphMX6 ppn1:: kanMX4	this study (made by crossing of JM85 and JM143)
JM146	upf1Δ ppn1Δ + pREP42-HA-Upf1		JM144 strain was transformed with pREP42-HA-Upf1 plasmid
JM147	air1-HA	h- air1:3HA:kanMX6, ade6- arg3D? his3D? leu1-32 ura4-	C terminal of air1 of SPJK002 was tagged with HA
Bioneer library mutant		h+ geneX:: KanMX4 ade6-M216 ura4-D18 leu1-32	Bioneer
Bioneer library mutant		h+ geneX:: KanMX4 ade6-M210 ura4-D18 leu1-32	Bioneer
upf3Δ		h+ upf3::KanMX4 ade6-M216 ura4-D18 leu1-32	Position V3-P01-08 in bioneer library M-3030H Version 2.0
SPJK030	MR3567	h- upf1 Δ::KanMX6, leu1-32; ura4D18	Rodríguez-Gabriel et al.,2006
SPJK031	MR3569	h- upf2::KanMX6, leu1-32; ura4D18	Rodríguez-Gabriel et al.,2006
SPJK032	MR3570	h- upf1::kanMX6 upf2::KanMX6, leu1-32; ura4D18;	Rodríguez-Gabriel et al.,2007
SPJK034	MR4022	upf1:HA:kanMX6	Rodríguez-Gabriel et al.,2006
upf1-HA cdc25-22	upf1-HA cdc25-22	h- cdc25-22 ade6-704 leu1-32 ura4-D18 upf1:HA:KanMX6	Sandip (made using one step PCR and JM1)
pab1Δ (SPAC57A7.04c)		h+ pab1::KanMX4 ade6-M216 leul-32 ura4-D18	Position V3-P06-01 in bioneer library M-3030H Version 3.0
ste7Δ		h+ ste7::KanMX4 ade6-M216 leul-32 ura4-D18	Position V3-P12-66 in bioneer library M-3030H Version 2.0

Appendix IV-plasmid maps

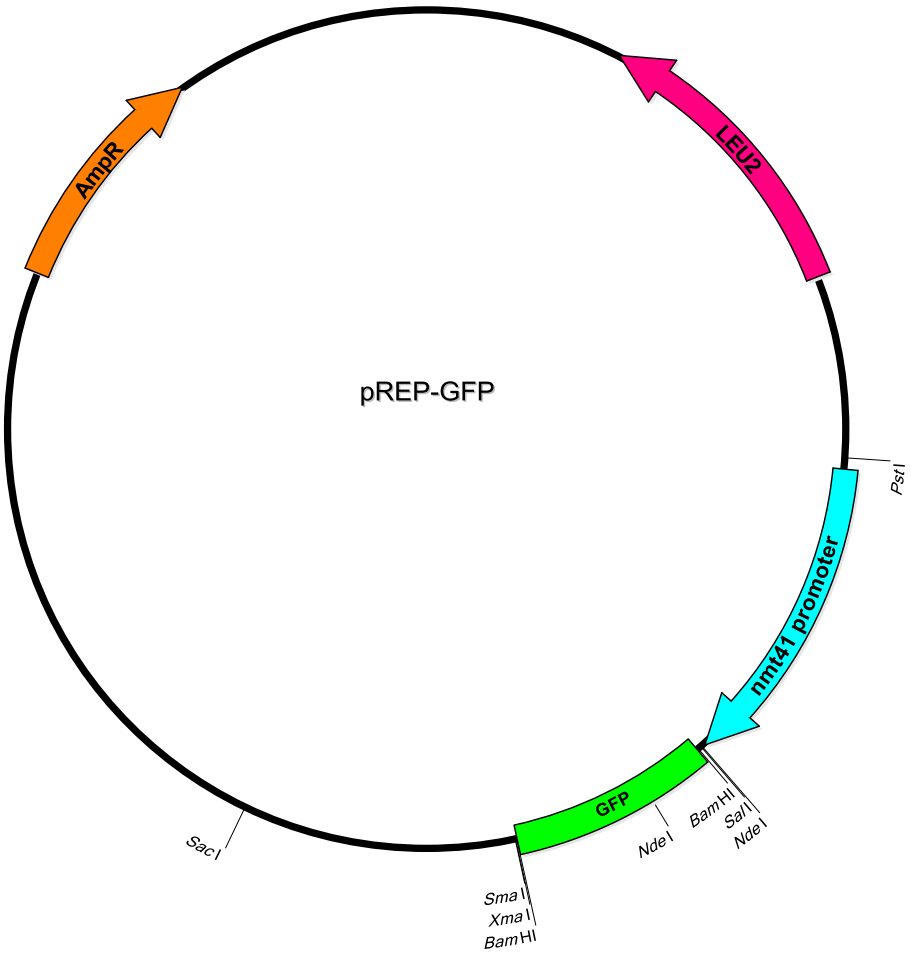

Map 1: pREP-GFP

The GFP reporters were constructed by inserting the GFP-coding sequence into the pREP41 plasmid vector under control of nmt41 promoter. The sequence of the NMD reporters PTC6+ is the same as GFP reporters except that there is a premature stop codon introduced at codon position 6 in GFP in NMD reporter. The construction of the plasmids was described by J WEN (Wen and Brogna, 2010).

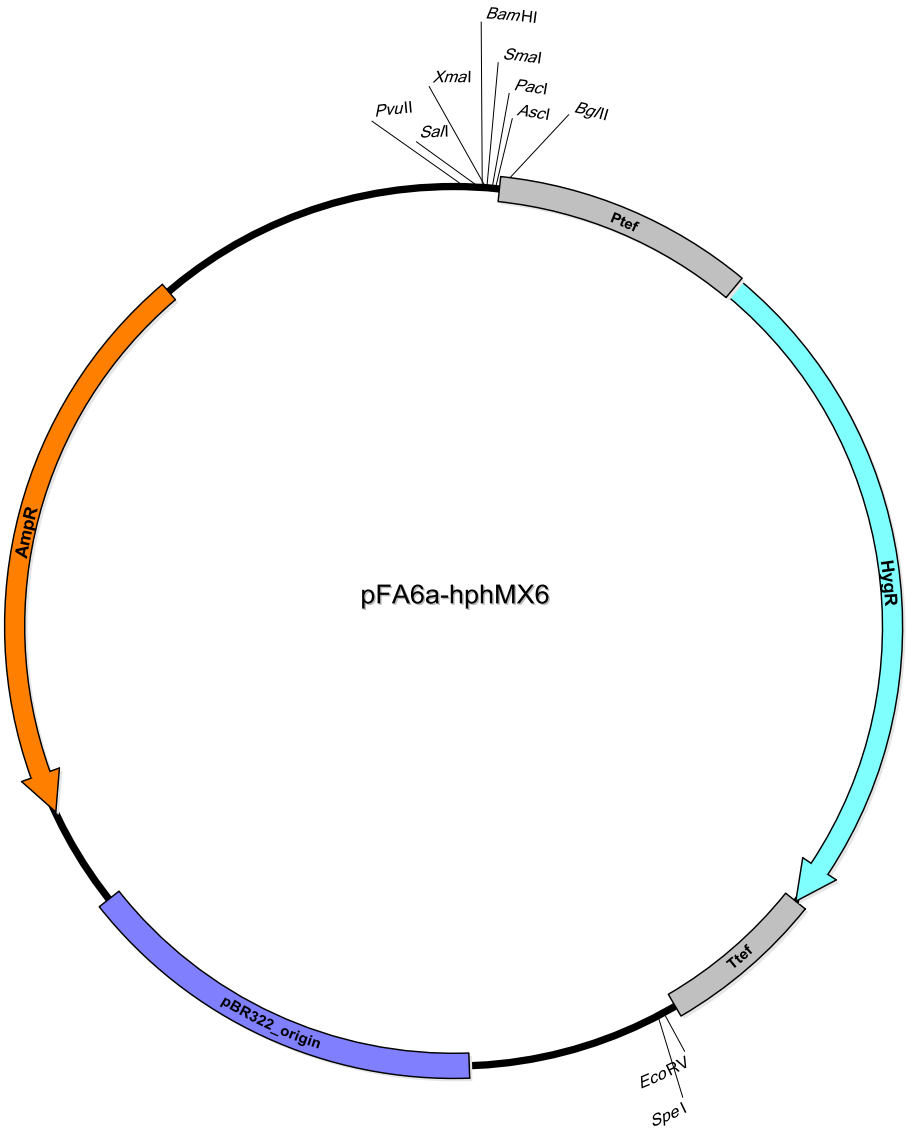

Map 2: pFA6a-hphMX6

The pFA6a-hphMX6 was constructed by replacing the kanMX6 cassette with hphMX6 cassette in the parental plasmid pFA6a-KanMX6. This plasmid is used for PCR-mediated gene disruption in *S. pombe*. The construction of the plasmids was described by Hentges (Hentges et al., 2005).

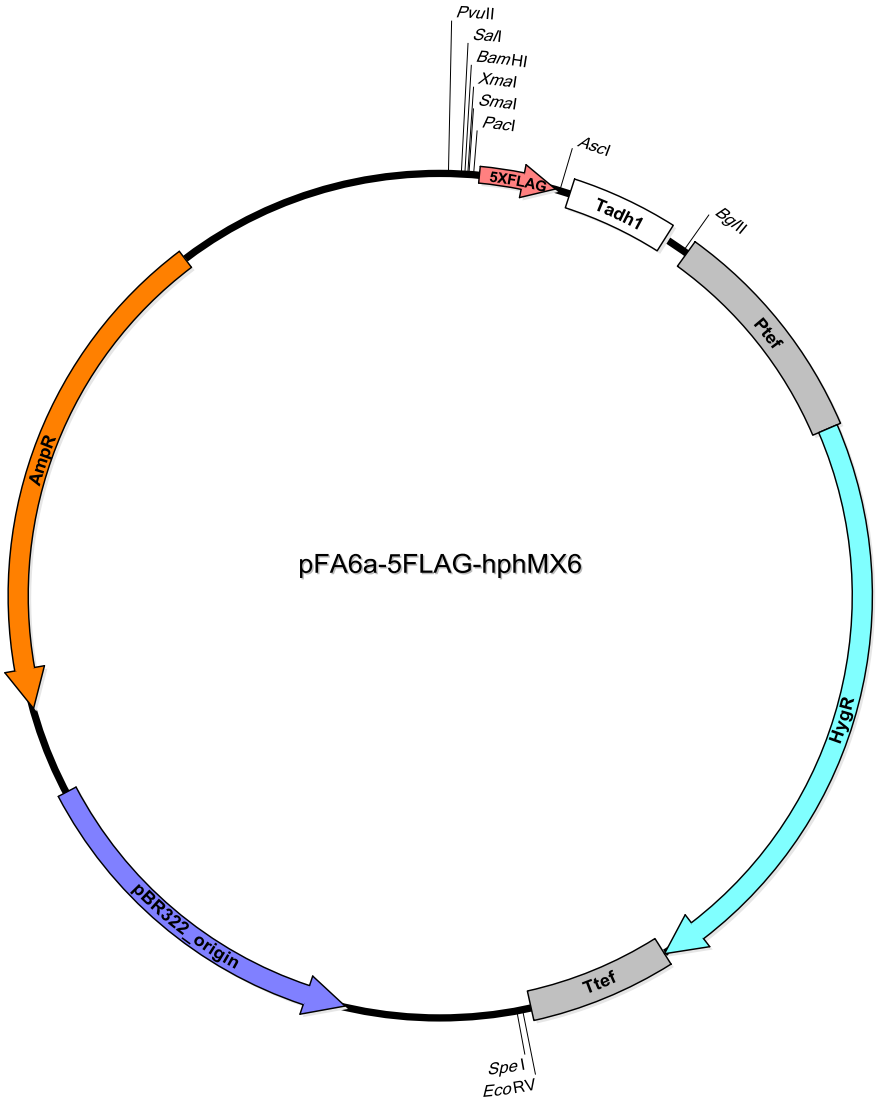

Map 3: pFA6a-5FLAG-hphMX6

The pFA6a-5FLAG-hphMX6 vector was designed for C-terminal FLAG epitope-tagging of proteins under the control of their native promoters at their own genomic loci in *S. pombe*. This vector contains hphMX6 marker which confers fission yeast the resistance to Hygromycin B Antibiotic. The construction of the plasmid was described by Noguchi (Noguchi et al., 2008).

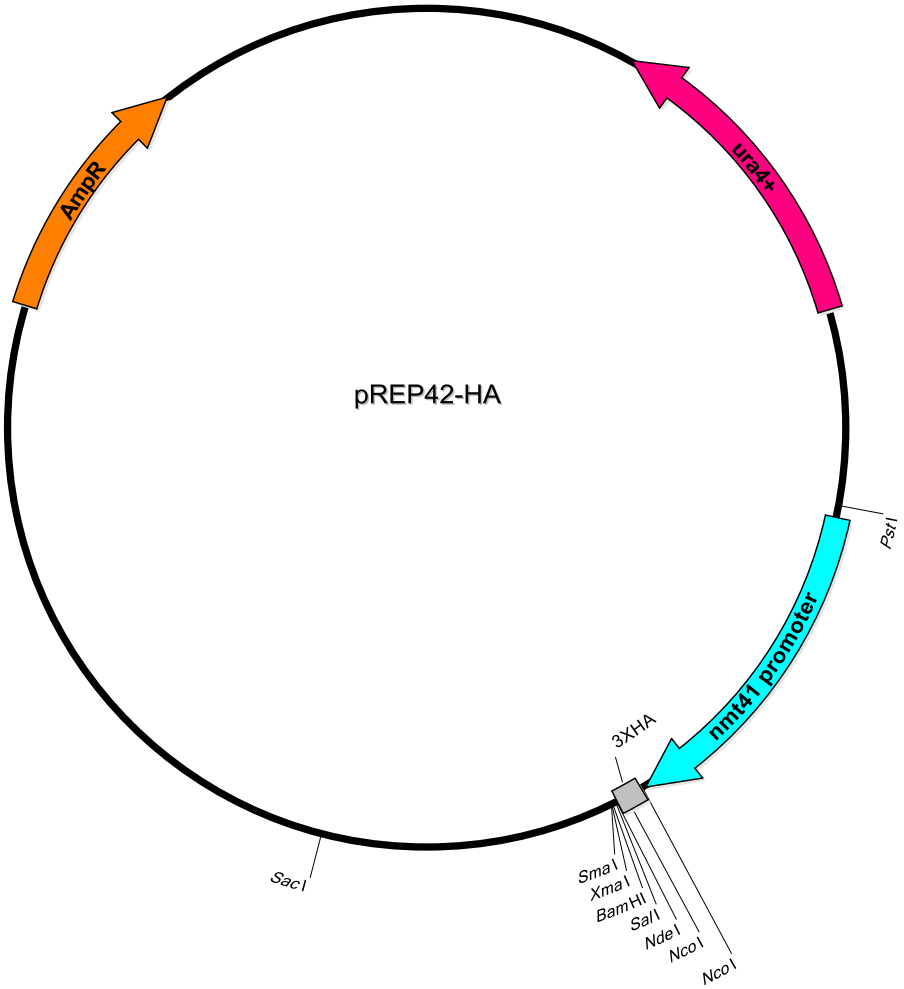

Map 4: pREP42-HA

The pREP42-HA vector was designed for N-terminal HA epitope-tagging of proteins under the control of nmt41 promoter in *S. pombe*. The construction of the plasmid was described by Craven (Craven et al., 1998).

Appendix V-Genetic screen results

Set correct?	set	rescue	M-3030H position	Systemic ID	Gene description
Y	1	B6	V3-P01-18	SPAC16A10.05c	DASH complex subunit Dad1
Y	3	F11(posi)?	V3-P03-71	SPAC15A10.06	CPA1 sodium ion/proton antiporter (predicted)
?	7	H9(positive)	V3-P07-93	SPBC21B10.05c	WD repeat protein Pop3
?A7(X)	10	E6(positive)	V3-P10-54	SPAC1851.04c	Ypt/Rab-specific guanyl-nucleotide exchange factor (GEF) subunit Ric1
?(H1X)	11	C5(positive)	V3-P11-29	SPBC1652.02	APC amino acid transporter (predicted)
?(H1X)	11	D2(positive)	V3-P11-38	SPBC1861.01c	CENP-C ortholog Cnp3
Y	13	G10(posi)	V3-P13-82	SPBC713.07c	vacuolar polyphosphatase (predicted)
Y	18	E5(posi)	V3-P18-53	SPBC11C11.09c	60S ribosomal protein L5
Y	18	G7(posi)	V3-P18-79	SPBC56F2.09c	arginine specific carbamoyl-phosphate synthase subunit Arg5 (predicted)
?	19	A2	V3-P19-02	SPCC1494.05c	CSN-associated deubiquitinating enzyme Ubp12
Y	20	F5(positive)	V3-P20-65	SPAC328.03	alpha,alpha-trehalose-phosphate synthase [UDP-forming]
Y	20	H4(positi)	V3-P20-88	SPBC12C2.01c	Schizosaccharomyces specific protein
Y	24	H1(posi)	V3-P24-85	SPBC19G7.16	transcription elongation factor complex subunit Iws1 (predicted)
Y	24	H7(posi)	V3-P24-91	SPBC713.08	mitochondrial TOM complex assembly protein Mim1 (predicted)
?F3(X)	26	C10(posi)	V3-P26-34	SPBC428.06c	histone deacetylase complex subunit Rxt2
?F3(X)	26	H4(posi)	V3-P26-88	SPAC22A12.04c	40S ribosomal protein S15a (predicted)
?H1(X)	30	F4(posi)	V3-P30-64	SPBC28F2.11	HMG box protein Hmo1
?H1(X)	30	H6(posi)	V3-P30-90	SPBC56F2.08c	RNA-binding protein (predicted)

set	lethal	M-3030H position	Systemic ID	Gene description
1	A5	V3-P01-05	SPAC11E3.15	60S ribosomal protein L22 (predicted)
1	G2	V3-P01-74	SPAC652.01	BC10 family protein
2	F10	V3-P02-70	SPBC3D6.15	40S ribosomal protein S25 (predicted)
4	C9	V3-P04-33	SPAC1D4.13	MAP kinase kinase Byr1
6	A5	V3-P06-05	SPAC5D6.06c	UDP-GlcNAc transferase associated protein Alg14 (predicted)
10	A7	V3-P10-07	SPCC553.08c	GTPase Ria1 (predicted)
21	C5	V3-P21-29	SPCC162.05	hexaprenyldihydroxybenzoate methyltransferase Coq3
22	A6	V3-P22-06	SPCC1795.06	P-factor pheromone Map2
25	E7	V3-P25-55	SPBC26H8.11c	thioesterase superfamily protein
25	E8	V3-P25-56	SPBC2G2.10c	Schizosaccharomyces specific protein Mug110
26	F3	V3-P26-63	SPAC323.04	mitochondrial ATPase (predicted)

set	very sick	M-3030H position	Systemic ID	Gene description
1	A10(YD sick3)	V3-P01-10	SPAC13G7.11	mitochondrial respiratory complex assembly protein (predicted),mba1
1	D6(YD sick1)	V3-P01-42	SPAC23A1.11	60S ribosomal protein L13/L16 (predicted)
1	G7 (YD sick3)	V3-P01-79	SPAC6B12.15	RACK1 ortholog Cpc2
2	C9(YD S2)	V3-P02-33	SPBC16A3.07c	MBF complex corepressor Nrm1
2	D10(YDS2)	V3-P02-46	SPBC18H10.07	WW domain-binding protein 4 (predicted)
2	H5(YD S1)	V3-P02-89	SPBCPT2R1.08c	RecQ type DNA helicase Tlh1
2	H6 (YD sick3)	V3-P02-90	SPBP22H7.08	40S ribosomal protein S10 (predicted)
2	H11(YDS2)	V3-P02-95	SPBPB2B2.02	esterase/lipase (predicted)
3	A12(lethal)	V3-P03-12	SPCC16C4.11	Pho85/PhoA-like cyclin-dependent kinase Pef1
3	D3(YDS3)	V3-P03-39	SPAC11E3.05	ubiquitin-protein ligase E3, human WDR559 ortholog
3	D5(YDS3)	V3-P03-41	SPAC11G7.02	HECT-type ubiquitin-protein ligase E3 Pub1
3	F1(YDS1)	V3-P03-61	SPAC13G6.09	SSU-rRNA maturation protein Tsr4 homolog 2 (predicted)
3	F4(YD1)	V3-P03-64	SPAC144.02	Ino80 complex subunit Iec1
3	G7(YDS1)	V3-P03-79	SPAC167.01	serine/threonine protein kinase Ppk4/ sensor for unfolded proteins in the ER (predicted)
3	G9(YDS1)	V3-P03-81	SPAC1687.05	SUMO E3 ligase Pli1
3	G10(YDS1)	V3-P03-82	SPAC1687.06c	60S ribosomal protein L28/L44 (predicted)
3	G11(YDS1)	V3-P03-83	SPAC1687.15	serine/threonine protein kinase Gsk3
3	H4(YDS3)	V3-P03-88	SPAC16C9.07	serine/threonine protein kinase Ppk5 (predicted)
4	B11(YDS1)	V3-P04-23	SPAC1851.03	CK2 family regulatory subunit Ckb1
4	G5(YDS1)	V3-P04-77	SPAC23G3.02c	ferrichrome synthetase Sib1

set	very sick	M-3030H position	Systemic ID	Gene description
4	H7(YDS1)	V3-P04-91	SPAC25G10.03	transcription factor Zip1
5	C3(YDS2)	V3-P05-27	SPAC2H10.01	transcription factor, zf-fungal binuclear cluster type (predicted)
5	C9(YDS2)	V3-P05-33	SPAC31G5.19	ATPase with bromodomain protein (predicted)
5	C11(YDS1)	V3-P05-35	SPAC328.02	ubiquitin-protein ligase involed in sporulation
5	D10(YDS1)	V3-P05-46	SPAC3A11.10c	dipeptidyl peptidase (predicted)
5	E8(YDs1)	V3-P05-56	SPAC3F10.11c	glutathione S-conjugate-exporting ATPase Abc2
5	G5(YDS2)	V3-P05-77	SPAC4G8.04	GTPase activating protein (predicted)
5	G6(YDS2)	V3-P05-78	SPAC4G8.05	serine/threonine protein kinase Ppk14 (predicted)
5	G7(YDS3)	V3-P05-79	SPAC4G8.08	mitochondrial iron ion transporter (predicted)
5	H3(YDs1)	V3-P05-87	SPAC521.02	WLM domain protein
5	H4(YDs1)	V3-P05-88	SPAC521.04c	calcium permease (predicted)
6	A1(YDS3)	V3-P06-01	SPAC57A7.04c	mRNA export shuttling protein,pab1
6	C8(YDS2)	V3-P06-32	SPAC821.05	translation initiation factor eIF3h (p40)
6	G4(YDS1)	V3-P06-76	SPBC106.02c	sulfiredoxin
7	B5?(YDS2)	V3-P07-17	SPBC1604.08c	importin alpha
7	F8(YDS3)	V3-P07-68	SPBC18H10.06c	Set1C complex subunit Swd2.1
7	G7(YDS2)	V3-P07-79	SPBC19G7.04	HMG box protein
8	A3(YDS2)	V3-P08-03	SPBC21C3.13	40S ribosomal protein S19 (predicted)
8	A7(YDS3)	V3-P08-07	SPBC21H7.04	ATP-dependent RNA helicase Dbp7 (predicted)
8	C11(YDS3)	V3-P08-35	SPBC2F12.11c	transcriptional activator, MBF subunit Rep2
8	H9(YDS2)	V3-P08-93	SPBC609.02	phosphatidylinositol-3,4,5-trisphosphate3-phosphatasePtn1

set	very sick	M-3030H position	Systemic ID	Gene description
9	A2(YDS2)	V3-P09-02	SPBC651.02	bis(5'-adenosyl)-triphosphatase (predicted)
9	D4(YDS1)	V3-P09-40	SPBP8B7.11	ubiquitin protease cofactor Glp1 (predicted)
10	C3(YDS2)	V3-P10-27	SPCC895.05	formin For3
10	C6(YDS3)	V3-P10-30	SPCC970.10c	ubiquitin-protein ligase E3 Brl2
11	A6?(YDS1)	V3-P11-06	SPAC821.03c	cell cortex node protein Slf1
11	B8(YDS2)	V3-P11-20	SPBC1105.04c	CENP-B homolog
11	B10(YDS3)	V3-P11-22	SPBC1198.06c	mannan endo-1,6-alpha-mannosidase (predicted)
11	B12(YDS3)	V3-P11-24	SPBC146.13c	myosin type I
11	F2(YDS1)	V3-P11-62	SPBC428.10	Schizosaccharomyces pombe specific protein
11	F3(YDS1)	V3-P11-63	SPBC4F6.06	microtubule affinity-regulating kinase Kin1
11	F5(YDS1)	V3-P11-65	SPBC530.06c	clustered mitochondria (cluA/CLU1) homolog Clu1 (predicted)
11	F8(YDS2)	V3-P11-68	SPBC800.03	histone deacetylase (class II) Clr3
11	F10(YDS2)	V3-P11-70	SPBC947.02	AP-1 adaptor complex subunit beta subunit Apl2
11	H6(YDS1)	V3-P11-90	SPCC1919.10c	myosin type V
11	H10()	V3-P11-94	SPCC338.16	F-box protein Pof3
12	A8(YDS1)	V3-P12-08	SPCP1E11.05c	acyl-coA-sterol acyltransferase Are2 (predicted)
12	A9(YDS1)	V3-P12-09	SPCP1E11.06	AP-1 adaptor complex gamma subunit Apl4
12	B12(YDS2)	V3-P12-24	SPAC1296.01c	phosphoacetylglucosamine mutase (predicted)
12	C3(YDS3)	V3-P12-27	SPAC1399.03	uracil permease
12	C5(YDS1)	V3-P12-29	SPAC13A11.06	pyruvate decarboxylase (predicted)
12	C9(YDS3)	V3-P12-33	SPAC15E1.04	thymidylate synthase/ flavoprotein fusion protein Hal3

set	very sick	M-3030H position	Systemic ID	Gene description
12	E2(YDS3)	V3-P12-50	SPAC1F7.01c	nucleosome remodeling protein Spt6
12	E11(YDS2)	V3-P12-59	SPAC222.07c	eIF2 alpha kinase Hri2
12	E12(YDS2)	V3-P12-60	SPAC222.13c	6-phosphofructo-2-kinase (predicted)
12	F6(YD lethal)	V3-P12-66	SPAC23E2.03c	arrestin family meiotic suppressor protein Ste7
12	F10(YDS2)	V3-P12-70	SPAC25B8.19c	transcription factor zf-C2H2 type (predicted)
12	G5(YDS1)	V3-P12-77	SPAC30C2.04	cofactor for cytoplasmic methionyl-and glutamyl-tRNA synthetases Asc1 (predicted)
12	G6(YDS2)	V3-P12-78	SPAC30D11.05	AP-3 adaptor complex subunit Aps3 (predicted)
12	H10(YDS2)	V3-P12-94	SPAC56F8.02	AMP binding enzyme (predicted)
12	H11(YDS2)	V3-P12-95	SPAC57A10.12c	dihydroorotate dehydrogenase Ura3
13	D1(YDS2)	V3-P13-37	SPBC1734.11	DNAJ domain protein Mas5 (predicted)
13	D10(YD lethal)	V3-P13-46	SPBC21.05c	Ras1-Scd pathway protein Ral2
13	E4(YD lethal)	V3-P13-52	SPBC24C6.06	G-protein alpha subunit
13	E6?(YDS2)	V3-P13-54	SPBC27B12.11c	transcription factor Pho7
13	H7(YD lethal)	V3-P13-91	SPBP35G2.08c	zinc knuckle TRAMP complex subunit Air1
14	E2?(YDS2)	V3-P14-50	SPAC11G7.01	serine-rich Schizosaccharomyces specific protein
14	H11(YDS2)	V3-P14-95	SPAC2G11.07c	protein phosphatase 2C Ptc3
15	A1(YDS2)	V3-P15-01	SPAC30C2.02	deoxyhypusine hydroxylase (predicted)
15	C7(YDS3)	V3-P15-31	SPACUNK4.12c	insulinase pombe homologue 1
15	D4(YDS2)	V3-P15-40	SPBC1289.14	adducin (predicted)
15	F3(YDS1)	V3-P15-63	SPBC2D10.17	SHREC complex subunit Clr1
15	F4(YDS2)	V3-P15-64	SPBC30D10.13c	pyruvate dehydrogenase e1 component beta subunit Pdb1

set	very sick	M-3030H position	Systemic ID	Gene description
15	G4(YDS2)	V3-P15-76	SPBC428.03c	thiamine-repressible acid phosphatase Pho4
15	H6(YDS3)	V3-P15-90	SPBC691.04	mitochondrial ATP-dependent RNA helicase Mss116 (predicted)
16	B5(YDS3)	V3-P16-17	SPCC31H12.05c	serine/threonine protein phosphatase Sds21
16	F6(YD lethal)	V3-P16-66	SPAC31G5.09c	MAP kinase Spk1
16	H3(YDS2)	V3-P16-87	SPAC922.05c	membrane transporter (predicted)
17	A7(YDS3)	V3-P17-07	SPBC14C8.17c	SAGA complex subunit Spt8
17	A12(YDS3, layp	V3-P17-12	SPBC16D10.07c	Sir2 family histone deacetylase Sir2
17	E4(YDS2)	V3-P17-52	SPBC887.17	transmembrane transporter (predicted)
17	F2(YDS3)	V3-P17-62	SPCC1442.01	guanyl-nucleotide exchange factor Ste6
17	H10(YDS3)	V3-P17-94	SPAC1142.05	copper transporter complex subunit Ctr5
18	A6(YD lethal)	V3-P18-06	SPAC1565.04c	adaptor protein Ste4
18	D1(YDS3)	V3-P18-37	SPAC4G8.10	SNARE Gos1 (predicted)
18	E6(YDS3)	V3-P18-54	SPBC1271.12	oxysterol binding protein (predicted)
19	C7	V3-P19-31	SPAC16C9.01c	carbohydrate kinase (predicted)
19	E1	V3-P19-49	SPAC23G3.10c	SWI/SNF and RSC complex subunit Ssr3
20	F1(JN lethal)	V3-P20-61	SPAC25B8.18	mitochondrial thioredoxin-related protein (predicted)
20	G2	V3-P20-74	SPAC630.04c	Schizosaccharomyces specific protein
21	A7	V3-P21-07	SPBC27B12.08	Pof6 interacting protein Sip1, predicted AP-1 accessory protein
21	E10	V3-P21-58	SPAC2G11.04	RNA-binding protein, G-patch type, splicing factor 45 ortholog (predicted)
21	F1	V3-P21-61	SPAC521.05	40S ribosomal protein S8 (predicted)
21	F10	V3-P21-70	SPAP8A3.07c	phospho-2-dehydro-3-deoxyheptonate aldolase (predicted)

set	very sick	M-3030H position	Systemic ID	Gene description
21	G9?	V3-P21-81	SPBC1718.07c	CCCH tandem zinc finger protein, human Tristetraprolin homolog Zfs1, involved in mRNA catabolism
21	H10	V3-P21-94	SPBP35G2.07	acetolactate synthase catalytic subunit
22	D11?	V3-P22-47	SPBC11B10.10c	histone H2A variant H2A.Z, Pht1
22	F8	V3-P22-68	SPCC736.02	Schizosaccharomyces specific protein
22	F9	V3-P22-69	SPAC1039.08	serine acetyltransferase (predicted)
22	G3	V3-P22-75	SPAC1610.02c	mitochondrial ribosomal protein subunit L1 (predicted)
22	G7	V3-P22-79	SPAC17C9.15c	Schizosaccharomyces specific protein
23	A5	V3-P23-05	SPBC902.03	Nem1-Spo7 complex regulatory subunit Spo7 (predicted)
23	H1	V3-P23-85	SPCC11E10.06c	elongator complex subunit Elp4 (predicted)
23	H9(not H8)	V3-P23-93	SPAC17H9.13c	glutamate 5-kinase (predicted)
24	C11	V3-P24-35	SPAC17G8.13c	histone acetyltransferase Mst2
24	F5?	V3-P24-65	SPBC29A10.16c	cytochrome b5 (predicted)
24	H5(JN lethal)	V3-P24-89	SPBC365.03c	60S ribosomal protein L21 (predicted)
25	C3	V3-P25-27	SPAC144.06	AP-3 adaptor complex subunit Apl5 (predicted)
25	C7	V3-P25-31	SPAC2G11.10c	URM1 activating enzyme (predicted)
25	E1	V3-P25-49	SPAC22F8.12c	small histone ubiquitination factor Shf1
26	A12	V3-P26-12	SPAC1F3.09	CwfJ family protein, splicing factor (predicted)
26	B7	V3-P26-19	SPBC27.06c	mitochondrial membrane protein Mgr2 (predicted)
26	D4	V3-P26-40	SPAC16C9.02c	S-methyl-5-thioadenosine phosphorylase (predicted)
26	D12	V3-P26-48	SPCC1235.09	Set3 complex subunit Hif2
26	E10	V3-P26-58	SPBC25B2.01	elongation factor 1 alpha related protein Hbs1 (predicted)

set	very sick	M-3030H position	Systemic ID	Gene description
26	F9	V3-P26-69	SPCC1442.02	central kinetochore associated family protein (predicted)
27	A2?	V3-P27-02	SPCC794.07	dihydrolipoamide S-acetyltransferase E2, Lat1 (predicted)
28	B12	V3-P28-24	SPAC22E12.04	superoxide dismutase copper chaperone Ccs1
28	D1	V3-P28-37	SPBC2F12.15c	palmitoyltransferase (predicted)
28	D3	V3-P28-39	SPCC1259.07	transcriptional regulatory protein Rxt3
28	G7	V3-P28-79	SPCC737.09c	ATP-binding cassette-type vacuolar membrane transporter Hmt1
29	A5	V3-P29-05	SPAC25B8.13c	2-OG-Fe(II) oxygenase superfamily protein
29	B7	V3-P29-19	SPBC146.11c	meiotically upregulated gene Mug97
29	E5	V3-P29-53	SPBP8B7.26	Schizosaccharomyces specific protein
30	D11	V3-P30-47	SPBC13E7.04	F1-ATPase delta subunit (predicted)
30	F11(JN lethal)	V3-P30-71	SPBC30B4.02c	R3H and G-patch domain, implicated in splicing (predicted)
30	G4	V3-P30-76	SPBC32H8.03	esterase/lipase (predicted)

Appendix VI-JM94 sequencing

upf1-flag sequence

caTAaGaGaCTCaTGTnnaAGaTcaCTATCTCCTATACAGAATGCCGGTTCTGCC
ATGTTACCTTCGTTTTctaATCTTCCGAACTTATACTCTTCCTCGTATCTTGA
AGAATGGAATGTCTTTGCTCAATACAAACGAAGAGAAAGCAACGCTACCG
ACTTTGAAGACTTTAGAAGTCAGGTTGGTGATGATGAAAGCAAGTTCGAC
GAACCTACTAGGTTCCGGATCCCCGGGTTAATTAATCATATGGACTACAA
GGACGACGATGACAAGGATTACAAAGATGACGACGATAAGCTTATGGAC
TACAAGGACGACGATGACAAGGATTACAAAGATGACGACGATAAGCTTA
TGGACTACAAGGACGACGATGACAAGCATATGGGCGCGCCACTTCTAAAT
AAGCGAATTTCTTATGATTTATGATTTTTATTATTAAATAAGTTATAAAAA
AAaTAAGTGTATACAAATTTTAAAGTGACTCTTAGGTTTTAAAACGAAAAT
TCTTATTCTTGAGTAACTCTTTCCTGTAGGTCAGGTTGCTTTCTCAGGTATA
GTATGAGGTCGCTCTTATTGACCACACCTCTACCGGCAGATCCGCTAGGG
ATAACAGGGTAATATAGATCTGTTTAGCTTGCCTCGTCCCCGCCGGGTCAC
CCGGCCAGCGACATGgagcCCCAGAATaaa

Note: The underlined sequence is the C terminal part of *upf1* open reading frame; the rest sequencing is originally from the plasmid pFa6a-5FLAG-hph, and includes the five repeats of *flag* sequence.

Appendix VII-Figure S1

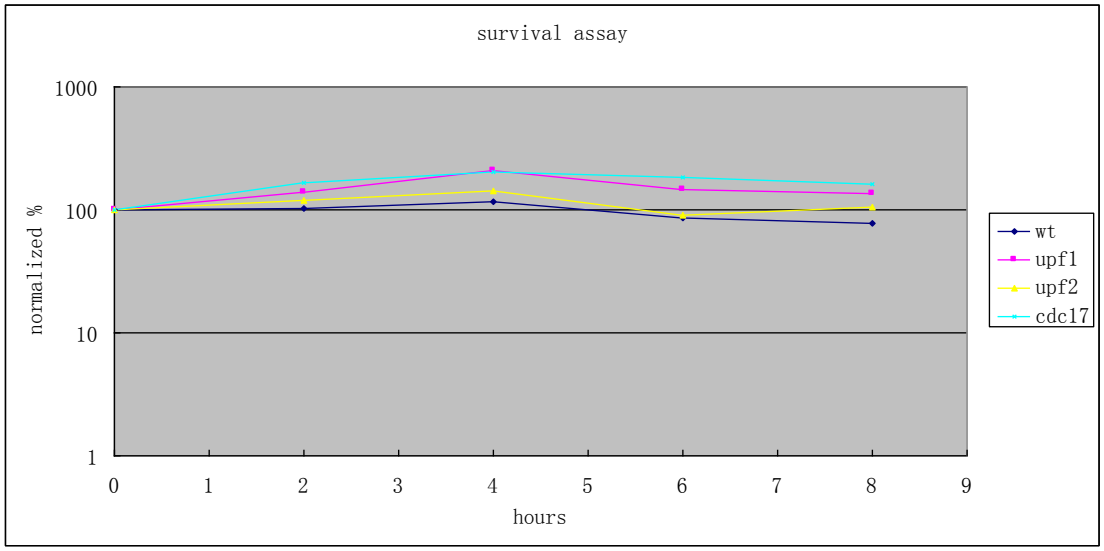

Figure S1. The growth rate of *upf1Δ* does not differ in short culturing times. For survival of acute exposure to HU, midlog phase cells were cultured in YES media in presence of 12 mM HU for 10 h. At 0 h, 1000 cells were plated onto YES agar plates in triplicate and, at the indicated time points, the same culture volume was taken, and the cells were plated in triplicate. Survival was estimated relative to untreated cells. For all survival assays, recovery was for 2-3 days at 30℃.

Appendix VIII-Figure S2

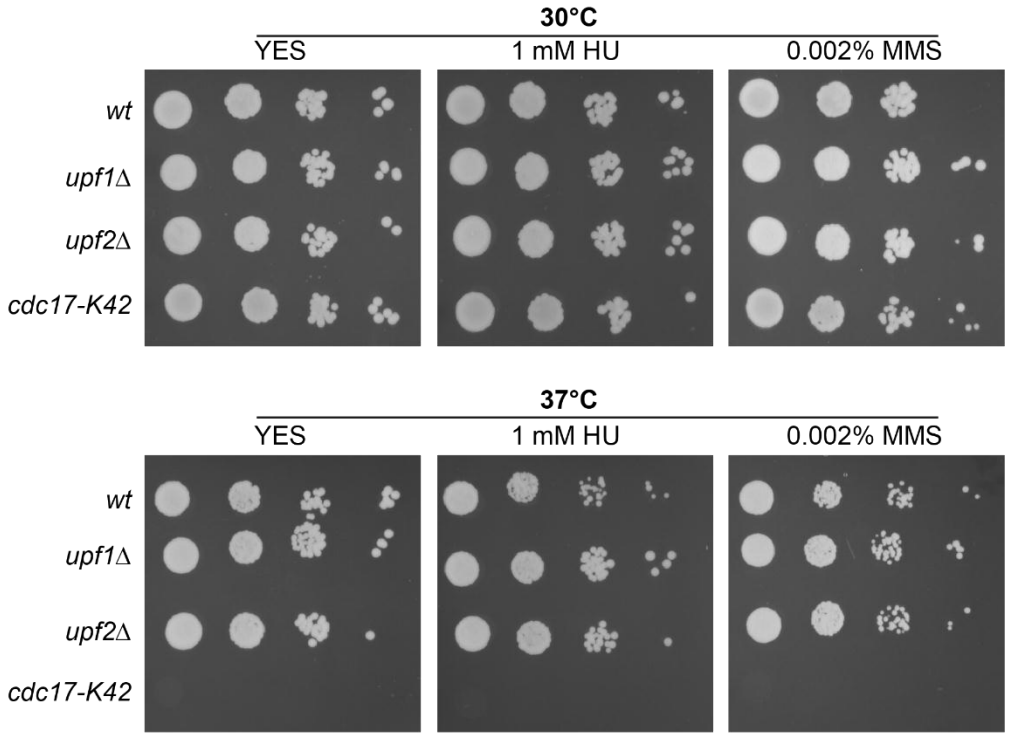

Figure S2． ***upf1Δ*** **and** ***upf2Δ*** **are not hypersensitive to low concentrations of DNA damaging drugs.** Wild type (JM1), *upf1Δ* (SPJK030), *upf2Δ* (SPJK031) and *cdc17-K42* mutants were grown on rich medium（YES）at 30 ℃. Approxymately 10^4, 10^3, 10^2, and 10 cells were spotted and grown for 4 days at either 30 ℃ or 37 ℃ in presence or absence of methyl methanesulfonate (MMS) or hydroxyurea (HU).

Appendix IX-Figure S3

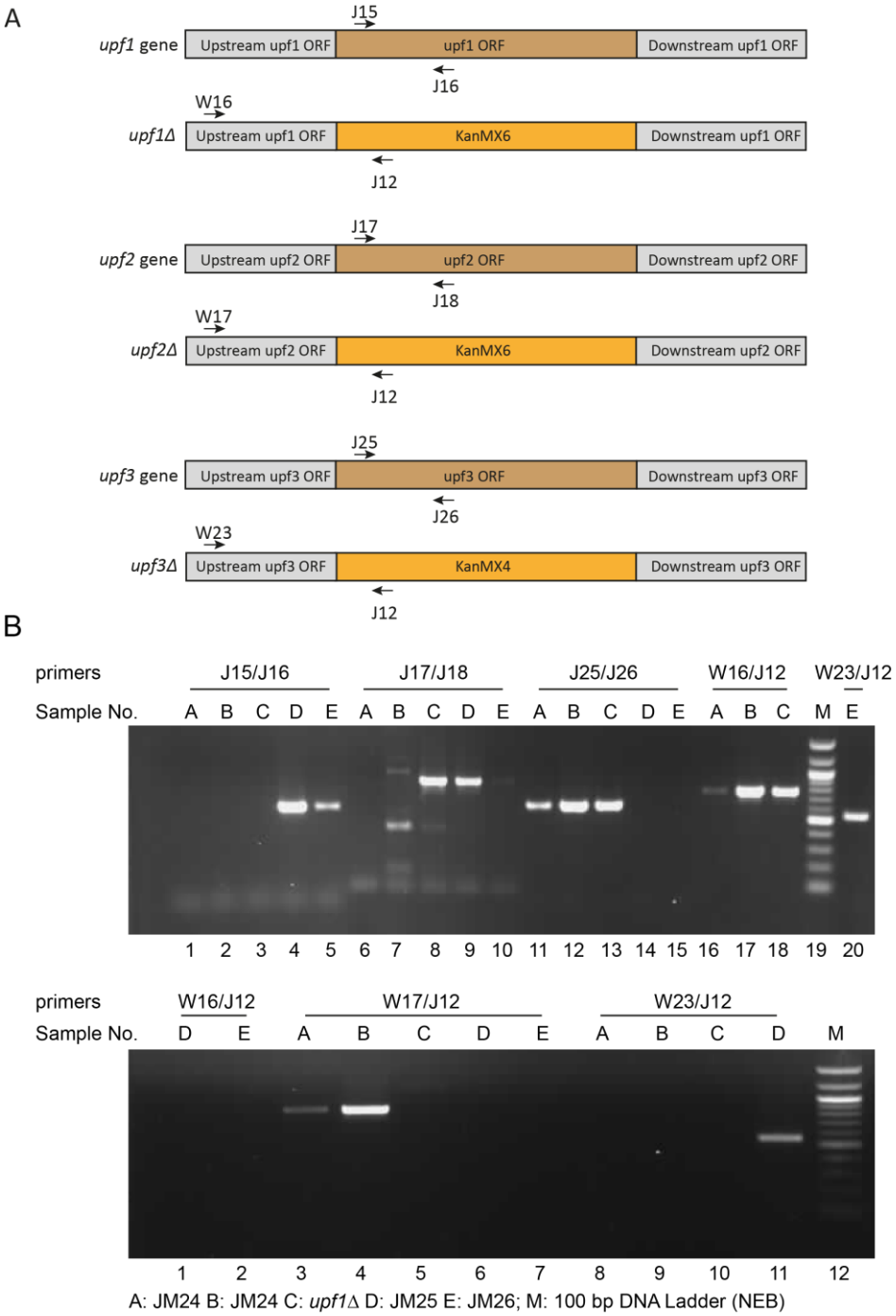

Figure S3. Verification of the deletion of *upf1* and *upf2* from JM24, and the deletion of *upf3* from JM25 and JM26 by colony PCR. (A) Diagram of the positions of the primers used for gene deletion verification. The primer sequences are listed in Appendix II (B) Confirmation of gene deletion from tested strains by colony PCR. Tested strains were

listed at the bottom of DNA agarose gel picture: JM24 (*upf1Δupf2Δ*), JM25 (h- *upf3Δ*), JM26 (h+ *upf3Δ*).